LUCAS RIBEIRO JARDULI

DADOS DE LANDMARK:

UMA NOVA LUZ NA FILOGENIA DE PSEUDOPIMELODIDAE (TELEOSTEI: SILURIFORMES)

Londrina
2017

LUCAS RIBEIRO JARDULI

DADOS DE LANDMARK:

UMA NOVA LUZ NA FILOGENIA DE PSEUDOPIMELODIDAE (TELEOSTEI: SILURIFORMES)

Tese apresentada ao Programa de Pósgraduação em Ciências Biológicas da Universidade Estadual de Londrina como um dos requisitos à obtenção do título de Doutor em Ciências Biológicas.

Orientador: Prof. Dr. Oscar Akio Shibatta.
Co-orientador: Prof. Dr. Fernando C. Jerep.

Londrina
2017

Ficha de identificação da obra elaborada pelo autor, através do Programa de Geração Automática do Sistema de Bibliotecas da UEL

Jarduli, Lucas Ribeiro.
Dados de landmark: uma nova luz na filogenia de Pseudopimelodidae (Teleostei: Siluriformes). / Lucas Ribeiro Jarduli. - Londrina, 2017.
127 f. : il.

Orientador: Oscar Akio Shibatta.
Coorientador: Fernando Camargo Jerep.
Tese (Doutorado em Ciências Biológicas) - Universidade Estadual de Londrina, Centro de Ciências Biológicas, Programa de Pós-Graduação em Ciências Biológicas, 2017.
Inclui bibliografia.

1. Sistemática - Tese. 2. Bagres - Tese. 3. Morfometria Geométrica - Tese. 4. Nova espécie. - Tese. I. Shibatta, Oscar Akio. II. Jerep, Fernando Camargo. III. Universidade Estadual de Londrina. Centro de Ciências Biológicas. Programa de Pós-Graduação em Ciências Biológicas. IV. Título.

UNIVERSIDADE ESTADUAL DE LONDRINA

201313090072

CENTRO DE CIÊNCIAS BIOLÓGICAS
PROGRAMA DE PÓS-GRADUAÇÃO EM CIÊNCIAS BIOLÓGICAS

DEFESA DE TESE DE DOUTORADO

Discente: **Lucas Ribeiro Jarduli**

Título: **"Dados de landmark: uma nova luz na filogenia de Pseudopimelodidae (Teleostei: Siluriformes)".**

Data da Defesa: 19 de julho de 2017 – 14:00hs, na sala nº7 de vídeo-conferência do LABESC da Universidade Estadual de Londrina.

Banca Examinadora		**Parecer**
PRESIDENTE:		
Dr. Oscar Akio Shibatta	UEL	Aprovado
TITULARES		
Dr. José Luís Olivan Birindelli	UEL	APROVADO
Dr. Santiago Andres Catalano	Unidad Ejecutora Lillo (UEL)	Aprovado
Dra. Fernanda de Oliveira Martins	IFPR	aprovado
Dra. Lenice Souza Shibatta	UEL	APROVADO
	Parecer Final	APROVADO

Dr. Oscar Akio Shibatta

Dr. José Luís Olivan Birindelli

Dr. Santiago Andres Catalano

Dra. Fernanda de Oliveira Martins

Dra. Lenice Souza Shibatta

Ao meus pais, Elias e Irene

Dedico

AGRADECIMENTOS

Aos meus pais, Elias Jarduli, Irene Ribeiro Jarduli, minha irmã, Luciana Ribeiro Jarduli, avó, Maria Farinha Ribeiro e a minha companheira Maquieli Menegusso, por todo apoio, incentivo e amor;

Ao Orientador Dr. Oscar Akio Shibatta, pela confiança, incentivo, orientação constante, pela minha formação enquanto pesquisador e pela grande amizade durante todos os anos em que trabalhamos juntos;

Ao Co-orientador Dr. Fernando C. Jerep, pelo incentivo, orientação e amizade;

Ao Dr. Santiago Catalano, por compartilhar seu conhecimento, scripts e auxílio nas análises com landmarks. Agradeço ainda, pela bolsa concedida para a realização do Curso: Análise de dados Morfométricos em Estudos Filogenéticos no Instituto Miguel Lillo, Argentina;

Ao Dr. Juan Marcos Mirande, Dr. Guillhermo Terán, Dr. Felipe Alonso, pela coleta e empréstimo de material para a descrição da espécie nova de *Microglanis*, além da amizade e conhecimento compartilhado;

À Sandra M. Ospina-Garcés e Eduardo Ascarrunz pelo auxilio com as análises de LAUP no TNT;

Ao Dr. Santiago Catalano, Dr. José L. O. Birindelli, Dra. Fernanda de Oliveira Martins, Dra. Lenice Souza Shibatta, Dr. Roberto Esser do Reis e Dra. Silvia Helena Sofia, por aceitar prontamente o convite para avaliação do meu trabalho e pelas valiosas considerações acrescentadas ao presente estudo;

Ao Dr. Paulo José dos Reis (Física-UEL), pela microtomografia dos exemplares de *Microglanis nigrolineatus*;

Aos Técnicos do MZUEL Edson e Aparecido, companheiros de coletas, risadas, cervejas (litrão) e amizade;

Aos amigos presentes e que já fizeram parte do MZUEL, Alex Claro, Fernando Assega, Ana Cecília, Nick Tramontina, Raul Henrique Cardoso, Vitor Abrahão, Fabio Mise, Gabriel Costa Silva, China (William Ohara), William Gotto Ruiz, Wanner Galves;

As Faculdades Integradas de Ourinhos (FIO), em especial, à Direção e aos amigos Yvana Britto, Odair Francisco, Anderson Garcia e Artur Rondina por todo apoio e amizade;

Aos amigos da UEL: Dr. Mário Orsi, Marcelo Yabu, Alexandro Costa, Ana Vidotto, Diego Garcia, Gean Leme, Camila Ribeiro, Armando Casimiro, Zé (Anderson Kikuchi), Tatiane Debiasi, Carol Brefari Batista, Guilherme Figueiredo, Wilson Frantine, Gabriela de

Oliveira, Gisele Porto, pela amizade, café, cervejas compartilhadas durante esses anos e almoços no RU;

Ao Programa de Pós-Graduação em Ciências Biológicas da Universidade Estadual de Londrina. Ao Dr. José Pimenta, Dr. Edmilson Bianchini, Dr. Luis dos Anjos, Dr. Oscar Akio Shibatta, Dr. José Birindelli, Dr. Fernando Jerep e a Secretária Rosana de Paula, por todo suporte obtido durante o Doutorado;

À Universidade Estadual de Londrina, pela minha formação profissional e parte de minha formação pessoal.

Muito obrigado!

“Ninguém é tão grande que não possa aprender,

nem tão pequeno que não possa ensinar. ”

Esopo

JARDULI, Lucas Ribeiro. **Dados de landmark:** uma nova luz na filogenia de Pseudopimelodidae (Teleostei: Siluriformes). 2017. 127 f. Tese (Doutorado em Ciências Biológicas) – Universidade Estadual de Londrina, Londrina, 2017.

RESUMO

A sistemática de Pseudopimelodidae, Fernández-Yépez & Antón, 1966 passou por análises e revisões acerca de sua posição filogenética e também de seus agrupamentos internos até o reconhecimento do monofiletismo e nível taxonômico atual. As filogenias produzidas até o momento para Pseudopimelodidae são baseadas em caracteres morfológicos e moleculares. Com o avanço de novas técnicas para o uso da morfometria geométrica em sistemática, implementações no programa TNT permitiram incorporar dados quantitativos diretamente em análises cladísticas. Isso possibilita traduzir os dados obtidos da morfometria geométrica em caracteres filogenéticos capazes de refletir homologias na forma das espécies. Afim de encontrar caracteres morfométricos para a família Pseudopimelodidae testamos o LAUP (Análise de Landmark sob Parcimônia) que estabelece estados ancestrais para um caráter que muda em duas ou três dimensões, escolhendo para cada ponto ancestral as posições que minimizam o deslocamento de um marco ao longo de todos os landmarks ancestrais/descendentes. Assim, as posições semelhantes de landmark em diferentes táxons podem ser explicadas por ancestralidade comum. A análise foi baseada em dados de morfologia externa, utilizando quatorze caracteres discretos e três configurações que representam diferentes estruturas. Trinta e oito marcos biologicamente homólogos foram selecionados para cada espécie. Foram testados diferentes alinhamentos e seus efeitos na melhoria da pontuação na árvore e das configurações de landmarks. Nossos dados mostram que a filogenia de Pseudopimelodidae baseada somente em configurações de landmark da morfologia externa não são informativas quando tratadas de forma independente, mas fornecem informações relevantes quando combinadas com dados discretos. Com base na morfologia externa, mostramos que os caracteres de morfometria geométrica podem ser adicionados em análises filogenéticas e fornecem evidências que somadas a outras fontes de caracteres trazem uma nova luz na filogenia de Pseudopimelodidade, como a compreensão da evolução morfológica da família. Esta foi a primeira hipótese filogenética produzida usando LAUP na sistemática de peixes de água doce neotropicais. Além deste estudo, descrevemos uma nova espécie de *Microglanis*, publicada recentemente na revista Ichthyological Exploration of Freshwaters, Volume 27, Número 3, páginas 193-202 (Apêndice 4). *Microglanis nigrolineatus*, é descrita de riachos da bacia do rio Bermejo, Argentina e se distingue de congêneres por possuir um padrão único de coloração: uma linha escura fina que se estende longitudinalmente através do meio do corpo e região dorsal da cabeça uniformemente escura sem áreas claras na região da nuca. Apesar dos estudos realizados por diversos autores, à medida que novas espécies vão sendo descobertas e novos táxons vão sendo adicionados à família, novas análises de relações filogenéticas são necessárias para compreender melhor a posição da família com relação as mais próximas, além das relações entre seus gêneros e espécies. Nesse sentido, os caracteres extraídos com esse novo método foram úteis para melhor compreensão da evolução morfológica dos Pseudopimedodidae.

Palavras-chave: Sistemática. Bagres. Morfometria geométrica. *Microglanis*. Nova espécie.

JARDULI, Lucas Ribeiro. **Landmark data:** a new light on the phylogeny of the Pseudopimelodidae (Teleostei: Siluriformes) 2017. 127 p. Thesis (Doctorate in Biological Sciences) – Universidade Estadual de Londrina, Londrina, 2017.

ABSTRACT

The systematics of Pseudopimelodidae Fernández-Yépez & Antón, 1966 has been target by a series of analyses and reviews concerning its phylogenetic position and the relationship of its internal groupings until reaching the current monophyletic and taxonomic status. The phylogenies produced so far, for Pseudopimelodidae, are based on traditional morphology and molecular characters. With the advancement of new techniques for the use of geometric morphometry in systematics, implementations in the TNT program allow the incorporation of quantitative data directly into cladistic analysis. This allows to translate the data obtained from geometric morphometry into phylogenetic characters capable of reflecting homologies in the form of species. To find morphometric characters for the Pseudopimelodidae we have tested LAUP (Landmark Analysis under Parsimony) that establishes ancestral states for a character that changes in two or three dimensions, choosing for each ancestral point the positions that minimize the displacement of landmarks along all ancestral/descendant. That is, the similar landmark positions in different taxa can be explained by common ancestry. The analysis was based on external morphology data, using fourteen discrete characters and three configurations representing different structures. Thirty-eight biologically homologous landmarks were selected for each species. Different alignments and their effects on the improvement of tree punctuation and landmarks configurations were tested. Our data show that the phylogeny of Pseudopimelodidae based only on landmark configurations of external morphology are not informative when treated independently but provide useful information when combined with discrete data. In this sense, landmark data helps support the branches with the new synapomorphies obtained for the family. Morphometric analysis using the body shape as a character, revealed changes of states in the landmarks characters that can be interpreted as synapomorphies and homoplasies. Based on the external morphology, we show that geometric morphometry can be added in phylogenetic analyses and provide evidence that when added to other sources of characters bring a new light in the phylogeny of Pseudopimelodidae, as the understanding of the morphological evolution of the family. This was the first phylogenetic hypothesis produced using LAUP in the systematics of neotropical freshwater fish. In addition to this study, we described a new species of *Microglanis*, recently published in the journal Ichthyological Exploration of Freshwaters, Volume 27, Number 3, pp. 193-202 (Appendix 4). *Microglanis nigrolineatus* is described from streams of the Bermejo River basin, Argentina and is distinguished from congeners by having a single-color pattern: a thin dark line that extends longitudinally through the middle of the body and dorsal region of the uniformly dark head without light areas on nuchal region. Despite the studies carried out by several authors, as new species are discovered and new taxa are added to the family, new analyzes of phylogenetic relationships are necessary to better understand the the position of the family with the closest ones, besides the relations between their genera and species. In this sense, the characters extracted with this new method were useful for a better understanding of the morphological evolution of the Pseudopimedodidae.

Keywords: Systematic. Catfish. Geometric morphometry. *Microglanis*, New species.

LISTA DE FIGURAS

INTRODUÇÃO GERAL

Landmark data: a new light on the phylogeny of the Pseudopimelodidae (Teleostei: Siluriformes)

LISTA DE TABELAS

SUMÁRIO

INTRODUÇÃO GERAL

A Morfometria Geométrica

A morfometria é o estudo da variação e covariação da forma biológica (Bookstein, 1997; Dryden, Mardia, 1998; Adams *et al.*, 2004), e conta com um conjunto de ferramentas importantes para a descrição e análises estatísticas da forma de um organismo (Rohlf, Marcus, 1993). Atualmente, existem duas abordagens disponíveis para estudos morfométricos: a morfometria tradicional, na qual a variação da forma é estudada por meio da variação entre pares de medidas lineares entre pontos de tangência ou extremos de estruturas (Cooper, 2000; Gumiel *et al.,* 2003; Mutanen, Pretorius, 2007), e a segunda abordagem que surgiu a partir do início dos anos 90 (Rohlf, Marcus, 1993) chamada de morfometria geométrica, abrange uma série de técnicas que visam descrever e representar a geometria das formas estudadas. Enquanto nas abordagens tradicionais a variação da forma evidencia que existem diferenças por vezes significativas, não é possível obter uma representação gráfica da localização destas diferenças que são deduzidas das análises das matrizes geradas pelos métodos multivariados. A morfometria geométrica é capaz de descrever e localizar mais claramente as regiões de mudanças na forma e, sobretudo, de construir e reconstituir graficamente essas diferenças. Essa descrição pode ser feita por meio do estabelecimento de pontos anatômicos de referência em estruturas homólogas (Rohlf, Marcus, 1993; Adams *et al.*, 2004). Os pontos de referência (*i.e.* landmarks) são locais anatômicos homólogos que podem ser reconhecidos como os mesmos em todos os espécimes em estudo (Zelditch *et al.*, 2004). Cada ponto de referência é expresso como um conjunto de duas posições de coordenadas (por exemplo, X e Y) ou tridimensional (por exemplo, X, Y e Z). O conjunto completo de marcos escolhidos para um objeto descreve sua forma com o objetivo de análise morfométrica (*i.e.* configurações).

Um dos primeiros passos da análise baseada em landmark é a eliminação do efeito do tamanho (Fig. 1), padronizando todas as configurações para uma mesma medida geral de tamanho. Assim, as diferenças observadas podem ser mais claramente atribuídas à forma. Além de eliminar o efeito de tamanho, os métodos de sobreposição alinham duas configurações de landmark (filtragem de diferenças devido à rotação e translação).

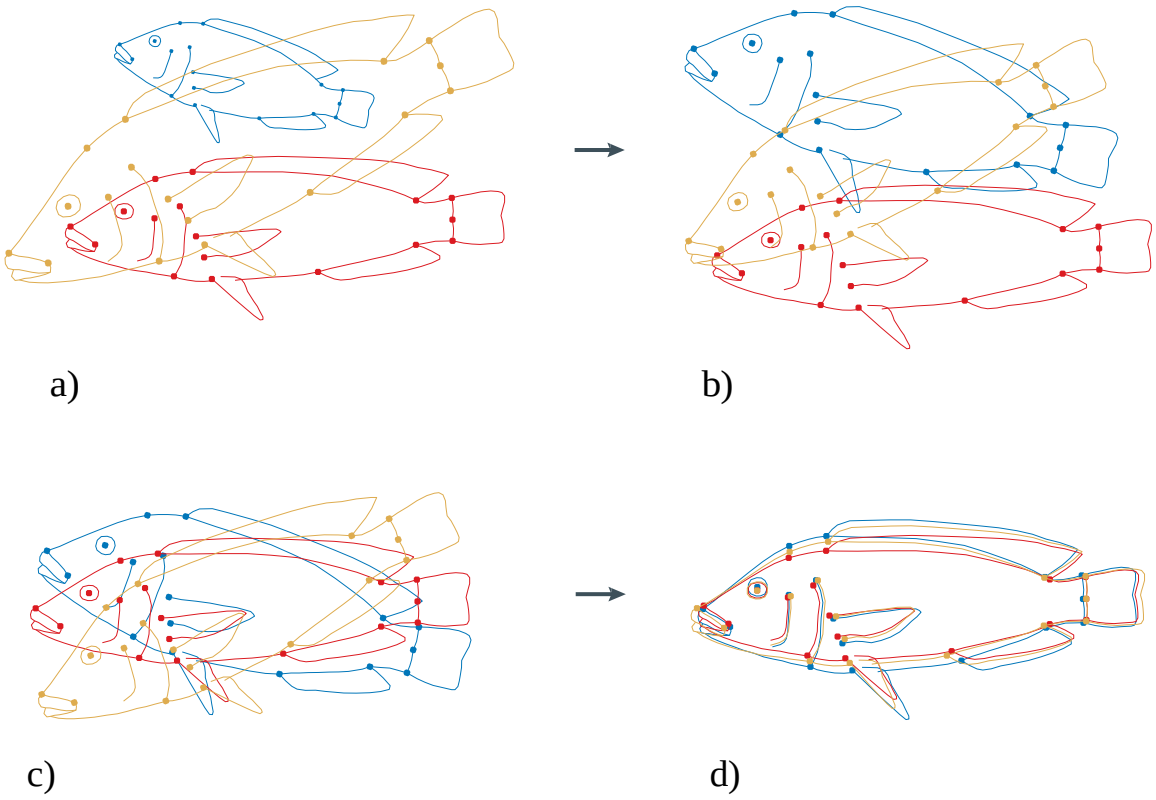

Figura 1. Etapas do processo de sobreposição de Procrustes (GPA): a) Configurações originais; b) Eliminação do efeito de tamanho; c) Translação para o mesmo local; d) Rotação para o ajuste ótimo. Fonte: Klingenberg (2010).

As diferenças de forma são determinadas a partir das mudanças na posição relativa de cada marco individual (Rohlf, Slice, 1990; Rohlf, Marcus, 1993; Slice, 1996; Rohlf, 1999; Adams *et al.*, 2004). A análise de GPA (Generalized Procrustes Analysis) faz a sobreposição de vários exemplares a uma dada configuração referência (Fig. 1). Os parâmetros de sobreposição são escolhidos de maneira a minimizar a soma de quadrados de distâncias entre

pontos de cada configuração e os pontos correspondentes à referência. A referência é a configuração de landmarks na qual os dados são sobrepostos. A referência pode ser qualquer exemplar da amostra ou a configuração média (consensus) da amostra (Chapman, 1990; Rohlf, Slice, 1990).

De acordo com Adams *et al.* (2004), essa nova abordagem levou Rohlf, Marcus (1993) a proclamar uma revolução na morfometria, e as estruturas de origem biológica que podem ser analisadas com técnicas de morfometria geométrica são quase infinitas. Nas últimas décadas, principalmente após a revolução morfométrica, muitos trabalhos vêm sendo publicados em diferentes áreas de interesse da biologia. Estes estudos de quantificação da forma dos organismos podem ser relacionados à ontogenia, variação geográfica intraespecífica, taxonomia, evolução de caracteres morfológicos, dimorfismo sexual, ecomorfologia, questões funcionais e biomecânicas das formas biológicas (Marcus *et al.,* 1996; Zelditch *et al.,* 2004). Além de todas essas áreas, atualmente os métodos morfométricos também podem ser utilizados como uma ferramenta para procurar caracteres convencionais que podem ser usados, juntamente com outras fontes de caracteres; ou até mesmo como única fonte de dados para se inferir hipóteses filogenéticas (Catalano, Torres, 2017).

A Morfometria Geométrica em estudos de Sistemática.

Com os avanços da morfometria geométrica, surgiram interesses na utilização desse método para resolver problemas em sistemática filogenética. As variáveis geométricas referentes à morfometria fornecem a quantificação da forma biológica que pode ser representada pela geometria das configurações de marcos anatômicos. Como tal, MacLeod (2002) considera natural que tais variáveis possam ser usadas para estimar árvores filogenéticas. Com isso, iniciou-se ao longo dos anos um debate sobre a legitimidade do uso de ferramentas morfométricas na obtenção de dados para a reconstrução filogenética (Roth, Mercer, 2000). É

verdade que os sistematas raramente usaram caracteres dessa natureza na prática, mas isso é devido mais à falta de implementação, do que a qualquer impossibilidade ou incompatibilidade teórica (Catalano, Goloboff, 2010). Desde então, vários artigos têm concentrado esforços na elaboração de novas técnicas para o uso da morfometria geométrica em sistemática (Zelditch *et al.*, 1995; Rohlf, 2002; Lockwood *et al.*, 2004; Cardini, Elton, 2007; González-José *et al.*, 2008; Catalano *et al.* 2010; Klingenberg, Gidaszewski, 2010; Catalano, Goloboff, 2012).

De acordo com Rohlf (2002), para estimar as formas correspondentes aos nós internos de uma árvore (as unidades taxonômicas hipotéticas, HTUs), é importante que os métodos produzam estimativas de forma que são invariantes aos efeitos da orientação dos espécimes ou às rotações do espaço tangente (Rohlf, 2000). Zelditch *et al.*, (1992), Zelditch *et al.* (1993) e Zelditch *et al.* (1995) utilizaram deformações parciais (*partial warps*) para encontrar variáveis que poderiam ser utilizadas em análises cladísticas. Para isto, são utilizadas regressões das deformações parciais para obter caracteres discretos. Adams, Rosenberg (1998) e Rohlf (1998) discutem alguns problemas com essa abordagem. Um dos pontos relevantes é que, ao reduzir as variáveis de forma contínua em estados discretos, perde-se a capacidade de visualizar mudanças de forma ao longo de um clado estimado e de estimar trajetórias evolutivas no espaço da forma. Outra questão técnica é que enquanto as *partial warps* são invariantes a orientação dos espécimes, as pontuações (*scores*) das *partial warps* são influenciadas pela orientação da referência. Há poucas razões para esperar que as coordenadas individuais do espaço tangente correspondam às variáveis taxonomicamente mais úteis ou biologicamente mais significativas individualmente, uma vez que são definidas *a priori* e não levam em consideração quaisquer padrões de covariação nos dados. Parece provável que as visualizações dos resultados de técnicas multivariadas, como análise de componentes principais (PCA, González-José *et al.*, 2008, Adams, Otarola-Castillo, 2013; Polly *et al,* 2013), análise de variáveis canônicas (CVA), ou regressão múltipla multivariada, possam ser utilizadas na descoberta de caracteres úteis. Para

maximizar a chance de encontrar recursos úteis, é desejável usar técnicas multivariadas que pesquisem completamente o espaço de forma multivariada (incluindo todas as rotações possíveis) e não limitam a estudar a variação ao longo de um único conjunto de eixos (Rohlf, 1998). González-José *et al.* (2008) propuseram reduzir os dados da forma de regiões anatômicas para um conjunto de variáveis com base nos principais eixos (PCA que explica pelo menos 75% da variação no espaço de forma dentro de cada região). Posteriormente, as pontuações classificadas em cada eixo de componente principal para cada espécie foram usadas para gerar um conjunto de estados de caracteres ordenados para uso em uma análise de parcimônia (Goloboff *et al.*, 2008). Como as tentativas anteriores de forçar variáveis de forma multivariada em uma forma compatível em análises cladísticas (Fink, Zelditch, 1995; Zelditch *et al.*, 1995), o método distorce a informação presente em tais variáveis e isso limita severamente as conclusões biológicas que podem ser extraídas. Usando métodos de morfometria geométrica, sabemos que a forma de cada espécie pode ser representada no espaço multivariado com base nas coordenadas alinhadas de análise generalizada de Procrustes (GPA) (Rohlf, 1999). Dessa forma, as diferenças de formas são descritas pela distância euclidiana entre espécies em um espaço tangente. A análise de PCA simplesmente gira esse espaço e, portanto, as distâncias são preservadas e nenhuma informação é perdida se todos os escores dos componentes principais forem usados. No entanto, a classificação separada dos objetos ao longo dos eixos individuais não preserva as distâncias entre os objetos e os estados de caracteres gerados a partir de eixos individuais mudará de maneira complexa se os eixos forem alternados de maneira diferente (Adams, Rosenberg, 1998; Rohlf, 1998; Monteiro, 2000, Adams *et al.* 2011), o que resultaria em um conjunto diferente de estados de caracteres ordenados para cada táxon (Fig. 2).

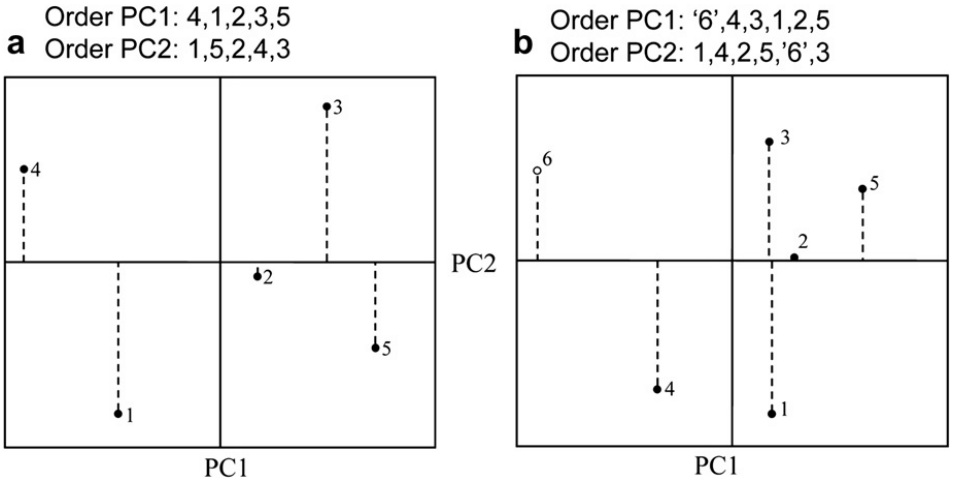

Figura 2. (a) Cinco espécies hipotéticas visualizadas ao longo de seus dois eixos de componentes principais. (b) Os mesmos dados com uma sexta espécie incluída. Observe que a ordem de classificação das espécies originais ao longo de ambos os eixos é alterada quando outro taxon é adicionado. Assim, diferentes estimativas de estados de caracteres (portanto, filogenia) seriam obtidas a partir de uma análise de parcimônia cladística. Fonte: Adams *et al*. (2011).

Klingenberg, Gidaszewski (2010) também afirmam que dados morfométricos são comumente considerados como fontes pobres ou pouco confiáveis para avaliação de relações filogenéticas. Apesar disso, há uma ampla defesa do tratamento de dados contínuos e, por conseguinte, estudo de formas bi ou tridimensionais por autores na última década (Goloboff *et al.*, 2006; Catalano *et al.*, 2010; Goloboff & Catalano, 2011; Catalano, Goloboff, 2012) e que estes podem ser significativamente congruentes com hipóteses filogenéticas robustas. Eles afirmam ainda, que os métodos de sobreposição existentes para alinhar os pontos de landmarks (encontrar o melhor ajuste para os dados através da rotação, translação e tamanho) são satisfatórios para comparar diferenças morfológicas, mas insuficientes para avaliar mudanças de formas ao longo de uma filogenia porque a mudança de forma é determinada a partir de mudanças na posição relativa de cada marco individual.

Análise de landmark sob parcimônia (LAUP).

Novas ferramentas para as análises filogenéticas como o programa TNT (*Tree Analysis Using New Technology*) permitiram usar caracteres contínuos, possibilitando traduzir os dados obtidos tanto da morfometria tradicional como da morfometria geométrica em caracteres filogenéticos capazes de refletir a forma das espécies (Goloboff *et al.*, 2006). Esses avanços teóricos permitem incorporar dados quantitativos, diretamente em estudos cladísticos (Goloboff *et al.*, 2006; Catalano *et al.*, 2010; Goloboff. Catalano, 2011; Catalano, Goloboff, 2012). Nesses casos, os caracteres utilizados não necessitam ser discretizados *a priori*, pois intervalos de medidas são analisados filogeneticamente com o emprego da otimização de Farris (1970). Os dados obtidos após a sobreposição de marcos anatômicos homólogos (landmarks) são analisados segundo um critério de minimização de custos justificável no contexto da parcimônia (Goloboff *et al.*, 2006; Catalano, Goloboff, 2012).

Catalano *et al.* (2010) implementaram um método que estabelece estados ancestrais para um caráter que muda em duas ou três dimensões (em espécimes que já estão alinhados). Esta abordagem usa uma extensão 3D da otimização de Farris, ou otimização espacial (Goloboff *et al.*, 2006), escolhendo para cada ponto ancestral as posições que minimizam o deslocamento deste marco ao longo de todos os pares ancestrais/descendentes (Fig. 3), ou seja, as posições semelhantes de landmark em diferentes táxons podem ser explicadas por ancestralidade comum.

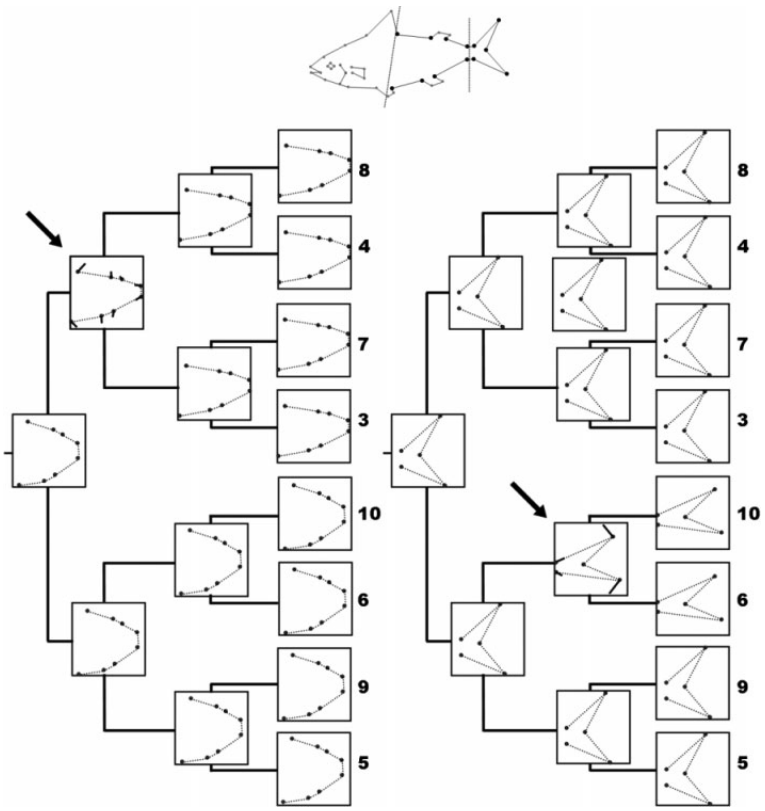

Figura 3. Configurações de landmarks ancestrais obtidas utilizando a otimização espacial para dois caracteres derivados de Naylor (1996) e MacLeod (2002). As setas indicam os nós das árvores com um deslocamento de landmark em relação ao estado ancestral, ou seja, sinapomorfias. Fonte: (Catalano et al, 2010).

Assim, a diferença de posição para cada landmark em cada ramo é calculada como a distância euclidiana entre a posição do landmark ancestral e a posição do landmark descendente. A pontuação total para cada landmark é obtida ao resumir essas distâncias em todos os nós. Finalmente, a pontuação para toda a configuração na árvore é obtida somando as pontuações em todos os landmarks. A escolha da métrica euclidiana para calcular a pontuação de cada landmark não é arbitrária: foi escolhida porque ela permite ampliar o critério de parcimônia para a análise de caracteres contínuos que mudam em mais de uma dimensão (Goloboff *et al.*, 2006, Catalano *et al.*, 2010). Dado que a pontuação da árvore para uma determinada configuração é calculada, resumindo a contribuição de cada landmark, a métrica correspondente para a pontuação da árvore é uma distância semelhante à distância de Manhattan. Essa

combinação de uma distância euclidiana para avaliar as mudanças entre configurações na posição de cada landmark e uma métrica de Manhattan para calcular a pontuação total, resumindo a contribuição de cada landmark, tem como conseqüência que nem a pontuação da árvore nem as inferências da mudança de forma são afetadas pela orientação original dos espécimes (Catalano *et al.*, 2010).

Como dito anteriormente, uma das principais preocupações sobre o uso de dados de landmarks em análises cladistas (Rohlf, 1998; Monteiro, 2000; Klingenberg, Monteiro, 2005) é sua multidimensionalidade. A otimização espacial proposta por Catalano *et al.* (2010) difere radicalmente dos métodos anteriores, na medida em que mantém a individualidade original dos landmarks ao longo da análise. Outras abordagens (por exemplo, as baseadas em *partial warps*, Rohlf, 2002, ou os resultados da análise de componentes principais, González-José *et al.*, 2008, Adams, Otarola-Castillo, 2013; Polly *et al*, 2013) usam as configurações de landmarks "projetadas" ao longo de diferentes eixos de um espaço multidimensional, representando efetivamente todos os pontos de referência em uma configuração por um único ponto em um espaço multidimensional (Fig. 2). O que é usado para a análise cladística são então "caracteres" que representam os valores das projeções deste ponto ao longo de diferentes eixos desse espaço multidimensional. Portanto, quando essa abordagem minimiza mudanças ao longo de cada eixo de projeção, consequentemente os valores ancestrais obtidos para os landmarks não têm qualquer significado em termos de parcimônia (Catalano *et al.*, 2010).

Os algoritmos para a otimização de landmarks sob parcimônia são descritos em (Goloboff. Catalano, 2011) e o método é baseado em uma primeira aproximação heurística usando grades (Fig. 4) com um refinamento posterior interativo dos pontos iniciais estimados (Goloboff, 1998). Esse refinamento é uma segunda abordagem que pode ser usada em combinação com a anterior, usando grades dentro de uma célula da grade (*nested grids*). Se os

pontos para cada nó foram colocados em posições subótimas, porque a grade era muito grosseira, usando uma grade menor (Fig. 4), centrada na melhor posição para cada nó calculado no passo anterior, e usando uma janela de algumas células, permitirá determinar a localização de cada ponto com muito mais precisão, mas sem aumentar o número total de pontos da grade.

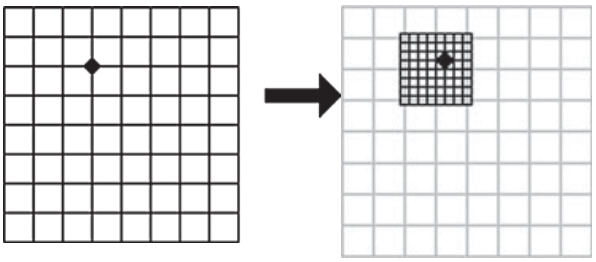

Figura 4. Exemplo que ilustra o uso de *nested grids* (com uma janela de 2x2 células), para melhorar a precisão da estimativa inicial. Fonte: Goloboff, Catalano (2011).

Esses algoritmos foram implementados no programa TNT (Goloboff *et al.*, 2003, 2008), e permitem "mapear" o caráter para obter ancestrais de maneira mais parcimoniosa e atribuir uma pontuação à árvore, que pode ser usada para selecionar a árvore que melhor representa as posições dos landmarks observados (Goloboff, Catalano, 2011).

Catalano, Goloboff (2012) apresentaram um método como uma extensão da abordagem proposta por Catalano *et al.* (2010) que combina as duas etapas, mapeamento e alinhamento, em um único procedimento que (para a árvore dada) produz um alinhamento múltiplo e atribui estados ancestrais, de modo que a soma das distâncias euclidianas entre os pontos de referência correspondentes ao longo dos nós de árvore é minimizado.

No método de Catalano *et al.* (2010), a otimização de caracteres considera uma sobreposição *a priori* que permanece não modificada durante o procedimento de mapeamento (alinhamento estático). No entanto, a pontuação da árvore pode ser melhorada, maximizando concomitantemente a quantidade de semelhança em posições de referência que podem ser explicadas por ancestralidade comum, se a sobreposição entre as configurações for modificada durante o procedimento de mapeamento. O método denominado “alinhamento dinâmico”

(Catalano, Goloboff, 2012) realiza uma sobreposição múltipla de configurações de landmarks usando parcimônia como critério de otimização. “Ciclos de perturbação” fazem com que as posições das configurações sejam randomizadas (heuristicamente) de tal forma que a estrutura da árvore é levada em consideração: as posições de todas as configurações pertencentes a um clado são modificadas aleatoriamente, e em cada ciclo de aleatorização, um certo número de clados são escolhidos aleatoriamente para serem modificados. Se um nó interno for escolhido, as configurações de todos os terminais pertencentes a esse nó são modificadas (Catalano, Goloboff, 2012). Embora essa abordagem não garanta atingir um ótimo global, a longo prazo aumenta consideravelmente as chances de fazê-lo.

Recentemente, Goloboff, Catalano (2016) implementaram as funcionalidades completas para buscas de árvores com landmarks na versão 1.5 do programa TNT, que integra completamente os dados de landmark em análises filogenéticas e possui comandos e opções (como os aplicados a outros tipos de dados) que podem ser usados através da interface do programa, onde as pesquisas filogenéticas podem ser executadas sem a necessidade de scripts, facilitando a utilização da morfometria geométrica em estudos de sistemática.

Sistemática da família Pseudopimelodidae

Pseudopimelodidae Fernández-Yépez & Antón, 1966, se encontra amplamente distribuída na América do Sul e pode ser encontrada desde o norte da Venezuela, no oeste dos Andes, até o Uruguai (Shibatta, 2003). É uma família monofilética (Shibatta, Vari, 2017) que atualmente possui 48 espécies válidas e sete gêneros e (*Batrochoglanis* Gill, 1858; *Cephalosilurus* Haseman, 1911; *Cruciglanis* Ortega-Lara & Lehmann, 2006; *Lophiosilurus* Steindachner, 1889; *Microglanis* Eigenmann, 1912; *Pseudopimelodus* Bleeker, 1858; *Rhyacoglanis* Shibatta & Vari, 2017). A monofilia da família Pseudopimelodidae foi proposta por Lundberg (1991) com as sinapomorfias: (1) etmóide lateral se projetando além do côndilo

do palatino; (2) metapterigóide muito curto, curvado dorsalmente em direção à parte interna e, geralmente, apoiado por uma crista; (3) endopterigóide e ectopterigóide largos, com formas distintas (sendo que o primeiro, no processo ântero-lateral, tem uma ponta afilada e no segundo tem forma de vírgula) e são fortemente ligados ao neurocrânio entre as suturas do etmóide lateral e orbitosfenóide no autopalatino; (4) terceiro ao sétimo radiais proximais da nadadeira dorsal em contato ao longo de sua extensão (nos grandes pseudopimelodídeos) ou mais separados (*Microglanis*); (5) ausência do osso hipohial dorsal. Além de caracteres osteológicos os membros da família Pseudopimelodidae podem ser identificados por possuírem boca larga, barbilhões curtos e olhos pequenos e sem margem orbital livre (Shibatta, 2003).

Anteriormente, espécies da família Pseudopimelodidae eram incluídas na família Pimelodidae. Posteriormente, foram incluídas em uma subfamília denominada Pseudopimelodinae por Lundberg *et al.*, (1991), que incluia os gêneros: *Cephalosilurus*, *Lophiosilurus*, *Pseudopimelodus*, *Microglanis*, *Zungaro* e, possivelmente, *Zungaropsis*. Mees (1974) considerava apenas *Pseudopimelodus*, *Microglanis* e *Lophiosilurus* até então como gêneros válidos. De Pinna (1993, 1998) e Shibatta (1998) levantaram caracteres sinapomórficos que reforçaram a hipótese de monofiletismo do grupo, inserindo o gênero *Batrochoglanis* e excluindo *Zungaro* e *Zungaropsis* (Shibatta, 1998). Ortega-Lara, Lehmann (2006) acrescentam *Cruciglanis*, um gênero monotípico, à família. Recentemente, Shibatta, Vari, (2017) descreveram um gênero novo, *Rhyacoglanis*, somado a descrição de quatro novas espécies.

Lundberg *et al.*, (1988, 1991) e Britto (2003) consideraram Pseudopimelodidae como grupo irmão de Rhamdiinae (= Heptapteridae). Diogo (2004) e Diogo *et al.*, (2004) consideraram Pseudopimelodidae como grupo irmão de um clado que inclui Pimelodidae e Heptapteridae. Outras análises de dados moleculares revelaram que a família Pseudopimelodidae é grupo irmão de Pimelodidae e este clado possui Heptapteridae como grupo irmão, compondo a superfamília Pimelodoidea (Hardman, 2005; Sullivan *et al.*, 2006).

A partir da análise da morfologia da bexiga natatória Birindelli, Shibatta (2011) encontraram uma sinapomorfia compartilhada exclusivamente por algumas espécies de Pimelodidae e Pseudopimelodidae, que não é encontrada nas espécies de Heptapteridae.

Os estudos das relações dentro da família se iniciaram com o trabalho de Shibatta (1998) que estabelece sinapomorfias e agrupa *Lophiosilurus* e *Cephalosilurus* em um clado. Segundo Shibatta (1998) *Pseudopimelodus* é grupo-irmão de todos os outros pseudopimelodídeos. Ortega-Lara e Lehmann (2006) propuseram uma nova hipótese, na qual o clado composto por *Cephalosilurus* e *Lophiosilurus* se manteve como grupo irmão do restante dos pseudopimelodídeos, um clado composto por *Pseudopimelodus*, *Cruciglanis* e *Batrochoglanis*, sendo este o grupo irmão de *Microglanis*. Shibatta, Vari (2017) separam a família em dois grandes clados: o primeiro composto por *Lophiosilurus*, *Cephalosilurus*, *Microglanis* e *Batrochoglanis*. O segundo composto por *Cruciglanis*, *Pseudopimelodus* e *Rhyacoglanis*. As relações internas são: *Lophiosilurus* grupo irmão de *Cephalosilurus*, *Microglanis* grupo irmão de *Batrochoglanis*, *Cruciglanis* grupo irmão de *Pseudopimelodus* e este clado grupo irmão de *Rhyacoglanis*. Apesar dos estudos realizados (Lundberg *et al.*, 1991; Shibatta, 1998, 2003; Ortega-Lara e Lehman, 2006; Birindelli e Shibatta, 2011, Shibatta, Vari, 2017), a adição de novos caracteres extraídos de diferentes métodos, serão mais um passo na busca pela organização e maior compreensão sistemática da família Pseudopimedodidae.

A cada ano são adciomadas novas espécies à família, como *M. nigrolineatus* descrita no Apêndice 4 deste trabalho. O gênero possui atualmente 29 espécies válidas (Shibatta, 2014; Terán *et al.* 2016), sendo encontrado a oeste dos Andes, no Peru, e nas bacias hidrográficas da região cisandina, desde a Venezuela até a bacia do rio da Prata, inclusive pelas drenagens costeiras do Brasil (Shibatta, 2003). Devido a sua ampla distribuição geográfica, algumas espécies de *Microglanis* ocorrem em simpatria com seus congêneres, o que ocasiona em alguns casos, confusões taxonômicas (Souza-Shibatta, 2015), indicando que novos estudos deverão ser

feitos para aumentar a compreensão sobre a sistemática do grupo. Dessa forma, a medida que novos táxons forem adicionados à família, novas análises de relações filogenéticas serão necessárias para aumentar o conhecimento acerca das relações de Pseudopimelodidae com outras famílias, além das relações entre seus gêneros e espécies.

REFERÊNCIAS

Adams DC, Cardini A, Monteiro LR, O'Higgins P, Rohlf FJ. Morphometrics and phylogenetics: principal components of shape from cranial modules are neither appropriate nor effective cladistic characters. J. Hum. Evol. 2011; 60(2): 240-243.

Adams DC, Otarola-Castillo E. Geomorph: An R package for the collection and analysis of geometric morphometric shape data. Methods Ecol. Evol. 2013; 4: 393–399.

Adams DC, Rohlf FJ, Slice DE. Geometric morphometrics: ten years of progress following the ‘‘revolution’’. Ital. J. Zool. 2004; 71: 5–16.

Adams DC, Rosenberg M. S. Partial warps, phylogeny, and ontogeny: A comment on Fink and Zelditch (1995). Syst. Biol. 1998; 46: 168-173.

Birindelli JLO, Shibatta OA. Morphology of the gas bladder in bumblebee catfishes (Siluriformes, Pseudopimelodidae). J Morphol. 2011; 272:890-896.

Bookstein FL. Morphometric tools for landmark data. Geometry and biology. Cambridge Univ. Press, New York. 1997.

Cardini A, Elton S. Does the skull carry a phylogenetic signal? Evolution and modularity in the guenons. Biol. J. Linn. Soc**.** 2007; 93: 813–83.

Catalano SA, Goloboff PA, Giannini NP. Phylogenetic morphometrics (I): the use of landmark data in a phylogenetic framework. Cladistics. 2010; 26: 539–549.

Catalano SA, Goloboff PA. Simultaneously mapping and superimposing landmark configurations with parsimony as optimality criterion. Syst. Biol. 2012; 61: 392-400.

Catalano SA, Torres A. Phylogenetic inference based on landmark data in 41 empirical datasets. Zool Scripta. 2017; 46: 1-11.

Chapman RE. Conventional Procrustes methods. In: Rohlf FJ, Bookstein FL, editors. Proceedings of the Michigan Morphometrics Workshop. University of Michigan, Museum of Zoology.1990; 251–267.

Cooper M. Five new species of *Agelaia lepeletier* (Hym, Vespidae, Polistinae) with a key to members of genus. New synonymy and notes. Entomol. Mon. Mag. 2000; 136:177-198.

de Pinna MCC. Higher-level phylogeny of Siluriformes (Teleostei: Ostariophysi), with a new classification of the order. [Phd Dissertação] City University of New York, New York. 1993; 482 p.

de Pinna MCC. Phylogenetic relationships of Neotropical Siluriformes (Teleostei: Ostariophysi): historical overview and synthesis of hypotheses. In: Malabarba LR, Reis RE, Vari RP, Lucena ZMS, Lucena CAS. Editors. Phylogeny and Classification of Neotropical Fishes. Porto Alegre, Edipucrs. 1998; 279–330 pp.

Diogo R. Osteology and myology of the cephalic region and pectoral girdle of *Heptapterus mustelinus*, comparison with other Heptapterins, and discussion on the synapomorphies and phylogenetic relationships of the Heptapterinae and the Pimelodidae (Teleostei: Siluriformes). Int J Morphol. 2007; 25:735-748.

Diogo R, Chardon M, Vandewalle P. Osteology and myology of the cephalic region and pectoral girdle of *Batrochoglanis raninus*, with a discussion on the synapomorphies and phylogenetic relationships of the Pseudopimelodinae and Pimelodidae (Teleostei: Siluriformes). Anim Biol. 2004; 54:261-280.

Dryden IL, Mardia KV. Statistical shape analysis. John Wiley & Sons. New York. 1998.

Farris J. Methods for computing wagner trees. Syst. Zool. 1970; 19: 83–92.

Goloboff PA. Tree searches under Sankoff parsimony. Cladistics. 1998; 14: 229–237.

Goloboff PA, Farris JS, Nixon KC. TNT, a free program for phylogenetic analysis. Cladistics. 2008; 24: 774-786.

Goloboff PA, Catalano SA. Phylogenetic morphometrics (II): algorithms for landmark optimization. Cladistics. 2011; 27: 42–51.

Goloboff PA, Catalano SA. TNT version 1.5, including a full implementation of phylogenetic morphometrics. Cladistics. 2016; 32: 221-237.

González-José R, Escapa I, Neves WA, Cúneo R, Pucciarelli HM. Cladistic analysis of continuous modularized traits provides phylogenetic signals in Homo evolution. Nature. 2008; 453(7196), 775.

Gumiel M, Catalã S, Noireau F, Rojas de Arias A, Garcia A, Dujardin J P. Wing. Geometry in *Triatoma infestans* (Klug) y *Triatoma melanosoma* Martínez, Olmedo & Carcavallo (Hemiptera: Reduvidae). Syst. Entomol. 2003; 28: 173-179.

Hardman M. The phylogenetic relationships among nondiplomystid catfishes as inferred from mitochondrial cytochrome *b* sequences; the search for the ictalurid sister taxon (Otophysi: Siluriformes). Mol Phylogenet Evol 2005; 37:700–720.

Klingenberg CP. Evolution and development of shape: integrating quantitative approaches. Nat. Rev. Genet. 2010; 11(9): 623-635.

Klingenberg P, Gidaszewski NA. Testing and quantifying phylogenetic signals and homoplasy in morphometric data. Syst. Biol. 2010; 59: 245–261.

Klingenberg CP, Monteiro LR. Distances and directions in multidimensional shape spaces: implications for morphometric applications. Syst. Biol. 2005; 54: 678–688.

Lockwood CA, Kimbel WH, Lynch JM. Morphometrics and hominoid phylogeny: support for a chimpanzee-human clade and differentiation among great ape subspecies. Proc. Natl. Acad. Sci. USA. 2004; 101: 4356–4360.

Lundberg JG, Bornbusch AH, Mago-Leccia F. *Gladioglanis conquistador* N. Sp. from Ecuador with diagnoses of the subfamilies Rhamdiinae Bleeker and Pseudopimelodinae N. Subf. (Siluriformes: Pimelodidae). Copeia. 1991; 1991:190-209.

Lundberg JG, Linares OJ, Antonio ME, Nass P. *Phractocephalus hemioliopterus* (Pimelodidae: Siluriformes) from the upper Miocene Urumaco formation, Venezuela: a further case of evolutionary stasis and local extinction among south American fishes. J. Vert. Paleont. 1988; 8:131-138.

MacLeod N. Phylogenetic signals in morphometric data. In: MacLeod N, Forey PL, editors. Morphology, shape and phylogeny. London: Taylor & Francis. 2002; 100–138.

Marcus LF, Corti M, Loy A, Naylor G, Slice DE, editors. Advances in morphometrics. New York: Plenum. 1996; 519–530.

Mees, GF. The Auchenipteridae and Pimelodidae of Suriname (Pisces, Nematognathi). Zoologische Verhandelingen, 1974; 132: 1-256.

Monteiro L. Why morphometrics is special: the problem with using partial warps as characters for phylogenetic inference. Syst. Biol. 2000; 49:796–800.

Mutanen M, Pretorius E. Subjective visual evaluation vs. traditional and geometric morphometrics in species delimitación: a comparison of moth genitalia. Syst. Entomol. 2007; 32(2): 371-386.

Naylor G. Can partial warp scores be used as cladistic characters? In: Marcus LF, Corti M, Loy A, Naylor G, Slice DE, editors. Advances in morphometrics. New York: Plenum. 1996; 519–530.

Ortega-Lara A, Lehmann P. Cruciglanis, a new genus of pseudopimelodid catfish (Ostariophysi, Siluriformes) with description of a new species from the Colombian Pacific coast. Neotrop Ichthyol. 2006; 4:147-156.

Polly PD, Lawing AM, Fabre AC & Goswami A. Phylogenetic principal components analysis and geometric morphometrics. Hystrix Ital. J. of Mamm. 2013; 24(1): 33-41.

Rohlf FJ. On application of geometric morphometrics to studies of ontogeny and phylogeny. Syst. Biol. 1998; 47:147–158.

Rohlf F.J. Shape statistics: procrustes superimpositions and tangent spaces. J. Classific. 1999; 16: 197–223.

Rohlf FJ. Geometric morphometrics and phylogeny. In: MacLeod N, Forey PL, editors. Morphology, shape, and phylogeny. London: Taylor & Francis. 2002; 175–193.

Rohlf FJ & Marcus LF. A revolution in morphometrics. Trends Ecol. Evol. 1993; 8: 129-132.

Rohlf FJ, Slice D. Extensions of the Procrustes method for the optimal superimposition of landmarks. Syst. Zool. 1990; 39:40–59.

Roth VL & Mercer JM. Morphometrics in Development and Evolution. Am. Zool. 2000; 40: 801–810.

Shibatta OA. Sistemática e evolução da família Pseudopimelodidae (Ostariophysi, Siluriformes), com a revisão taxonômica do gênero Pseudopimelodus. [PhD Thesis]. São Carlos, SP: Universidade Federal de São Carlos; 1998.

Shibatta OA. Family Pseudopimelodidae (Bumblebee catfishes, dwarf marbled catfishes. In: Reis RE, Kullander SO, Ferraris Jr CJ, editors. Check List of the Freshwater Fishes of South and Central America. Porto Alegre: Edipucrs; 2003. p. 401-405.

Shibatta OA, Vari, RP. *Rhyacoglanis*, a new genus of Neotropical rheophilic catfishes, with four new species (Teleostei: Siluriformes Pseudopimelodidae) Neotrop Ichthyol. 2017; 15(2): e160132.

Small C. G. The statistical theory of shape. Springer-Verlag. New York. 1996.

Souza-Shibatta L. Filogeografia de *Microglanis cottoides* (Boulenger, 1891) (Siluriformes: Pseudopimelodidae). Tese (Doutorado em Ciências Biológicas). Universidade Estadual de Londrina. 127p.

Sullivan JP, Lundberg JG, Hardman M. A phylogenetic analysis of the major groups of catfishes (Teleostei: Siluriformes) using rag1 and rag2 nuclear gene sequences. Mol Phylogenet Evol. 2006; 41:635-662.

Terán GE, Jarduli LR, Alonso F, Mirande JM, Shibatta OA. *Microglanis nigrolineatus*, a new species from northwestern Argentina (Ostariophysi: Pseudopimelodidae). Ichthyol. Explor. Freshw. 2016; 27(3): 193-202.

Zelditch ML, Bookstein FL, Lundrigan BL. Ontogeny of integrated skull growth in the cotton rat Sigmodon fulviventer. Evolution. 1992; 46: 1164- 1180.

Zelditch ML, Bookstein FL, Lundrigan BL. The ontogenetic complexity of developmental constraints. J. Evol. Biol. 1993; 6: 121-141.

Zelditch ML, Fink WL, Swiderski D. Morphometrics, homology, and phylogenetics: quantified characters as synapomorphies. Syst. Biol. 1995: 44:179–189.

Zelditch ML, Swiderski DL, Sheets DH, Fink W. Geometrics morphometrics for biologist: A primer. London: Elsevier Academic Press. 2004.

Landmark data: a new light on the phylogeny of the Pseudopimelodidae (Teleostei: Siluriformes)

Abstract

The relationship between morphometric and phylogenetic analysis has been quite controversial and discussed over the years. Regardless, there is a growing effort to use morphometric characters in phylogenetic reconstruction without discretization. In this sense, the use of landmark data in phylogenetic analyses of Neotropical freshwater fish remains largely unexplored. Herein the method of landmark analysis under parsimony (LAUP) was tested in a phylogenetic analysis of Pseudopimelodidae, a monophyletic family of Siluriformes composed of seven genera and 48 species. This analysis seeks for ancestral landmark configurations that minimize point displacements between ancestral and descendant nodes along all branches of the tree, so the similar landmark positions at different taxa can be explained by common ancestry. The analysis was based on external morphology data, using fourteen discrete characters and three configurations representing different structures. Thirty-eight biologically homologous landmarks were selected for each species, producing the first hypothesis of phylogeny using LAUP in the Neotropical freshwater fish systematics. The influence of dynamic and static alignment and its effects on the improvement of the tree score also was tested using matrix combined with discrete and geometric morphometry data. The data confirmed that the alignment method used may influence LAUP results. In addition, landmark settings from external morphology, are unreliable when treated independently, but provide useful information when combined with other data. A symmetric resampling was necessary for the colapse of the over-estimated nodes revealing that the landmark data aid in supporting the branches. The morphometric analysis using body shape as a character, revealed changes in landmarks characters that can be interpreted as synapomorphies and homoplasies. Finally, based on the external morphology, we showed that the geometric morphometry can be added in the phylogenetic analysis, composing a new source of synapomorphies for Pseudopimelodidae family.

Resumo

A relação entre as análises morfométrica e filogenética tem sido bastante controversa e discutida ao longo dos anos. Há um esforço crescente para usar caracteres morfométricos na reconstrução filogenética sem discretizá-los. Nesse sentido, o uso de dados de lardmark em análises filogenéticas de peixes de água doce Neotropicais permanece amplamente inexplorado. Neste trabalho, o método de análise de landmark sob parcimônia (LAUP) foi testado em uma análise filogenética de Pseudopimelodidae, uma família monofilética de siluriformes composta por sete gêneros e 48 espécies. Esta análise busca configurações de landmark ancestrais que minimizam os deslocamentos de pontos entre nós ancestral e descendente ao longo de todos os ramos da árvore, de modo que as posições de landmark similares em diferentes táxons podem ser explicadas por ancestralidade comum. A análise foi feita com base em dados de morfologia externa, utilizando quatorze caracteres discretos e três configurações que representam diferentes estruturas. Trinta e oito landmarks biologicamente homólogos foram selecionados para cada espécie, produzindo a primeira hipótese de filogenia usando LAUP na sistemática de peixes de água doce Neotropicais. A influência do alinhamento dinâmico e estático e seus efeitos na melhoria da pontuação da árvore foram testados usando matriz combinada com dados discretos e de morfometria geométrica. Os dados confirmaram que o método de alinhamento usado pode influenciar os resultados de LAUP. Além disso, as configurações de landmark da morfologia externa, não são confiáveis quando tratadas de forma independente, mas fornecem informações úteis quando combinadas com outros dados. Uma reamostragem simétrica foi necessária para o colapso dos nós superestimados, revelando que os dados de landmark ajudam a suportar os ramos. A análise morfométrica usando a forma do corpo como caráter, revelou mudanças nos caracteres de landmarks que podem ser interpretadas como sinapomorfias e homoplasias. Finalmente, com base na morfologia externa, mostramos que os caracteres de morfometria geométrica podem ser adicionados em análises filogenéticas, constituindo uma nova fonte de sinapomorfias para a família Pseudopimelodidae.

Key words. Catfish, Systematics, Geometric Morphometric, Morphometry

Introduction

Phylogenetic analyses require a matrix of character data and these characters, either morphological or molecular, have traditionally been composed of discrete states in studies on freshwater fishes of the Neotropical region (e.g. Lundberg *et al.*, 1991; Shibatta, 1998; Sullivan *et al.*, 2006; Birindelli, Shibatta, 2011; Sullivan *et al.*, 2013; Shibatta, Vari, 2017). However, new routines are being implemented to use additive characters, such as morphometry data, in computational softwares for phylogenetic analysis using parsimony (Catalano, *et al.* 2010).

Although morphometry is widely explored in taxonomy, only recently it has been used in phylogenetic analyses. However, in most cases, those methods usually ignore valuable information from the shape of the species (Adams *et al.*, 2004; Catalano *et al.*, 2010; Klingenberg, Gidaszewski, 2010; Catalano, Goloboff, 2012). Shape is one of the most important and easily measured elements of phenotype, and expresses the interaction of many, if not most, genes (Ollier *et al.*, 2006; Covain *et al.*, 2008). Although the shape has information on the evolution of a group, there is a discussion of how morphometric characters can be used in the phylogenetic context (Felsenstein, 1988, 2002; Zelditch *et al.*, 1995; Naylor, 1996; Collard, Wood 2000; Monteiro, 2000; Cannon, Manos 2001; Polly, 2001; MacLeod, 2002; Rohlf, 2002; Lockwood *et al.*, 2004; Caumul, Polly, 2005; Lycett, Collard, 2005, Cardini, Elton 2008, Klingenberg, Gidaszewski, 2010).

There is a controversy about the correct way to deal with continuous and landmark characters in phylogenetic frameworks. The definition of what a character represents is not an easy task in phylogenetics, in addition, there is a discussion about the adequation of different phylogenetic methods to analyze this type of data (Smith, 1990; Bookstein, 1994; Zelditch *et al.*, 1995, 1998; Naylor 1996; Adams, Rosenberg 1998; Rohlf, 1998, 2002; Monteiro, 2000; Bookstein, 2002; MacLeod, 2002; Stone, 2003). Despite that, the use of geometric

morphometric data in phylogenies has become increasingly common in empirical studies due to the creation of new approaches for the phylogenetic treatment of landmark data (Rohlf, 2002; Lockwood *et al.*, 2004; Cardini, Elton, 2008; González-José *et al.*, 2008; Catalano *et al.* 2010; Klingenberg, Gidaszewski, 2010; Catalano, Goloboff, 2012). One of this approaches, the LAUP (landmark analysis under parsimony), developed by Catalano *et al.* (2010) and Goloboff, Catalano (2011), provides a rationale use for the morphogeometric data in phylogenetic studies. The approach is equivalent to an analysis using parcimony. This analysis establishes ancestral landmark configurations that minimize point displacements between ancestral and descendant nodes along all branches of the tree, so the similar landmark positions at different taxa can be explained by common ancestry (Catalano *et al.*, 2010).

In order to better understand the addition of geometric morphometry characters in phylogenetic studies, we tested the use of landmarks in a phylogenetic reconstruction of the Pseudopimelodidae Fernández-Yépez & Antón, 1966, a monophyletic family of siluriforms composed of seven genera (*Batrochoglanis* Gill, 1858; *Cephalosilurus* Haseman, 1911; *Cruciglanis* Ortega-Lara & Lehmann, 2006; *Lophiosilurus* Steindachner, 1889; *Microglanis* Eigenmann, 1912; *Pseudopimelodus* Bleeker, 1858 and *Rhyacoglanis* Shibatta & Vari, 2017). Pseudopimelodidae encompasses 48 valid species widely distributed in South America, from northern Venezuela to Uruguay, and also western slope of the Andes (Shibatta, 2003) with a large diversity of forms and sizes (e.g. *Microglanis* spp. and *Lophiosilurus alexandri*) (Ferraris, 2007; Jarduli, Shibatta, 2013; Shibatta, Vari, 2017).

Pseudopimelodids are rare and many species have been described with few individuals (e.g. Shibatta, Pavanelli, 2005; Ortega-Lara & Lehmann, 2006; Jarduli, Shibatta, 2013; Shibatta, 2014, 2016; Shibatta, Vari, 2017). The family has a small number of specimens present in museum collections. Thus, it is not possible to extract osteological characters and tissues for molecular analysis for the phylogenetic reconstruction of most species of

Pseudopimelodidae. This reflects in the use of a low number of species used in the studies published until now. (Lundberg *et al.*, 1991; Shibatta, 1998; Sullivan *et al.*, 2006, Birindelli, Shibatta, 2011; Sullivan *et al.*, 2013; Shibatta, Vari, 2017). The use of geometric morphometry is a fast, inexpensive (Bichuette *et al.*, 2014), and simple approach that allows the inclusion of the majority of species of Pseudopimelodidae in a single phylogenetic analysis. In addition, as this is a relatively new area of research, the present analysis also provides a discussion about the new possibility of the use of landmark data to infer phylogenetic relationships. The present study is a contribution to help those who wish to include such data as additional source of evidence in studies of the Neotropical freshwater fish systematics.

Material and methods

Examined material and taxa selection. The phylogenetic analysis included 440 specimens belonging to 40 of the 48 valid species of all genera of Pseudopimelodidae, in addtion four species of the family Pimelodidae and Heptapiteridae as outgroup terminals, for being closely related to the Pseudopimelodidae. *Rhamdia quelen* was used for rooting the tree (Tab. 1). This choice was based on previous phylogenetic hypotheses for Siluriformes groups (Lundberg *et al.*, 1991; Britto, 2002; Diogo, 2004; Diogo *et al.*, 2004; Hardman, 2005; Sullivan *et al.*, 2006; Birindelli, Shibatta, 2011; Sullivan *et al.*, 2013) and the monophyly of the superfamily Pimelodoidea, composed by those three families, as presented by Sullivan *et al.* (2006).

Samples from the following institutions were studied: American Museum of Natural History, New York (AMNH), Academy of Natural Sciences of Drexel University, Philadelphia (ANSP), California Academy of Sciences, San Francisco (CAS), Colección ictiológica Fundación Miguel Lillo, San Miguel de Tucumán (CI-FML), Field Museum of Natural History, Chicago (FMNH), Instituto Nacional de Pesquisas da Amazônia, Manaus (INPA), Museo de

Ciencias Instituto para la Investigación y Preservación del Patrimonio Cultural y Natural del Valle del Cauca, Cali (IMCN), Laboratório de Biologia e Genética de Peixes, Botucatu (LBP), Laboratório de Ictiologia, Ribeirão Preto (LIRP), Museu de Ciências e Tecnologia da PUCRS, Porto Alegre (MCP), Museo de Historia Natural de la Escuela Politecnia Nacional, Quito (MEPN), Muséum d'histoire naturelle, Genève (MHNG), Museo Nacional de Historia Natural del Paraguay, Asunción (MNHNP), Museu Nacional, Rio de Janeiro (MNRJ), Museu Paraense Emilio Goeldi, Belém (MPEG), Museu de Zoologia da Universidade Estadual de Londrina, Londrina (MZUEL), Museu de Zoologia da Universidade de São Paulo, São Paulo (MZUSP), Núcleo de Pesquisas em Limnologia, Ictiologia e Aquicultura, Maringá (NUPELIA), Swedish Museum of Natural History, Stockholm (NRM), Royal Ontario Museum, Toronto (ROM), National Museum of Natural History, Washington DC (USNM) and Coleção Zoológica de Referência da Universidade Federal de Mato Grosso do Sul, Campo Grande (ZUFMS).

Tab. 1. List of ingroup and outgroup species used in this study. (N = sample size).

Taxon	N	Taxon	N
Pseudopimelodidae		*Microglanis nigrolineatus* Terán, Jarduli, Alonso, Mirande & Shibatta, 2016	10
Batrochoglanis acanthochiroides (Güntert, 1942)	11	*Microglanis oliveirai* Ruiz & Shibatta, 2011	12
Batrochoglanis melanurus Shibatta & Pavanelli, 2005	5	*Microglanis parahybae* (Steindachner 1880)	10
Batrochoglanis raninus (Valenciennes, 1840)	12	*Microglanis pataxo* Sarmento-Soares, Martins-Pinheiro, Aranda & Chamon, 2006	10
Batrochoglanis transmontanus (Regan, 1913)	4	*Microglanis pellopterygius* Mees, 1978	3
Batrochoglanis villosus (Eigenmann, 1912)	30	*Microglanis poecilus* Eigenmann, 1912	12
Cephalosilurus albomarginatus Eigenmann, 1912	22	*Microglanis robustus* Ruiz & Shibatta, 2010	17
Cephalosilurus apurensis Mees, 1978	5	*Microglanis secundus* Mees, 1974	16
Cephalosilurus fowleri Haseman, 1911	9	*Microglanis variegatus* Eigenmann & Henn, 1914	5
Cephalosilurus nigricaudus (Mees 1974)	1	*Microglanis xylographicus* Ruiz & Shibatta, 2011	7
Cruciglanis pacifici Ortega-Lara & Lehmann, 2006	1	*Pseudopimelodus bufonius* (Valenciennes, 1840)	22
Lophiosilurus alexandri Steindachner, 1876	8	*Pseudopimelodus charus* (Valenciennes, 1840)	7
Microglanis carlae Vera Alcaraz *et al.*, 2008	6	*Pseudopimelodus mangurus* (Valenciennes, 1835)	13
Microglanis cibelae Malabarba & Mahler, 1998	32	*Pseudopimelodus schultzi* (Dahl, 1955):	2
Microglanis cottoides (Boulenger, 1891)	20	*Rhyacoglanis epiblepsi* Shibatta & Vari, 2017	25
Microglanis eurystoma Malabarba & Mahler, 1998	11	*Rhyacoglanis paranae* Shibatta & Vari, 2017	23
Microglanis garavelloi Shibatta & Benine, 2005	7	*Rhyacoglanis seminiger* Shibatta & Vari, 2017	14
Microglanis iheringi Gomes, 1946	4	**Outgroup**	
Microglanis leniceae Shibatta 2016	7	**Pimelodidae**	
Microglanis leptostriatus Mori & Shibatta, 2006	8	*Steindachneridion melanodermatum* Garavello, 2005	6
Microglanis lundbergi Jarduli & Shibatta, 2013	8	*Steindachneridion parahybae* (Steindachner, 1877)	12
Microglanis maculatus Shibatta, 2014	4	S*teindachneridion scriptum* (Miranda Ribeiro, 1918)	12
Microglanis malabarbai Bertaco & Cardoso, 2005	14	**Heptapiteridae**	
Microglanis nigripinnis Bizerril & Perez-Neto, 1992	3	*Rhamdia quelen* Quoy & Gaimard, 1824	15

Geometric morphometrics. Digital images of the dorsal, ventral and left lateral views of each specimen was taken with a Canon G16 digital camera, resulting in three data sources, that represent also different structures, for each species. Thirty-eight biologically homologous landmarks were digitalized in two dimensions using TPSDig 2.21 (Rohlf, 2015) (Fig. 1, Tab. 2). The procedure performed to obtain the landmark data follow Catalano *et al.* (2015). First, all specimens from each species were superimposed using a General Procrustes Analysis (GPA, Gower, 1975; Rohlf, Slice, 1990). The consensus configurations derived from this step represent the shape of each species, and this procedure was repeated for all of the structures analyzed. Next, the consensus configurations representing each species were used to define a multiple superimposition by means of a new GPA, and this was again repeated for each structure. After a standardization step, the multiple superimposition of each structure was incorporated into a matrix as a different character, generating a combined data set. Finally, the matrix was used to conduct the phylogenetic search. The TPSRelw 1.65 program (Rohlf, 2016) was used to obtain the GPA and consensus settings.

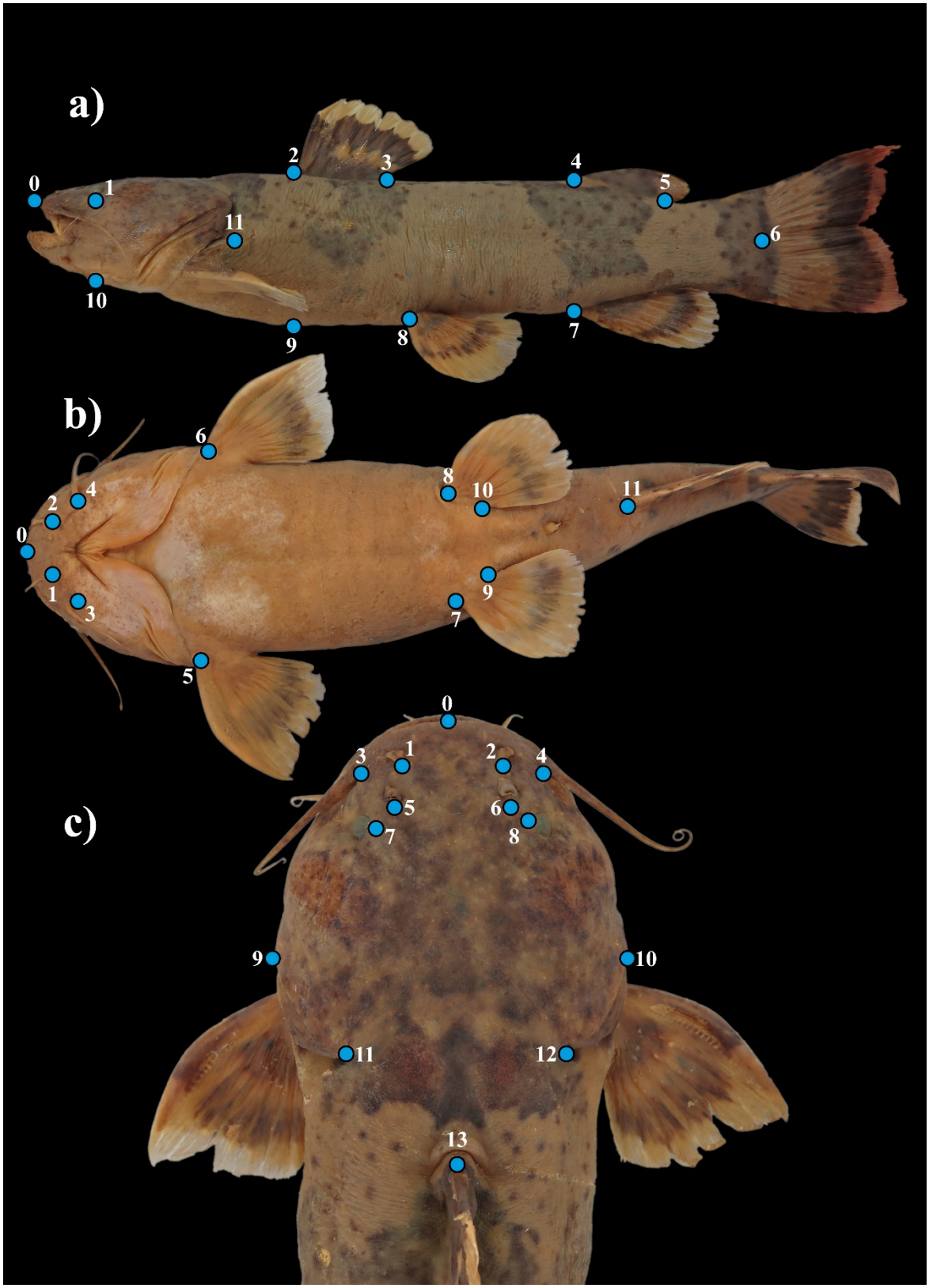

Fig. 1. *Pseudopimelodus mangurus*, MZUEL 1073, 185.2 mm SL, showing the position of each landmark: a) lateral, b) ventral and c) dorsal views. See Table 2 for definitions.

Tab. 2. Description of landmarks as shown in fig. 1. (L= left side, R= rigth side).

Landmark number	Definition
	Dorsal
0	Tip of snout
1	Posterior margin of the anterior nostril L
2	Posterior margin of the anterior nostril R
3	Insertion of maxillary barbel L
4	Insertion of maxillary barbel R
5	Posterior margin of the posterior nostril L
6	Posterior margin of the posterior nostril R
7	Internal lateral margin of eye L
8	Internal lateral margin of eye R
9	Most lateral point of the head L
10	Most lateral point of the head R
11	Upper end of the operculum L
12	Upper end of the operculum R
13	Insertion of dorsal fin spine
	Lateral
0	Tip of snout
1	Base of the orbit
2	Anterior insertion of dorsal fin
3	Posterior insertion of dorsal fin
4	Anterior insertion of adipose fin
5	Posterior insertion of adipose fin
6	End of vertebral column
7	Anterior insertion of anal fin
8	Anterior insertion of pelvic fin
9	Ventral margin of body below Landmark 1
10	Ventral margin of head below Landmark 2
11	Tip of posterior cleithral process
	Ventral
0	Tip of lower jaw
1	Insertion of anterior mental barbel R
2	Insertion of anterior mental barbel L
3	Insertion of posterior mental barbel R
4	Insertion of posterior mental barbel L
5	Insertion of pectoral fin spine L
6	Insertion of pectoral fin spine R
7	Anterior Insertion of pelvic fin L
8	Anterior insertion of pelvic fin R
9	Posterior Insertion of pelvic fin L

10	Posterior insertion of pelvic fin R
11	Anterior insertion of anal fin

Landmark analysis under parsimony. After the standardization step (see below), multiple superimposition of each structure was incorporated into a matrix as a different character generating a combined data set. The phylogenetic analysis was performed following the approach proposed by Catalano *et al.* (2010) for the analysis of landmark data in phylogenetics (LAUP - landmark analysis under parsimony). This approach maximizes the degree to which the similarity in landmark position in different taxa can be accounted for by common ancestry. The tree score was given by the sum of the landmark displacements along the tree (Catalano *et al.*, 2015). This method is implemented in Tree Analysis using New Technology (TNT) phylogenetic software (Goloboff *et al.,* 2008) and is a direct extension of the parsimony principle (Farris 1983) for the analysis of landmark data. Since phylogenetic searches for landmark are implemented natively in TNT in recent version 1.5 (Goloboff, Catalano, 2016) including a full implementation on phylogenetic morphometrics. The implementation allows the user to define different parameters for the LAUP (Catalano *et al.*, 2015). These parameters included the number of search replicates, the accuracy of the grids used to reconstruct the ancestral landmark positions, the number of nested grids used to refine the estimation of the ancestral landmark position, the number of cells covered by the nested grids during this refinement step and the use of dynamic realignment. Dynamic realignment is the superposition of the configurations during the tree search to minimize landmark displacements along the tree (Goloboff, Catalano, 2011, Catalano, Goloboff, 2012). The matrix for analysis in TNT was compiled by adding the generated geometric morphometric characters to discrete characters as a separate block within a .tnt file (Appendix 3). The search strategy consisted of 100 Random

Addition Sequences (RAS = Wagner trees) followed by TBR (Tree Bisection and Reconnection algorithm). Phylogenetic uncertainty in relation to configuration and landmark sampling was analyzed by means of resampling analysis. The resampling was done in the same way as in the implementation of symmetric resampling (Goloboff *et al.* 2003, 2008) in TNT: Each configuration/landmark had a 0.33 probability of being deleted, a 0.33 probability of having its weight duplicated, and a 0.33 probability of remaining unaltered. A total of 100 pseudoreplicates were conducted, with a single run of RAS + TBR per pseudoreplicate (Catalano *et al.*, 2015).

Optimization of landmark data on tree. The tree score and ancestral shapes were established using the algorithms described in Goloboff, Catalano (2011) to optimize landmark data on a tree. In summary, this approach consists of establishing the optimal ancestral positions of each landmark by means of a heuristic approximation, in wich a grid is placed over the space occupied by all the observed positions for a given landmark. Each cell of the grid is considered as a possible state (i.e., position) for the inner nodes. A cost matrix is built where the costs between states are the distances between the centers of each of the cells. Once each of the observed positions has been assigned to the corresponding cell, the optimal positions are established using a cost matrix algorithm (Sankoff, Rousseau, 1975, Goloboff, 1998). The score can then be improved by repeating this Sankoff step, but this time superimposing a new grid over the optimal cell and the neighboring cells for each node. This step is called “nested grid.” Finally, the score can also be improved, modifying the position of each landmark at each internal node (Fig. 2). The precision depends on the number of cells included in the grid: the higher the number of cells the higher the level of precision. However, the execution time of Sankoff algorithm increases quadratically with the number of states, being necessary to find a

value of compromise. In this study, the landmark optimization was run with the following settings: A 8×8 grid of cells, two level of nested grids, observed landmark positions included as states and a final iterative improvement of the positions. Once optimal positions (Fermat point) are assigned to all nodes of the tree it is possible to improve the score by modifying the positions node by node. In each visited node the position of each landmark is modified considering the position of the neighbor nodes to minimize the different in position between the chosen node and the position in the neighbor nodes (Catalano, *et al.* 2010).

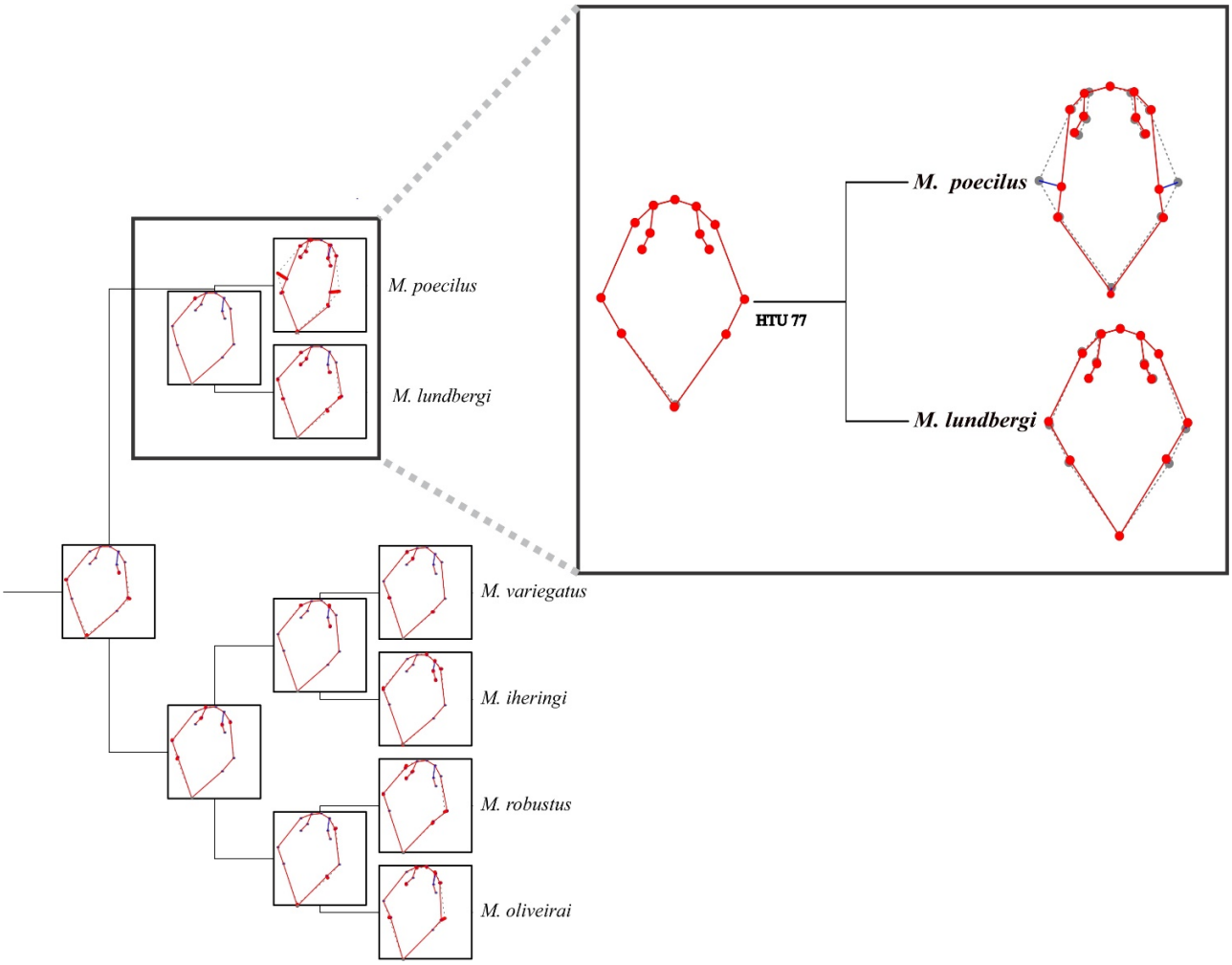

Fig. 2. Optimization of landmark data on tree. In all landmark configurations, deformation vectors at each point indicate displacements from the ancestral configurations to each of the descendant configurations, as optimized with spatial parsimony with TNT. The ancestral configurations are in gray dotted lines. Red line represents reconstructed shapes. Blue line indicates the change in position of each landmark from the ancestor to the corresponding node. HTU (Hypothetical Taxonomic Unit).

Standardization. For the simultaneous analysis of multiple landmark configurations, it is necessary to decide how the information of the different configurations is combined. Otherwise, some configurations might have much more influence than the rest in the election of the optimal phylogenetic hypothesis due to uncontrolled and possibly unwanted factors. For instance, if configurations representing different structures have different sizes, the phylogenetic results may be driven by larger configurations (Catalano *et al.*, 2015). These factors affect the analysis, as long as these can produce differential contribution of the configurations to the election of the final hypothesis (i.e. produce the domination of some characters over others). There are different approaches that can be followed to address these issues. In this study was followed an approach where the contribution of each configuration to the election of the phylogenetic hypothesis was equal. After the standardization, a simultaneous displacement along the range in each of the landmarks of the configuration is equivalent to one step in a discrete character. It is also possible to calculate standardization factors in such a way that the contribution of all landmarks within a configuration is similar irrespective of the total displacement suffer by each landmark. This standardization within each configuration is combined with the standardization among the configurations (Goloboff, Catalano, 2011).

Superimposition of configurations. Two parameters of the superimposition method were tested: the Procrustes alignment (the original alignment resulting from a GPA) and Dynamic alignment. Recently, Catalano, Goloboff (2012) presented a method that merges both steps, map and align, into a single procedure that (for the given tree) produces a multiple alignment and ancestral assignments such that the sum of the euclidean distances between the corresponding landmarks along tree nodes is minimized (script available from the authors). The retention index and the consistency index were computed to estimate shape changes that can be

interpreted as synapomorphies, or as homoplasies for each configuration (Klingenberg, Gidaszewski, 2010; Ospina-Garcés, Luna, 2017). GPA was considered as the “static” alignment and it was used for compare results.

Discrete morphological characters. The list of characters used and their correspondence with literature is presented in Table 3. Fourteen discrete characters were selected from Shibatta, Vari (2017) and included in the analysis. Only characters based on external morphology to encompass the largest number of Pseudopimedidae species were examined. The characters were analyzed and polarized for all the samples and a new matrix of discrete characters was made, including several species never used in phylogenetic analyses of Pseudopimelodidae.

Tab. 3. Discrete morphological characters used for phylogenetic analysis of Pseudopimelodidae, based on external morphology. Character numbers between parentheses follows Shibatta, Vari (2017).

Character		Description	States
		Skin and dermal structures	
4	(2)	Degree of development of unculiferous epidermal structures	(0) little developed; (1) well developed
5	(3)	Skin covering pectoral-fin spine	(0) thin; (1) thick
6	(4)	Axillary pore	(0) present; (1) absent
		Pigmentation	
7	(5)	Light blotch on cheek	(0) absent; (1) present
8	(6)	Dark band on predorsal region	(0) absent; (1) present
9	(7)	Fusion of dark predorsal and subdorsal bands	(0) absent (1) partial, (2) complete
10	(11)	Dark caudal-fin stripe	(0) absent; (1) present
		Jaws	
11	(14)	Premaxillary tooth plate form	(0) somewhat rounded; not posterolaterally extended; (1) posterolaterally extended
		Head	
12	(15)	Location of anterior nostril	(0) distant from margin of mouth; (1) near margin of mouth
		Appendicular skeleton	

13	(25)	Posterior cleithral process	(0) elongate, more than half exposed after opercular membrane; (1) short, broadly covered by opercular membrane
14	(26)	Number of branched pectoral-fin rays	(0) 8 or more; (1) 7; (2) 6; (3) 5
15	(29)	Tip of pectoral-fin spine	(0) pointed; (1) bifurcated
16	(34)	Length of ventral versus dorsal caudal-fin lobes	(0) lobes approximately equal; (1) ventral lobe longer; (2) dorsal lobe longer
		Laterosensory system	
17	(39)	Lateral line	(0) complete; (1) incomplete but long; extending beyond vertical through adipose fin; (2) incomplete and short; falling short of vertical through adipose fin

Results

Phylogenetic analysis with landmark data

Combined analysis. The analysis included the discrete morphological characters and landmarks in the combined matrix (Appendix 3). This dataset was analyzed under a dynamic approach, where the score for each tree evaluated during searches is calculated considering the best (heuristic) superimposition. The parsimony analysis of the combined geometric morphometric and discrete data found one most parsimonious tree (score = 44.844). The tree obtained with the combined matrix (Fig. 3) had consistency index of 0.51 and retention index of 0.88.

All clades are supported by landmarks data with different states in relation to the corresponding ancestor position (Figs. 2 and 4), besides the synapomorphies supported by landmarks in all clades. Monophyly of the Pseudopimelodidae is supported by characters 1 in landmarks 3 and 4 showing differences in the insertion of the maxillary barbel, where the snout is narrow, increase in distance from the anterior nostril to the posterior nostril (landmarks 5 and 6), with eyes closer to the posterior nostril (landmarks 7 and 8). Landmarks 9 and 10 show that Pseudopimelodidae has a larger head than the outgroup. In character 2, the main synapomorphy is in landmark 11: Tip of the posterior cleithral process longer in relation to the ancestral state. Other sinapomorphies (character 3) were differences in the position of the mental barbels, being restricted in Pseudopimelodidae the distal part of mental region (landmarks 1-4) and large ventral fin base in landmarks 7 to 10 (Figs. 1 and 4). *Cruciglanis*, *Pseudopimelodus* and *Rhyacoglanis* are supported by sinapomorphies: anterior nostril distant from anterior margin of the mouth (character 1, landmarks 1 and 2) and base of the dorsal fin larger (character 2,

landmarks 2 and 3). *Rhyacoglanis* is supported by character 1, landmarks 1, 2, 5 and 6 with anterior and posterior nostrils closer, longer tip of the posterior cleithral process (character 2, landmark 11). The sister relationship between *Cruciglanis* and *Pseudopimelodus* is supported by the greater distance interorbital (character 1, landmarks 7 and 8), longer snout tip (character 2, landmark 0) and greater length of caudal peduncle (character 3, landmark 11). The clade formed by *Cephalosilurus*, *Lophiosilurus*, *Batrochoglanis* and *Microglanis* is supported by smaller distance between the tip of the snout and the base of the dorsal fin (character 1, landmark 13). *Cephalosilurus* and *Lophiosilurus* share the wider head, with smaller distance interorbital, posterior and anterior nostrils (character 1, landmarks 1-8), smaller base of the adipose fin (character 2, landmarks 4 and 5) and greater body width (character 3, landmarks 5 and 6). The sister group formed by *Batrochoglanis* and *Microglanis* shares greater distance between the opercular openings (character 1, landmarks 11 and 12) and shorter ventral fin base (character 3, landmarks 7-10). *Microglanis* is supported by lower distance between the anterior nostrils, posterior nostril closer to the posterior margin of the eye, greater interorbital distance (character 1, landmarks 1,2, 5,6, 7 and 8), longer tip of the posterior cleithral process (character 2, landmark 11).

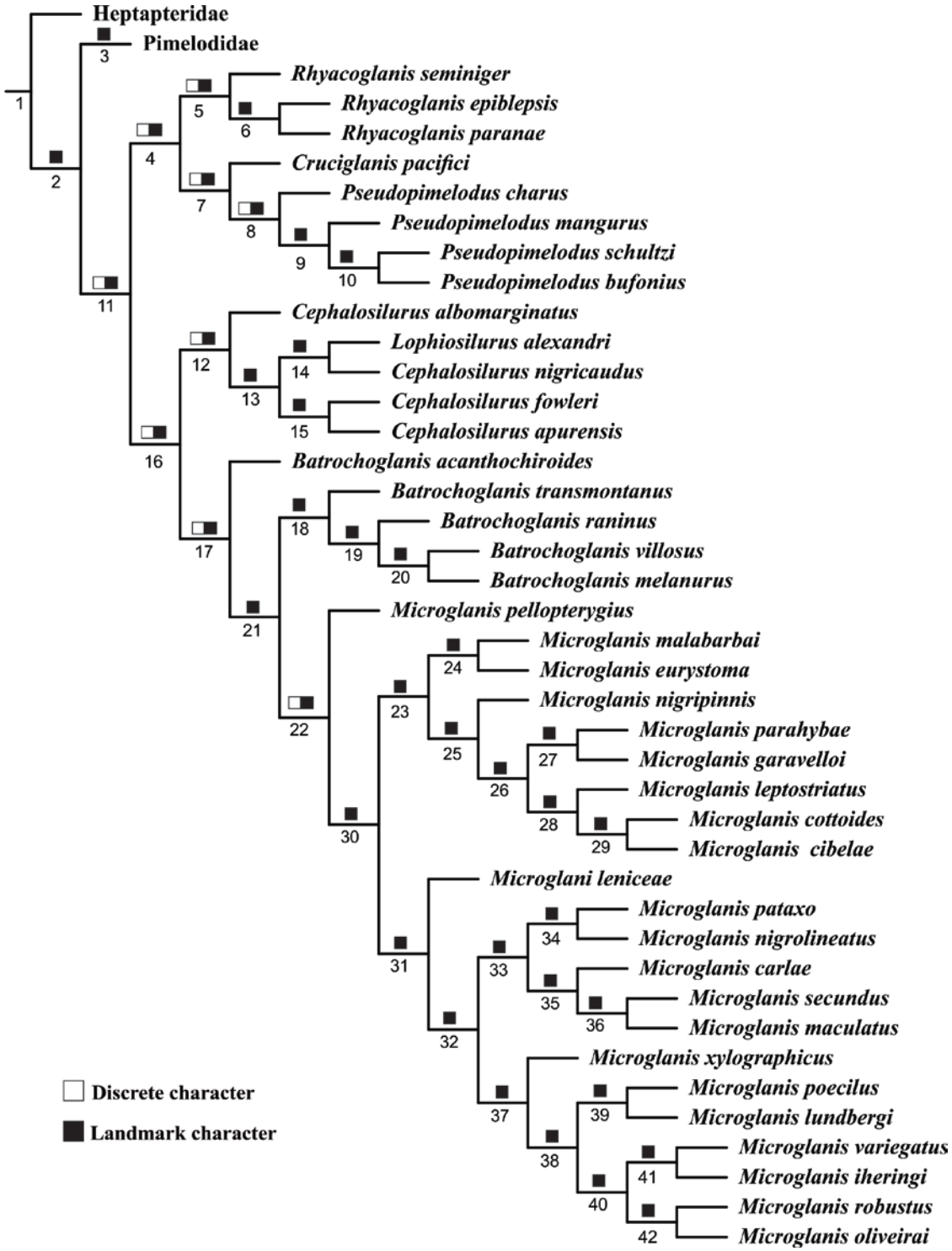

Fig. 3. Phylogeny of Pseudopimelodidae obtained from the parsimony analysis of combined discrete and landmark data of three configurations in TNT, under dynamic alignment. Black squares represent landmark synapomorphies and white squares represent synapomorphies with the discrete characters. Numbers below branches indicate internal nodes (see Appendix 1 and 2).

Some clades are supported by discrete character (Tab. 3) sets along with landmarks characters: Monophyly of the Pseudopimelodidae is supported by one discrete character [14 (0>2)]. Within the family, the clade *Cruciglanis*, *Pseudopimelodus* and *Rhyacoglanis* is supported by two characters [5 (0> 1), 15 (0> 1]. *Rhyacoglanis* is supported by one synapomorphies [character 7 [0> 1)]. The sister relationship between *Cruciglanis* and *Pseudopimelodus* is supported by two states of characters [8(0> 1), and 14 (2> 1)]. *Pseudopimelodus* is supported by one character [13 (0> 1)]. The clade formed by *Cephalosilurus albomarginatus*, *Cephalosilurus* and *Lophiosilurus* shares two characters [3 (0> 1) and 13 (0> 1)], and that clade, in turn, shares one character [11 (0> 1)], with its sister formed by *Batrochoglanis* and *Microglanis*, a clade supported by four characters [6 (0> 1), 8 (0> 1) 9 (0> 2), and 16 (0> 1)]. *Microglanis* is supported by four characters [11 (1> 0), 14 (2> 3) 16 (0> 2), and 17 (1> 2)]. The complete list of autopomorphies and synapomorphies and character mapping (see numbers of internal nodes Fig. 3) are given in Appendix 1 and 2.

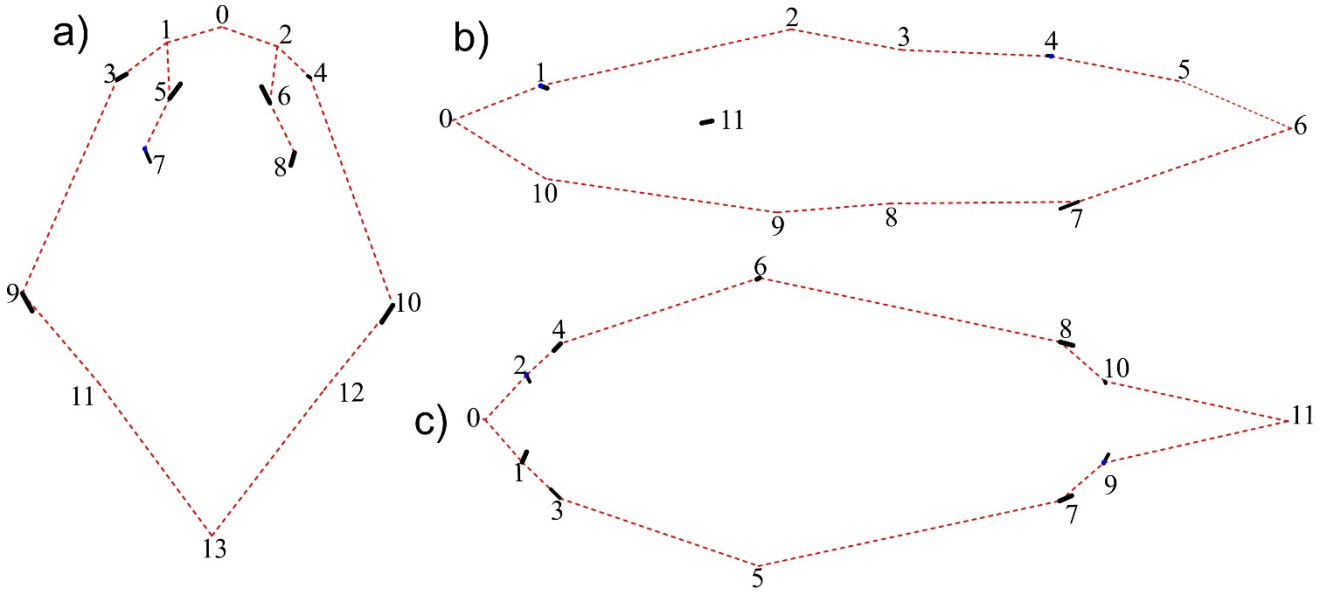

Fig. 4. Landmark synapomorphies of the Pseudopimelodidae: a) character 1 (dorsal view of head), b) character 2 (lateral view of body), c) character 3 (ventral view of body). Dashed lines represent reconstructed shapes. Solid lines indicate the change in position of each landmark from the ancestor to the corresponding node.

Group support. The support values derived from resampling configurations were highly variable along the tree (from 2% to 100%) when configurations were resampled. Symmetric resampling did not support some nodes (Fig. 5). Despite demonstrating different topologies with the parsimony tree result (Fig. 3), the taxonomic groupings between the genera of Pseudopimelodidae was the same, having support values of 48% to 100%. The characters formed by configurations of landmarks, supported in 76% the hypothesis of a monophyletic Pseudopimelodidae (Figs. 3 and 4). The clade formed by *Cephalosilurus* and *Lophiosilurus*, with 92% of support, suggests that *Lophiosilurus* may belong to the genus *Cephalosilurus* forming a monophyletic group. *Cruciglanis*, *Pseudopimelodus* and *Rhyacoglanis* formed one clade supported by 48%. *Rhyacoglanis*, the genus recently described, is monophyletic and supported with 58%. *Pseudopimelodus*, although presenting a polytomy involving *P. schultzi*, *P. mangurus* and *P. bufonios*, is monophyletic with 70% support when we applied symmetric resampling. *Batrochoglanis* had *Microglanis* as sister group, forming a clade supported in 91%. *Microglanis* is strongly supported, remaining monophyletic in symmetric resampling with 100% of support.

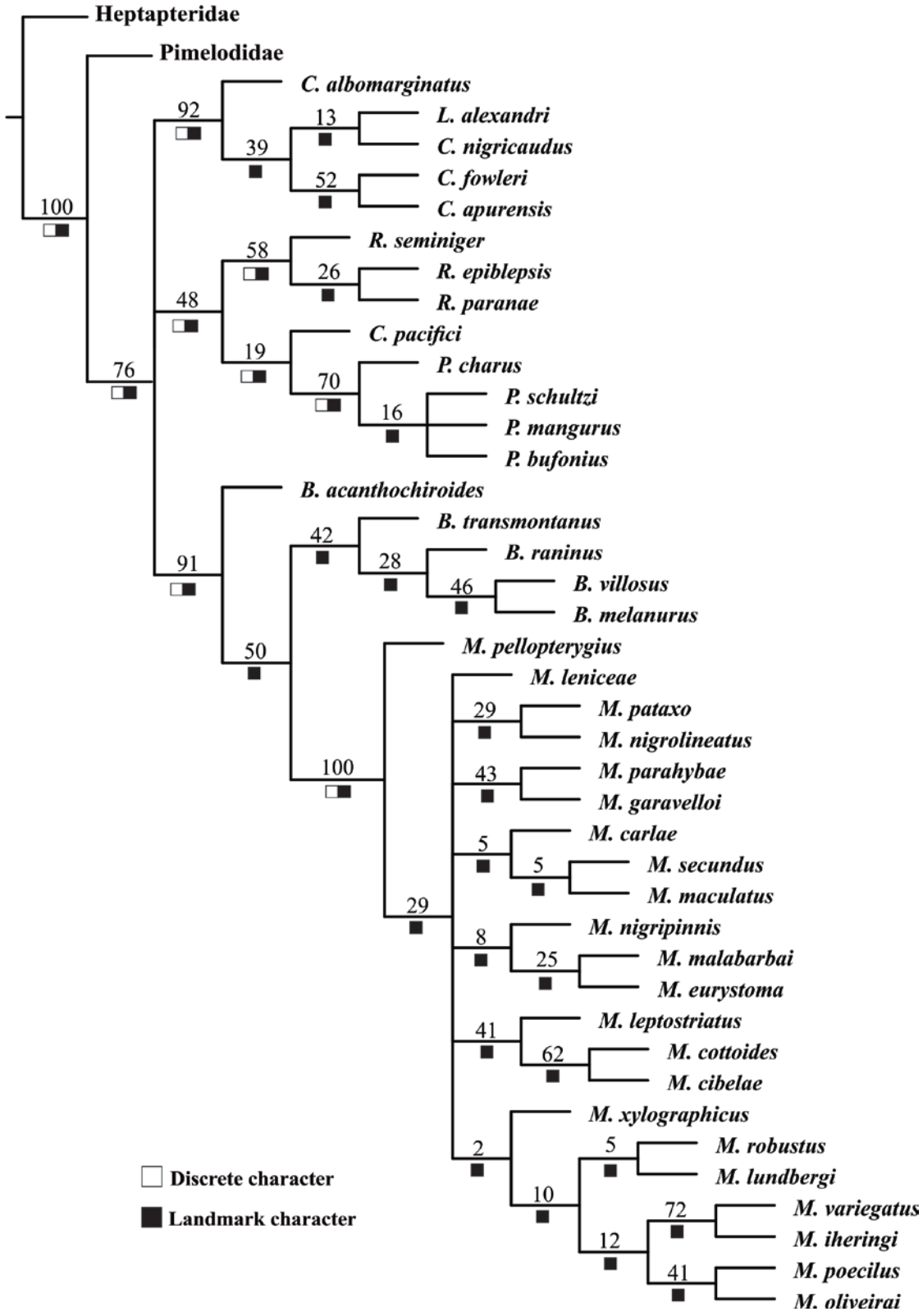

Fig. 5. Resampled tree from the Pseudopimelodidae obtained from the landmark analysis under parsimony (LAUP) and discrete data in TNT. Numbers above branches indicate support values when configurations were resampled. Black squares represent landmark synapomorphies and white squares represent synapomorphies with the discrete characters.

Different superimposition strategies. The analysis starts with a static superimposition that remains unaltered during the tree search. The best tree obtained in this analysis (score = 45.170), was not similar to that obtained in the dynamic approach, differing in the relationship of species of the genera *Batrochoglanis* and *Microglanis* (Figs. 3, 5 and 6). The consistency index was 0.50 and retention index 0.88, similar to values found in the tree with dynamic approach. However, the two approaches differed in the values of the landmarks parsimony scores (s) as shown in table 3. The dynamic approach in this data set produced an improvement in tree score and landmarks scores compared to static alignment.

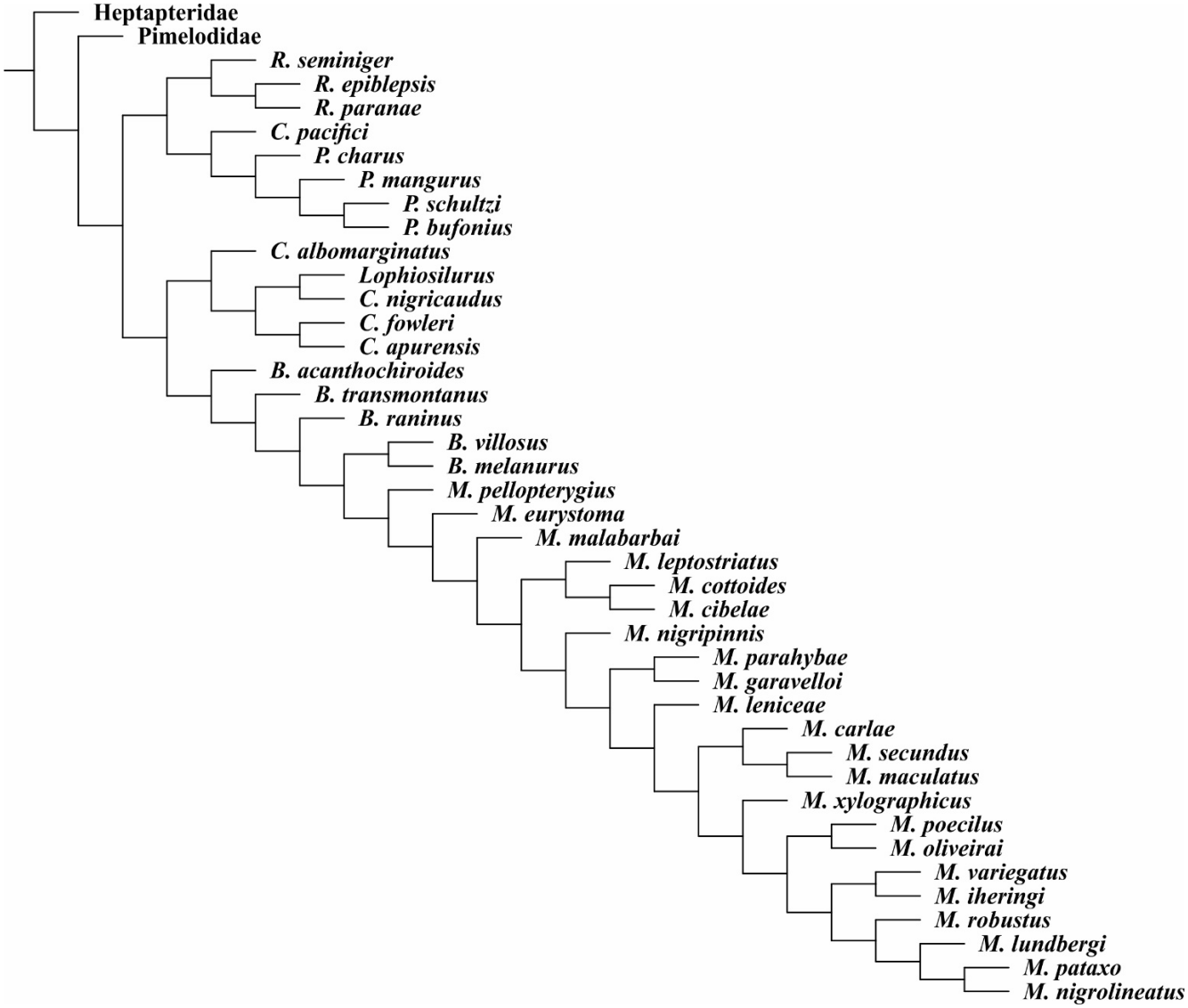

Fig. 6. Phylogeny of Pseudopimelodidae obtained from LAUP of combined discrete and landmark data in TNT, under static alignment.

Independent parsimony scores were computed with TNT for each landmark configuration (40 species, outgroups pruned) on the combined discrete and morphometric tree. Optimization settings enabled us to calculate the parsimony scores (*s*) with high precision over our combined discrete and morphometric tree, the minimum possible steps (*m*) on the single character best tree, and the minimum steps on a bush tree (*g*) for each shape character

(characters 1-3). From these values, we estimated the character consistency (*ci*) and retention (*ri*) indices as usual (*ci* = *m*/*s*; *ri* = *g*-s/*g*-*m*).

Tab. 4. Parsimony scores estimated in TNT for the dynamic and static approach, with the following metrics: *s* atual steps of a character on the combined tree, m minimum possible steps for the character alone, *g* minimum steps on a bush, *h* = s−m homoplasy index for a character, *ci* = *m*/*s* character consistency index, *ri* = *g*−s/*g*-*m* retention index.

Character	s	m	g	h	ci	Ri
			Dynamic Alignment			
1. Dorsal	5,56	5,12	9,35	0,44	0,92	0,90
2. Lateral	5,65	4,99	8,48	0,66	0,88	0,81
3. Ventral	5,61	4,97	8,33	0,64	0,89	0,81
			Static Alignment			
1. Dorsal	5,63	5,12	9,35	0,51	0,91	0,88
2. Lateral	5,75	4,99	8,48	0,77	0,87	0,78
3. Ventral	5,75	4,97	8,33	0,78	0,86	0,77

Our morphometric analysis using the body shape as a character, revealed changes of landmark configurations consisting of synapomorphy and homoplasy (Figs. 3, 4 and 5, Tab. 4). The characters 2 and 3, lateral and ventral view, shows higher homoplasy changes in the two alignment approaches. The dorsal region (character 1) shows lower homoplasy (*h* = 0.44 and 0.51). This is the shape character with the highest consistency index (*ci* = 0.91 and 0.92, Tab. 4).

The use of dynamic realignment had improvements not only on the tree score obtained (score = 44.844 vs. 45.170, Figs. 3 and 6) as well as character scores, resulting in a lower homoplasy and higher consistency and retention index (Tab. 4). The character 2, for example, had 15% of the score improved, in the homoplasy index of the character 2 (lateral configuration) using the dynamic alignment (*h* = 0.66 *vs.* 0.77). There was also a small increase in the consistency index (*ci* = 0.88 *vs.* 0.87) and retention index (*ri* = 0.81 *vs.* 0.78). The analysis showed that the tree scores and landmark parsimony score obtained by the dynamic approach

were considerably better and the results demonstrate that topologies are different depending on the initial alignment, optimization parameters and realignment.

Phylogenetic analysis of geometric morphometry data. Two matrices with geometric morphometry data were analyzed. The first includes the discrete characters and the landmarks in a single matrix combined (Fig. 3, Appendix 3). The second includes only the configuration of the shape coordinates, that is, the consensus by species for the set of aligned anatomical landmarks. A matrix with only the landmark characters was extracted from the combined matrix and was analyzed with the same initial alignment, optimization parameters, and dynamic realignment. Only one tree was retained as being the most parsimonious (score = 16.218) and obtained a low consistency (*ci* = 0.23) and retention index (*ri* = 0.41). The obtained tree using only landmark data of body shape (Fig. 7) proved to be not informative to unravel the phylogenetic relationships of Pseudopimelodidae due to the high number of convergences. This result is not congruent with the phylogenetic proposal of combined matrix data previously analyzed. Genera suck as *Rhyacoglanis* and *Batrochoglanis* have become polyphyletic (Fig 7). Thus, *Microglanis* and *Pseudopimelodus* that once formed a clade, are now paraphyletic.

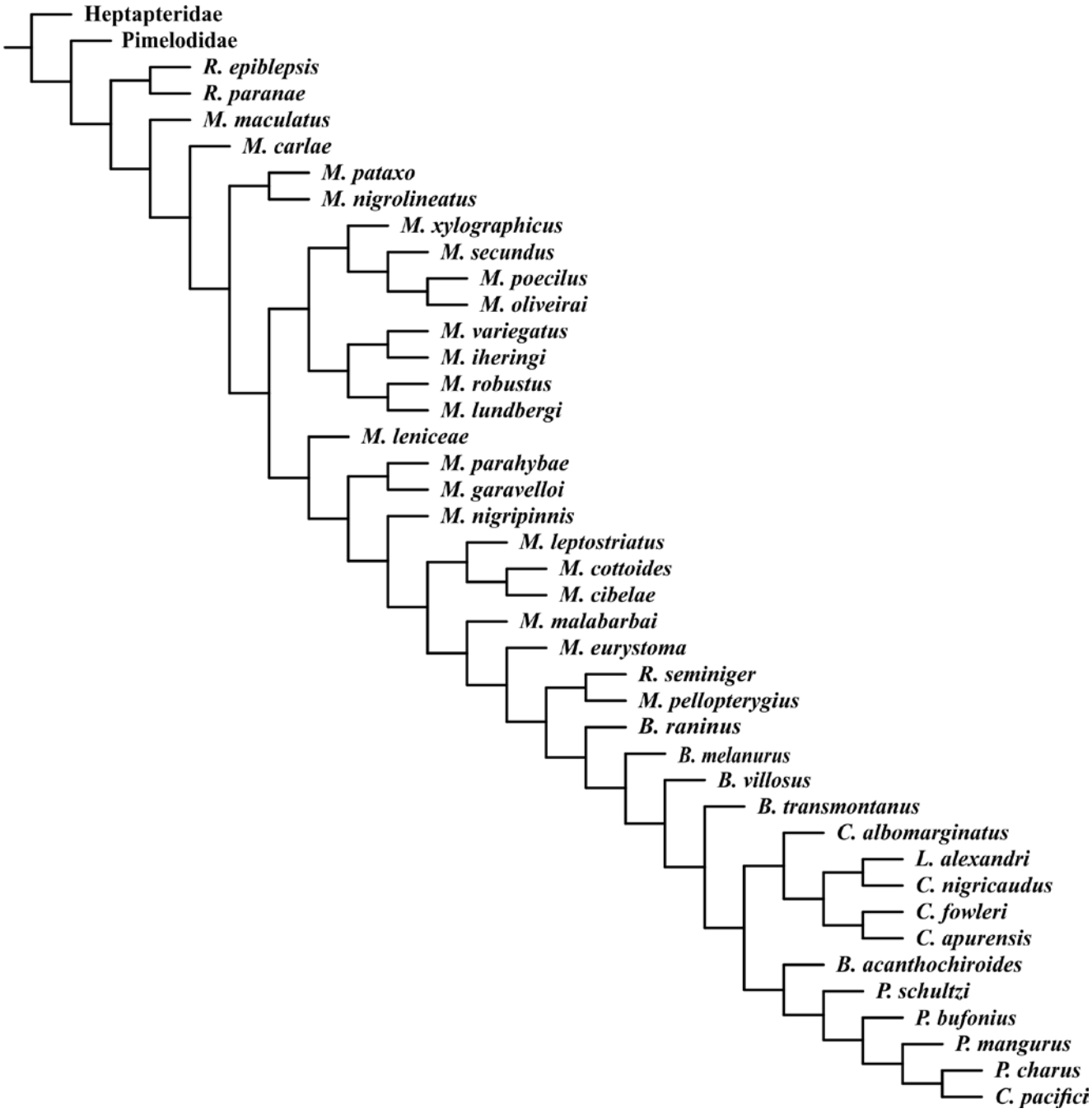

Fig. 7. Tree obtained from landmark characters only with LAUP, under dynamic alignment.

Discussion

Morphological evolution in Pseudopimelodidae.

The current systematics of Pseudopimelodidae is based mainly on morphological and molecular data (*e.g.* Shibatta, 1998; Ortega-Lara, Lehmann, 2006; Birindelli, Shibatta 2011; Sullivan *et al.*; 2013, Shibatta, Vari, 2017). The analysis of the combined matrix shows that it is possible to add phylogenetically informative morphometric characters, that in addition to other characters, help to support the monophyly of Pseudopimelodidae. The new Pseudopimelodidae synapomorphies based on landmarks data (Fig. 4, Appendix 1 and 2), include the presence of a wider head and narrower snout, resulting in changes in the positions of the maxillary and mental barbels, the tip of the longer cleithral process and the wider base of pelvic fins. These new characters that reveal the morphological evolution of the group have never been observed in previous studies (*i.e.* Lundberg *et al.*, 1991; Shibatta, 1998, 2003; Diogo *et al.*, 2004; Hardman, 2005; Sullivan *et al.*, 2006; Diogo, 2007; Sullivan *et al.*, 2013; Shibatta, Vari, 2017).

The tree obtained in this study (Figs. 3 and 5) have greater congruence with previous studies (Shibatta, 1998; Birindelli, Shibatta, 2011 (cladogram A); Shibatta, Vari, 2017). *Cruciglanis*, *Pseudopimelodus* and *Rhyacoglanis* form a clade that is supported by the greater distance from the anterior nostril compared to the anterior margin of the mouth. The recently described genus *Rhyacoglanis* is supported, in this study by have a longer tip of the posterior cleithral process as synapomorphy. These synapomorphies are also found by Shibatta, Vari (2017), demonstrating that it is possible through LAUP to include morphometric characters, without these to be previously discretized, obtaining informative morphometric characters (Catalano et al., 2010; Goloboff, Catalano, 2016). The method can aid the inclusion of

characters where it is difficult to establish a range of discrete states (Rohlf, 1998). *Cruciglanis* and *Pseudopimelodus* differ from *Rhyacoglanis*, by the newly recognized synapomorphies: greater interorbital distance, longer snout tip, greater length of caudal peduncle.

The clade formed by *Cephalosilurus*, *Lophiosilurus*, *Batrochoglanis* and *Microglanis* has the smaller and wider head (dorsal view) compared to other pseudopimelodids. This change in the pattern of head shape was observed by Assega, *et al.* (2016) in the study of ontogenetic development of *L. alexandri*, in which the relative depths of head and body decrease from post-larval to juvenile stages, besides the decreases of nout length, anal-fin base length, caudal-peduncle length, interorbital width. In this study, this becomes even more evident in *Cephalosilurus* and *Lophiosilurus* that shares the wider head, with smaller distance between the posterior and anterior nostrils. Although *Lophiosilurus* also exhibits the most highly modified morphology for the family (Assega, *et al.*, 2016), *Lophiosilurus* and *Cephalosilurus* formed a monophyletic group as proposed by Shibatta (1998), Birindelli, Shibatta (2011) and Shibatta, Vari (2017).

The sister group formed by *Batrochoglanis* and *Microglanis*, shares greater distance between the opercular openings and shorter ventral fin base. *Batrochoglanis* and *Microglanis* also share the absence of axillary pore (Shibatta, Pavanelli, 2005), a synapomorphic character proposed for these two genera by Shibatta (2003), however, this state of character is also shared by *Cruciglanis* (Ortega-Lara, Lehmann, 2006). In this way, the addition of new morphometric characters helps to support the relationship between *Batrochoglanis* and *Microglanis*. The hypothesis that *Microglanis* is a monophyletic group (Jarduli, Shibatta, 2013, Terán, *et al.*, 2016; Shibatta, Vari, 2017) is corroborated in our study. Species of this clade also share a longer tip of the posterior cleithral process, as in *Rhyacoglanis*, demonstrating that some characters of the body shape are convergent and independently evolved in Pseudopimeldidae.

The results obtained in the present study, based on landmark data, show that some changes in each of the morphometric characters can be interpreted as homology hypotheses and some are better interpreted as homoplasy (Table 4). The highest number of synapomorphies in our data is in the dorsal view of head (character 1, Fig. 4a), with a lower homoplasy index and a higher index of consistency and retention (0.92 and 0.90). Homoplasy levels were higher for characters 2 and 3 (Fig 4b and 4c) corresponding to the lateral and dorsal configuration of the body (0.66 and 0.64, respectively). Therefore, the homoplasy index, consistency index and retention index for each character provide evidence to interpret informative phylogenetic changes in landmark configurations (Klingenberg, Gidaszewski, 2010; Ospina-Garcés, Luna, 2017).

Landmark data inference based on the phylogenetic relationships of Pseudopimelodidae.

In the resampled tree, the highest support values are in the synapomorphies from branches supported by the two types of characters (Fig 3). Under equal weigh, it is expected that discrete characters have a higher influence on topology once they are in greater number when compared to the three characters of landmark included in the analysis. Despite of that, the landmark characters presented a high retention index and consistency, both above 75% (Table 3) which, according to Perrard *et al.* (2016), support internal nodes.

The TNT considers each configuration of landmarks as a character. By default, TNT standardizes the configurations so that the contribution of each configuration is similar to a discrete character irrespective of the scale of the configurations or the number of landmarks. In the end, there are no significant differences with the definition of discrete characters in any phylogenetic systematic procedure (Catalano *et al.*, 2010, Goloboff, Catalano, 2011, Goloboff,

Catalano, 2016). In this way, it is possible to consider that the characters derived from the geometric morphometry, with the LAUP approach, aid to support branches.

As observed in Table 3, characters representing the body shape are homoplastic. In fact, it is expected a negative association between degree of homoplasy in morphometric data and the strength of phylogenetic signal (Klingenberg, Gidaszewski, 2010). Since the analyzed structures are generally associated with processes of adaptation, they would be prone to reversals and parallelisms that would in turn complicate the inference of phylogenetic relationships from landmark data. Nevertheless, we consider that landmark data should not be disqualified for supposedly lacking historical information, as generalized by Klingenberg, Gidaszewki (2010). The use of GM of wing venation to understand the evolution of social wasps (Perrard *et al.*, 2016), and the inclusion of landmark data of osteology of mammals (Gonzalez-José *et al.*, 2008, Catalano, Torres, 2015, Ospina-Garcés, Luna, 2017), have shown important congruences with the phylogenies of discrete morphological characters previously proposed for the groups.

As in the case of any other evidence, GM may contain historical information, and the phylogenetic analyses of landmark coordinates can reveal which shape changes are homologous and which are homoplastic (Wenzel, 2002; Ospina-Garcés, Luna, 2017). Although in this work the GM alone were incapable of revealing a phylogenetic pattern congruent with previous hypotheses based on traditional morphology (Fig. 7), the advantages of including GM in phylogenetic inferences have already been noted by several authors (David, Laurin,1996; Larson, 2005; Gonzalez-José *et al.*, 2008; Catalano *et al.*, 2015; Catalano, Torres, 2017; Ospina-Garcés, Luna, 2017). The most obvious advantage is the potential for including taxa known only from fossils as well as species that are rare or difficult to collect (Catalano, Torres, 2017), but are available in museum collections. In addition, the analysis of GM also provides a

potential source of evidence, as the synapomorphies that help the discrete characters to support the monophyly of the Pseudopimelodidae and its genera (Fig. 4 and 5). Recently, it had been demonstrated that the inclusion of more landmark configurations improves the results of the phylogenetic analysis (Catalano, Torres, 2017). Thus, GM are alternative that can be used to compose total evidence analyses along with discrete morphological and molecular characters.

The results obtained in the study of Catalano *et al.* (2015), show that including structures associated with adaptive processes does not necessary lead to incorrect phylogenetic conclusions. The results found by the authors, strongly suggest that to obtain good results the number of structures to be included in a phylogenetic analysis should be much higher than previously considered, probably including a similar number of structures as those included in the analysis of traditional morphological characters. This suggests that retrieving incorrect groupings in Pseudopimelodidae using only landmarks characters may be related to the lack of further information, or the addition of a larger number of characters such as the gemmetric morphometry of osteological configurations, for example.

Scores of Dynamic versus Static Approach. The use of dynamic realignment and the initial alignment had effects on the tree score and topology obtained (Fig. 3 and 6). There was a 0.7% improvement in the score obtained in relation to the tree with static alignment (GPA), decreasing the index of homoplasy and increasing the retention and consistency index of the characters (Tab. 4). The analysis of the four real data sets performed by Catalano, Goloboff (2012) showed improvements in tree score of up to 5%. In other terms, it means that 5% of the shape changes inferred on the trees when mapping a fixed alignment were not changes in shape but merely differences produced by suboptimal alignments.

The higher number of cells and nested grids also improve the scores (Catalano, Goloboff, 2012). However, in our work we did not compare different numbers of cells and nested grids, because the changes are minimal for a number of cells above 6 x 6 and a number of nested grids above of one (Perrard, *et al.*, 2016). In general, grids of 6x6 or 10x10 cells are a good compromise between precision and execution time (Goloboff, Catalano, 2011).

Considering that the topology was impacted by the alignment method, the dynamic superimposition is a prerequisite to obtaining the best tree possible, as this is the alignment consistent with the LAUP frame-work (Perrard *et al.*, 2016). In the context of phylogenetics, this method allows maximizing the degree to which similarity in landmark positions can be accounted for by common ancestry. In the context of morphometrics, this approach guarantees (heuristics aside) that all the transformations inferred on the tree represent changes in shape. However, a limitation for this method is that both the increase of LAUP parameters and the dynamic realignment greatly increase computational time (Goloboff, Catalano, 2016). In this context, it might be the case that prior alignments provide a good enough approximation to the values and results obtained with the dynamic alignment. This question can be evaluated empirically by examining whether the dynamic approach produces a marked improvement on tree scores compared with the nonphylogenetic alignments. Should the results be very similar, this would indicate that the static approach is a good and fast approximation to the real (=optimal) solution (Catalano, Goloboff, 2012).

LAUP considerations. Although there are no systematic studies of fish using GM on phylogeny, the LAUP provides a way to use landmark data in a cladistics context. The current implementation of the method likely produces over-resolved trees, emphasizing the necessity of resampling methods to collapse over-estimated nodes (Catalano, *et al.*, 2015, Catalano,

Torres, 2017). LAUP should be run preferably with grids of more than 6x6 cells, one nested grids and several iterations, to avoid biases related to the orientation of the shapes (Perrard *et al.*, 2016). The use of dynamic alignment is also recommended (Catalano, Goloboff, 2012). Our results show that body shape is more susceptible to homoplasy, but can provide insights in poorly resolved clades by enhancing signals from other data. The inclusion of more landmarks configurations, like any other type of character, can improve the analysis so that they are significantly congruent with other phylogenetic hypotheses. The lardmark data have enormous potential not only as an additional source of information for phylogenetic reconstruction but for a greater understanding of how the evolution of phenotypic characteristics occurs.

Material examined.

Batrochoglanis acanthochiroides (Güntert, 1942): **Venezuela:** USNM 121270, holotype, 106.0 mm SL, USNM 121271, paratypes, 4, 33.6–54.1. USNM 121273, 2, 51.0–80.4 mm SL. USNM 121276, 2, 41.1–53.2 mm SL. USNM 121278, 1, 27.2 mm SL. MZUEL 6675, 1, 227.4 mm SL. *Batrochoglanis melanurus* Shibatta & Pavanelli, 2005: **Brazil**: MZUSP 87240, holotype, 136.7 mm SL. MZUEL 3669, 1, 60.8 mm SL. MZUEL 3670, 1, 151.7 mm SL. MZUEL 3671, 1, 49.1 mm SL. NUP 3430, 1, 92.8 mm SL. *Batrochoglanis raninus* (Valenciennes, 1840): **Brazil:** INPA 1979, 1, 108.0 mm SL. INPA 7343, 1, 65.8 mm SL. INPA 8057, 1, 67.8 mm SL. INPA 19863, 2, 102.2-107.0 mm SL. INPA 34130, 3, 46.2-54.6 mm SL. LIRP 9435, 1, 51.8 mm SL. MZUEL 6035, 1, 77.6 mm SL.MZUSP 23407, 2, 50.7–74.4 mm SL. *Batrochoglanis transmontanus* (Regan, 1913): **Colombia:** CAS 76668, 1, 56.8 mm SL. NRM 15990, 1, 191.9 mm SL. NRM 15992, 1, 138.1 mm SL. NRM 15994, 1, 58.4 mm SL. *Batrochoglanis villosus* (Eigenmann, 1912): **Brazil**: INPA 3088, 1, 163.2 mm SL. INPA 5719, 1. 98.6 mm SL.INPA 4884, 1, 191.9 mm SL. INPA 6202, 1, 142.7 mm SL. INPA 7085, 1, 117.2 mm SL. INPA

31808, 6, 64.2-142.2 mm SL. MPEG 12645, 1, 96,9 mm SL. MZUSP 24903, 1, 178.1 mm SL. MZUSP 30836, 1, 138.8 mm SL. MZUSP 37786, 8, 31.58-109.8 mm SL. **Peru:** ANSP 139056, 1, 125.8 mm SL. **Venezuela:** ANSP 135903, 1, 91.4 mm SL. ANSP 160315, 1, 61.3 mm SL. CAS 158745, 5, 74.13-124.2 mm SL. *Cephalosilurus albomarginatus* Eigenmann, 1912: **Guyana**: FMNH 53221, holotype, 75 mm SL. FMNH 53572, paratype, 68.8 mm SL, FMNH 53222, 8, 21.5-58.5 mm SL. ROM 61482, 2, 50.5-78.8 mm SL. ROM 61336, 10 of 27, 29.0-88.4 mm SL. *Cephalosilurus apurensis* Mees, 1978: **Colombia:** NRM 15995, 1, 201.9 mm SL. V**enezuela**: MZUEL 6492, 1, 186.0 mm SL. MZUEL 6493, 1, 188.4 mm SL. MZUSP 110996, 1, 180.3 mm SL. MZUSP 11099, 1, 200.2 mm SL. *Cephalosilurus fowleri* Haseman, 1911: **Brazil**: FMNH 54254, holotype, 301.4 mm SL. MCP 16675, 2, 44.9-128,0 mm SL. ANSP 172158, 2, 39.2-199.5 mm SL. MCP 14094, 1, 328.8 mm SL. MCP 14126, 1, 262.7 mm SL. MZUSP 38097, 1, 244.6 mm SL. MZUSP 24647, 1, 277.0 mm SL. *Cephalosilurus nigrucaudus* (Mees 1974): **Suriname:** INPA 21632, 1, 57.5 mm SL. *Cruciglanis pacifici* Ortega-Lara & Lehmann, 2006: **Colombia**: INCIVA (IMCN) 113, 1, 91.6 mm SL. *Lophiosilurus alexandri* Steindachner, 1876: **Brazil**: MZUEL 5377, 3, 120.5-160.5 mm SL. MZUEL 13823, 1, 256.9 mm SL. MZUEL 16486, 1, 279.8 mm SL. MZUEL 19691, 2, 181.0-265.5 mm SL. MZUSP 96276, 1, 70.1 mm SL. *Microglanis carlae* Vera Alcaraz, da Graça & Shibatta, 2008: **Paraguay**: MNHP 3667, holotype, 34.1 mm SL. MZUSP 98255, paratypes, 5, 23.4-29.1 mm SL. *Microglanis cibelae* Malabarba & Mahler, 1998: **Brazil**: MCP 19822, paratypes, 3, 34.9-48.7 mm SL. MCP 21190, 9, 24.6-42.4 mm SL. *Microglanis cottoides* (Boulenger,1891): LBP 17014, 15, 39.3-51.3 mm SL. MCP 10826, 5, 38.2-49.5 mm SL. *Microglanis eurystoma* Malabarba & Mahler, 1998: MCP 13405, holotype, 77.6 mm SL. MCP 12698, paratypes, 10, 26.3-41.1 mm SL. *Microglanis garavelloi* Shibatta & Benine, 2005: MZUSP 88006, holotype, 31.7 mm SL. MCP 1678, paratypes, 4, 24.6-27.9 mm SL MZUSP 1732, paratypes, 2, 23.7-30.8

mm SL. *Microglanis iheringi* Gomes, 1946: **Venezuela:** USNM 121985, paratype, 31.3 mm SL. CAS 64403, 3, 27.4- 41.0 mm SL. *Microglanis leniceae* Shibatta 2016: **Brazil:** ZUFMS 4148, holotype, 33.0 mm SL. ZUFMS 4143, paratype, 30.1 mm SL. INPA 27582, paratype, 4, 19.5-21.0 mm SL. NUP 3533, paratype, 29.1 mm SL. *Microglanis leptostriatus* Mori & Shibatta, 2006: MZUEL 3733, paratypes, 6, 19.3-27.4 mm SL. MZUSP 47456, paratypes, 2, 28.4- 28.7 mm SL. *Microglanis lundbergi* Jarduli & Shibatta, 2013: INPA 28577, holotype, 27.7 mm SL. INPA 18774, paratypes, 3, 22.3-24.7 mm SL. MZUSP 112217, paratype, 23.3 mm SL.MZUSP 112218, paratype, 23.1 mm SL. MZUSP 112219, paratypes 2, 21.2-25.7 mm SL. MZUSP 112220, paratype, 24.5 mm SL. MZUSP 112221, paratype, 20.8 mm SL. *Microglanis maculatus* Shibatta, 2014: INPA 41133, holotype, 36.5 mm SL. INPA 24044, paratypes, 2, 21.4- 25.8 mm SL. MZUEL 5825, paratype, 20.5 mm SL. *Microglanis malabarbai* Bertaco & Cardoso, 2005: MCP 37252, 1, 47.7 mm SL. MCP 37187, 1, 50.1 mm SL. MZUEL 17065, 12, 2.77-52.6 mm SL. *Microglanis nigripinnis* Bizerril & Perez-Neto, 1992: MZUSP 80223, 1, 47.2 mm SL. MZUSP 80229, 2, 38.3-43.5 mm SL. *Microglanis nigrolineatus* Terán, Jarduli, Alonso, Mirande & Shibatta, 2016: **Argentina**: CI-FML 6596, holotype, 32.6 mm SL. CI-FML 4841, paratype, 40.1 mm SL. CI-FML 6260, paratype, 21.8 mm SL. CI-FML 6261, paratype, 34.2 mm SL. CI-FML 6595, 4, paratypes, 27.6-43.6 mm SL. MZUEL 14122, 2, paratypes, 17.5-30.1 mm SL. *Microglanis oliveirai* Ruiz & Shibatta, 2011: **Brazil:** INPA 35623, holotype, 26.3 mm SL. MZUEL 5175, paratypes, 11, 19.6- 25.4 mm SL. *Microglanis parahybae* (Steindachner 1880): MNRJ 15989, 5, 30.3-34.2 mm SL. MNRJ 16047, 5, 28.6-38.9 mm SL. *Microglanis pataxo* Sarmento-Soares, Martins-Pinheiro, Aranda & Chamon, 2006: MZUSP 54516, 10, 24.9-31.4 mm SL. *Microglanis pellopterygius* Mees, 1978: **Ecuador:** ANSP 130437, holotype, 68.1 mm SL; MEPN 88.4-12, 2, 22.4-23.1 mm SL. *Microglanis poecilus* Eigenmann, 1912: **Brazil:** INPA 28575, 3, 18.6-20.6 mm SL. INPA 28576, 3, 19.8-

20.4 mm SL. INPA 8052, 3, 24.8-26.2 mm SL. INPA 6828, 3, 19.2-25.8 mm SL. **Guiana:** ROM 60738, 1, 22.5 mm SL. ROM 62390, 1, 17,1 mm SL. ROM 62391, 1, 17.1 mm SL. *Microglanis robustus* Ruiz & Shibatta, 2010: **Brazil:** INPA 8053, holotype, 20.3 mm SL. INPA 7943, paratypes, 2, 20.0-22.2 mm SL. INPA 7957, paratypes, 3, 19.2-21.7 mm SL. INPA 32885, paratypes, 11, 18.4-23.3 mm SL. *Microglanis secundus* Mees, 1974: INPA 5730, 7, 18.5-31.1 mm SL. INPA 7950, 3, 24.4-3.1 mm SL. **Suriname:** MHNG 2621.038, 6, 18.9-27.1 mm SL. *Microglanis variegatus* Eigenmann & Henn, 1914. **Ecuador:** USNM 083653, paratype, 29.1 mm SL. MHNG 298.033, 2, 25.2-27.7 mm SL. MHNG 1232.11, 2, 23.6-26.2 mm SL. *Microglanis xylographicus* Ruiz & Shibatta, 2011: **Brazil:** NPA 35624, holotype, 27.8 mm SL. MZUEL 5173, paratypes, 4, 18.2-22.3 mm SL. MZUEL 5174, paratypes, 2, 23.1-26.2 mm SL. *Pseudopimelodus bufonius* (Valenciennes, 1840) MZUEL 5744, 20 of 42, 88.28-260.49 mm SL. MZUEL 07715, 1, 85.77 mm SL. INPA 8058, 1, 68.8 mm SL. *Pseudopimelodus charus* (Valenciennes, 1840): MZUSP 39278, 1, 93.4 mm SL. MZUSP 39752, 3, 121.2-123.4 mm SL. ANSP 172157, 2, 70.0-71.6 mm SL. ANSP 172156, 1, 53.4 mm SL. *Pseudopimelodus mangurus* (Valenciennes, 1835): MZUEL 829, 1, 140.8 mm SL. MZUEL 1073, 1, 185.2 mm SL. MZUEL 3681, 1, 97.3 mm SL. MZUEL 6618, 1, 127 mm SL. MZUEL 1477, 2, 87.55-111.7 mm SL. MZUEL 1777, 1, 144, 53 mm SL. MZUEL 38278, 1, 83.55 mm SL. MZUEL 5741, 2, 159.9-208.2 mm SL. MCP 10336, 1, 129.0 mm SL. MCP 12685, 1, 146.1 mm SL. MCP 13087, 1, 173.7 mm SL. *Pseudopimelodus schultzi* (Dahl, 1955): **Colombia**: USNM 121258, 1, 150.2 mm SL. USNM 175310, 1, 99.9 mm SL. *Rhamdia quelen* Quoy & Gaimard, 1824: **Brazil**: MZUEL 3845, 15 of 30, 104.6-193.3 mm. *Rhyacoglanis epiblepsi* Shibatta & Vari, 2017: **Bolivia***:* AMNH 40127, paratypes, 25, 41.0-54.2 mm SL. *Rhyacoglanis paranae* Shibatta & Vari, 2017: **Brazil:** MZUEL 6034, 10, 44.6-38.7 mm SL. MZUEL 14121, 1, 89.3 mm SL, MZUEL 12159, 12, 33.7-27.6 mm SL. *Rhyacoglanis seminiger* Shibatta &

Vari, 2017: LIRP 8042, paratypes, 9, 48.3-74.8 mm SL. MZUEL 14123, 2, 60.4 - 64.8 mm SL. MZUSP 82085, 3, 44.4-70.4 mm SL. *Steindachneridion melanodermatum* Garavello, 2005: MZUEL 5227, 6, 99.14-143.2 mm SL. *Steindachneridion parahybae* (Steindachner, 1877): Brazil: MZUEL 14552, 12, 114.2-131.8 mm SL. S*teindachneridion scriptum* (Miranda Ribeiro, 1918): MZUEL 866, 1, 602.2 mm SL. MZUEL 1482, 1, 163.3 mm SL. MZUEL 16238, 10, 101-125.9 mm SL.

Acknowledgments

We are most grateful to Santiago Catalano for sharing his knowledge and his scripts to run the LAUP analysis and for the scholarship granted to LRJ in the accomplishment of the postgraduate course in the Instituto Miguel Lillo. Special thanks to Sandra M. Ospina-Garcés and Eduardo Ascarrunz for the assistance in the analysis of landmarks; Guillermo Terán and Juan Marcos Mirande for suggestions on the analysis in TNT software; Programa de Pós-Graduação em Ciências Biológicas, Universidade Estadual de Londrina for financial support granted to LRJ; and all curators of the fish collections herein cited that loaned material for this study. We also thank the Willi Hennig Society for subsidizing the program TNT and making it freely available.

References

Adams DC, Rosenberg M. 1998. Partial warps, phylogeny, and ontogeny: a comment on Fink and Zelditch. Syst. 1995; Biol. 47: 168–173.

Adams DC, Rohlf FJ, Slice DE. Geometric morphometrics: ten years of progress following the ‘‘revolution’’. Ital. J. Zool. 2004; 71: 5–16.

Assega FM., Birindelli JLO, Bialetzki A, Shibatta, OA. External Morphology of *Lophiosilurus alexandri* Steindachner, 1876 during Early Stages of Development, and Its Implications for the Evolution of Pseudopimelodidae (Siluriformes). PloS one. 2016; 11(4), e0153123.

Bichuette ME, Rantin B, Hingst-Zaher E, Trajano, E. (2015). Geometric morphometrics throws light on evolution of the subterranean catfish *Rhamdiopsis krugi* (Teleostei: Siluriformes: Heptapteridae) in eastern Brazil. Biol. J. Linn. Soc**.** 2015; 114(1): 136-151.

Birindelli JLO, Shibatta OA. Morphology of the gas bladder in bumblebee catfishes (Siluriformes, Pseudopimelodidae). J Morphol. 2011; 272: 890-896.

Bookstein FL. Can biometrical shape be a homologous character? In: Hall BK, editor. Homology: the hierarchical basis of comparative biology. New York: Academic Press. 1994; 197–227.

Bookstein FL. Creases as morphometric characters. In: MacLeod N, Forey P, editors. Morphology, shape and phylogeny. Systematics association special volume series 64. London: Taylor & Francis. 2002; 139–174.

Britto MR. Análise filogenética da ordem Siluriformes com ênfase nas relações da superfamília Loricarioidea (Teleostei: Ostariophysi). [PhD Thesis]. São Paulo, SP: Universidade de São Paulo; 2002.

Caumul R, Polly PD. Phylogenetic and environmental components of morphological variation: skull, mandible, and molar shape in marmots (Marmota, Rodentia). Evolution. 2005; 59: 2460–2472.

Cardini, A, Elton, S. Does the skull carry a phylogenetic signal? Evolution and modularity in the guenons. Biol. J. Linn. Soc**.** 2007; 93: 813–83

Catalano SA, Goloboff PA. Simultaneously mapping and superimposing landmark configurations with parsimony as optimality criterion. Syst. Biol. 2012; 61: 392-400.

Catalano SA, Torres A. Phylogenetic inference based on landmark data in 41 empirical datasets. Zool Scripta. 2017; 46: 1-11.

Catalano SA, Goloboff PA, Giannini NP. Phylogenetic morphometrics (I): the use of landmark data in a phylogenetic framework. Cladistics, 2010; 26: 539–549.

Catalano SA, Ercoli M, Prevosti F. 2015. The More, the Better: The Use of Multiple Landmark Configurations to Solve the Phylogenetic Relationships in Musteloids. Syst. Biol. 2015; 64: 294-306.

Covain RS, Dray S, Fisch-Muller, Montoya-Burgos JI. Assessing phylogenetic dependence of morphological traits using co-inertia prior to investigate character evolution in Loricariinae catfishes. Mol. Phylogen. Evol. 2008; 46: 986-1002.

David B, Laurin B. Morphometrics and cladistics: measuring phylogeny in the sea urchin Echinocardium. Evolution. 1996; 50: 348–359.

Diogo R. Osteology and myology of the cephalic region and pectoral girdle of *Heptapterus mustelinus*, comparison with other Heptapterins, and discussion on the synapomorphies and phylogenetic relationships of the Heptapterinae and the Pimelodidae (Teleostei: Siluriformes). Int J Morphol. 2007; 25: 735-748.

Diogo R, Chardon M, Vandewalle P. Osteology and myology of the cephalic region and pectoral girdle of *Batrochoglanis raninus*, with a discussion on the synapomorphies and phylogenetic relationships of the Pseudopimelodinae and Pimelodidae (Teleostei: Siluriformes). Anim Biol. 2004; 54: 261-280.

Esguícero, ALH, Arcifa MS. Which is the best environment for the development of the early life stages of fish during the dryseason? Acta Limnologica Brasiliensia, 2010; 22: 267-275.

Farris J. The logical basis of phylogenetic analysis. In: Platnick NI, Funk VA, editors. Advances in cladistics II. New York, Columbia University Press. 1983; 7–36.

Ferraris Jr, CJ. Checklist of catfishes, recent and fossil (Osteichthyes: Siluriformes), and catalogue of siluriform primary types. Zootaxa 2007; 1418: 1-628.

Felsenstein J. Phylogenies and quantitative characters. Annu.Rev. Ecol. Syst. 1988; 19:455–471.

Felsenstein J. Quantitative characters, phylogenies, and morphometrics. In: MacLeod N, Forey PL, editors. Morphology, shape and phylogeny. London: Taylor & Francis. 2002; p. 27–44.

Goloboff, PA. Tree searches under Sankoff parsimony. Cladistics. 1998; 14: 229–237.

Goloboff PA, Catalano SA. Phylogenetic morphometrics (II): algorithms for landmark optimization. Cladistics, 2011; 27: 42–51.

Goloboff PA, Catalano SA. TNT version 1.5, including a full implementation of phylogenetic morphometrics. Cladistics. 2016; 32: 221-237.

Goloboff PA, Farris JS, Källersjö M, Oxelman B, Szumik CA. Improvements to resampling measures of group support. Cladistics, 2003; 19(4), 324-332.

Goloboff PA., Farris JS, Nixon KC. TNT, a free program for phylogenetic analysis. Cladistics. 2008; 24: 774-786.

Goloboff PA, Farris JS, Källersjö M., Oxelman B., Ramírez M.J., Szumik C.A. 2003. Improvements to resampling measures of group support. Cladistics 19: 324–332.

González-José R, Escapa I, Neves WA, Cúneo R, Pucciarelli HM. Cladistic analysis of continuous modularized traits provides phylogenetic signals in *Homo* evolution. Nature, 2008; 453 (7196), 775.

Gower JC. Generalized Procrustes analysis. Psychometrika 1975; 40: 33–51.

Hardman M. The phylogenetic relationships among nondiplomystid catfishes as inferred from mitochondrial cytochrome *b* sequences; the search for the ictalurid sister taxon (Otophysi: Siluriformes). Mol Phylogenet Evol 2005; 37: 700–720.

Jarduli LR; Shibatta OA. Description of a new species of *Microglanis* (Siluriformes: Pseudopimelodidae) from the Amazon basin, Amazonas State, Brazil. Neotrop Ichthyol. 2013; 11(3): 507-512.

Klingenberg P, Gidaszewski NA. Testing and quantifying phylogenetic signals and homoplasy in morphometric data. Syst. Biol. 2010; 59: 245–261.

Larson PM. Ontogeny, phylogeny, and morphology in anuran larvae: morphometric analysis of cranial development and evolution in *Rana tadpoles* (Anura: Ranidae). J. Morphol. 2005; 264:34–52. 35: 105-111

Lockwood CA, Kimbel WH, Lynch JM. Morphometrics and hominoid phylogeny: support for a chimpanzee-human clade and differentiation among great ape subspecies. Proc. Natl. Acad. Sci. USA. 2004; 101: 4356–4360.

Lundberg JG, Bornbusch AH, Mago-Leccia F. *Gladioglanis conquistador* N. Sp. from Ecuador with diagnoses of the subfamilies Rhamdiinae Bleeker and Pseudopimelodinae N. Subf. (Siluriformes: Pimelodidae). Copeia. 1991; 1991: 190-209.

Lycett SJ, Collard M. Do homoiologies impede phylogenetic analyses of the fossil hominids? An assessment based on extant papionin craniodental morphology. J. Hum. Evol. 2005; 49: 618–642.

MacLeod N. Phylogenetic signals in morphometric data. In: MacLeod N, Forey PL, editors. Morphology, shape and phylogeny. London: Taylor & Francis. 2002; 100–138.

Monteiro L. Why morphometrics is special: the problem with using partial warps as characters for phylogenetic inference. Syst. Biol. 2000; 49: 796–800.

Naylor G. Can partial warp scores be used as cladistic characters? In: Marcus LF., Corti M, Loy A, Naylor G, Slice DE, editors. Advances in morphometrics. New York: Plenum. 1996; p. 519–530.

Ollier S, Couteron P, Chessel D. Orthonormal transform to decompose the variance of a life-history trait across a phylogenetic tree. Biometrics 2006; 62: 471-477.

Ortega-Lara A, Lehmann P. Cruciglanis, a new genus of pseudopimelodid catfish (Ostariophysi, Siluriformes) with description of a new species from the Colombian Pacific coast. Neotrop Ichthyol. 2006; 4: 147-156.

Ospina-Garcés SM, Luna ED. Phylogenetic analysis of landmark data and the morphological evolution of cranial shape and diets in species of *Myotis* (Chiroptera: Vespertilionidae). Zoomorphology. 2017; 136(2): 251-265.

Perrard A, Lopez-Osorio F, Carpenter JM. Phylogeny, landmark analysis and the use of wing venation to study the evolution of social wasps (Hymenoptera: Vespidae: Vespinae). Cladistics 2016; 32: 406–425.

Polly PD. On morphological clocks and paleophylogeography: towards a timescale for Sorex hybrid zones. Genetica. 2001; 112–113: 339–357.

Rohlf FJ. On application of geometric morphometrics to studies of ontogeny and phylogeny. Syst. Biol. 1998; 47: 147–158.

Rohlf FJ. 2002. Geometric morphometrics and phylogeny. In: MacLeod N, Forey PL, editors. Morphology, shape, and phylogeny. London: Taylor & Francis. 2002; p. 175–193.

Rohlf FJ. tpsDig v.2.21. Distributed by the author, Department of Ecology and Evolution, State University of New York, Stony Brook, NY. 2015.

Rohlf FJ. tpsRelw v.1.65. Distributed by the author, Department of Ecology and Evolution, State University of New York, Stony Brook, NY. 2016.

Rohlf FJ, Slice D. Extensions of the Procrustes method for the optimal superimposition of landmarks. Syst. Zool. 1990; 39: 40–59.

Sankoff D, Rousseau P. Locating the vertices of a Steiner tree in an arbitrary space. Math. Program. 1975; 9: 240–246.

Shibatta OA. Sistemática e evolução da família Pseudopimelodidae (Ostariophysi, Siluriformes), com a revisão taxonômica do gênero *Pseudopimelodus*. [PhD Thesis]. São Carlos, SP: Universidade Federal de São Carlos; 1998.

Shibatta OA. Family Pseudopimelodidae (Bumblebee catfishes, dwarf marbled catfishes. In: Reis RE, Kullander SO, Ferraris Jr CJ, editors. Check List of the Freshwater Fishes of South and Central America. Porto Alegre: Edipucrs; 2003. 401-405.

Shibatta OA. A new species of *Microglanis* (Siluriformes: Pseudopimelodidae) from the upper Rio Tocantins basin, Goiás State, Central Brazil. Neotrop Ichthyol. 2014; 12: 81-87.

Shibatta OA. A new species of bumblebee catfish of the genus *Microglanis* (Siluriformes: Pseudopimelodidae) from upper Rio Paraguay basin, Brazil. Neotrop Ichthyol. 2016; 14(3): 525-532.

Shibatta OA, Pavanelli CS. Description of a new *Batrochoglanis* species (Siluriformes, Pseudopimelodidae) from the Rio Paraguai basin, State of Mato Grosso, Brazil. Zootaxa. 2005; 1092: 21-30.

Shibatta OA, Vari, RP. *Rhyacoglanis*, a new genus of Neotropical rheophilic catfishes, with four new species (Teleostei: Siluriformes Pseudopimelodidae) Neotrop Ichthyol. 2017; 15(2): e160132.

Smith GR. Homology in morphometrics and phylogenetics. In: Rohlf FJ, Bookstein FL, editors. Proceedings of the Michigan morphometrics workshop. Museum of Zoology, University of Michigan. Special Publication 2. 1990.

Stone JR. Mapping cladograms into morphospaces. Acta Zool. 2003; 84: 63–68.

Sullivan JP, Lundberg JG, Hardman M. A phylogenetic analysis of the major groups of catfishes (Teleostei: Siluriformes) using rag1 and rag2 nuclear gene sequences. Mol Phylogenet Evol. 2006; 41: 635-662.

Sullivan JP, Muriel-Cunha J, Lundberg JG. Phylogenetic relationship and molecular dating of the major groups of catfishes of the Neotropical superfamily Pimelodoidea (Teleostei, Siluriformes). Proc Acad Nat Sci Philadelphia. 2013; 162: 89-110.

Terán GE, Jarduli LR., Alonso F, Mirande, JM, Shibatta, OA. *Microglanis nigrolineatus*, a new species from northwestern Argentina (Ostariophysi: Pseudopimelodidae). Ichthyol. Explor. Freshw. 2016; 27(3): 193-202.

Zelditch ML, Fink WL, Swiderski D. Morphometrics, homology, and phylogenetics: quantified characters as synapomorphies. Syst. Biol. 1995: 44: 179–189.

Wenzel J. Phylogenetic analysis: the basic method. In: DeSalle R, Giribet G, Wheeler W, editors. Techniques in molecular systematics and evolution. Birkhäuser, Basel, 2002; 4–30.

CONCLUSÃO GERAL

A utilização da Análise de Landmark sob Parcimônia, apresenta uma abordagem satisfatória para tratar dados de morfometria geométrica. Essa área tem um enorme potencial não apenas como fonte de dados adicionais para a reconstrução filogenética dos grupos, mas para a compreensão detalhada de como se dá a evolução de características fenotípicas. As análises filogenéticas dos dados de morfometria geométrica isoladamente para as relações entre os gêneros de Pseudopimelodidae mostraram resultados incongruentes daqueles obtidos em estudos prévios. Homoplasias presentes na morfologia externa de Pseudopimelodidae, demostram que é possível que os caracteres morfométricos estejam respondendo a pressões seletivas semelhantes em clados diferentes. Os resultados obtidos através da análise filogenética de caracteres discretos e dados de landmark são uma demonstração de que é possível inserir caracteres quantitativos, sem que estes sejam discretizados a priori e, que se combinados com outras fontes de caracteres podem ser informativos. Dessa forma, a ferramenta da morfometria geométrica usando o LAUP para a reconstrução de estados ancestrais fornece informação filogenética trazendo novas sinapomorfias para a sistemática do grupo. Finalmente, o estudo mostra que o estudo detalhado da evolução da forma permite o reconhecimento dos pontos em que possíveis pressões evolutivas, moldaram a evolução morfológica dos pseudopimelodídeos.

A família apresenta um grande potencial para descoberta e descrição de novas espécies como as do gênero *Microglanis*, aumentando a compreensão sobre a distribuição do grupo na América do Sul e incorporando novos táxons nas análises filogenéticas futuras. A análise filogenética utilizando a morfologia externa do grupo, permitiu acrescentar o maior número de

espécies utilizadas até o momento para a família. Além disso é a primeira vez que essa metologia é utilizada para sistemática de peixes de água doce da região Neotropical.

Appendix 1. List of autapomorphies and synapomorphies from the phylogeny of the Pseudopimelodidae. List obtained from the parsimony analysis of combined discrete and landmark data of three configurations in TNT, under dynamic alignment (Fig. 3).

Autapomorphies

Rhamdia quelen:

No autapomorphies

Batrochoglanis acanthochiroides:

Char. 1: landmark(s) 0, 1, 2, 4, 5, 6, 9, 10, 12

Char. 2: landmark(s) 0, 1, 2, 3, 4, 5, 7

Char. 3: landmark(s) 0, 1, 2, 3, 4, 5, 7, 8, 10, 11

Batrochoglanis melanurus:

Char. 1: landmark(s) 2, 3, 4, 6, 9, 12, 13

Char. 2: landmark(s) 0, 1, 2, 3, 4, 5, 6, 7, 8, 9, 10, 11

Char. 3: landmark(s) 1, 4, 5, 6, 8, 9

Batrochoglanis raninus:

Char. 1: landmark(s) 0, 1, 3, 4, 5, 6, 7, 8, 10, 11, 12, 13

Char. 2: landmark(s) 0, 1, 2, 3, 4, 6, 8, 9, 10, 11

Char. 3: landmark(s) 0, 1, 3, 6, 7, 11

Batrochoglanis transmontanus:

Char. 1: landmark(s) 0, 2, 3, 4, 7, 8, 12, 13

Char. 2: landmark(s) 0, 2, 4, 5, 6, 8, 9, 11

Char. 3: landmark(s) 0, 1, 2, 3, 5, 7, 9, 10

Batrochoglanis villosus:

Char. 1: landmark(s) 0, 1, 2, 3, 5, 6, 7, 8, 9, 10, 11, 13

Char. 2: landmark(s) 1, 2, 3, 5, 7, 10

Char. 3: landmark(s) 0, 2, 3, 5, 6, 7, 8, 9, 10, 11

Cephalocilurus albomarginatus:

Char. 1: landmark(s) 1, 3, 4, 7, 8, 9, 10, 11, 12, 13

Char. 2: landmark(s) 0, 1, 2, 5, 6, 7, 8, 9, 11

Char. 3: landmark(s) 0, 1, 2, 10, 11

Cephalocilurus apurensis:

Char. 1: landmark(s) 0, 1, 2, 3, 4, 5, 6, 7, 8, 9, 10, 11, 12, 13

Char. 2: landmark(s) 0, 1, 2, 3, 4, 7, 8, 9, 10, 11

Char. 3: landmark(s) 0, 1, 2, 3, 4, 5, 6, 7, 8, 9, 10, 11

Cephalocilurus fowleri:

Char. 1: landmark(s) 1, 2, 3, 4, 9, 10, 11, 12, 13

Char. 2: landmark(s) 1, 2, 4, 5, 6, 7, 9, 10, 11

Char. 3: landmark(s) 1, 2, 3, 4, 5, 6, 7, 11

Cephalocilurus nigricaudus:

Char. 1: landmark(s) 0, 1, 2, 3, 7, 8, 9

Char. 2: landmark(s) 0, 1, 2, 3, 5, 6, 7, 9, 10, 11

Char. 3: landmark(s) 1, 2, 3, 4, 5, 7, 8, 9, 10, 11

Cruciglanis pacifici:

Char. 1: landmark(s) 3, 4, 9, 10, 13

Char. 2: landmark(s) 0, 1, 2, 3, 4, 5, 6, 7, 11

Char. 3: landmark(s) 2, 4, 5, 7, 8, 9, 10, 11

Char. 9: 0 > 1

Char. 17: 0 > 1

Lophiosilurus alexandri:

Char. 1: landmark(s) 0, 1, 2, 3, 4, 5, 6, 7, 8, 9, 10, 11, 12, 13

Char. 2: landmark(s) 1, 2, 3, 4, 5, 6, 8, 10, 11

Char. 3: landmark(s) 0, 2, 3, 4, 5, 6, 7, 8, 9, 10

Char. 14: 2 > 1

Microglanis carlae:

Char. 1: landmark(s) 2, 3, 4, 6, 7, 8, 9, 12, 13

Char. 2: landmark(s) 4, 5, 7, 8, 11

Char. 3: landmark(s) 0, 2, 6, 7, 8, 9, 10

Microglanis cibelae:

Char. 1: landmark(s) 5, 6, 8, 10, 12

Char. 2: landmark(s) 3, 4, 5, 7, 8, 9, 11

Char. 3: landmark(s) 0, 1, 4, 5, 6, 8, 9, 10, 11

Microglanis cottoides:

Char. 1: landmark(s) 0, 1, 2, 3, 4, 5, 6, 7, 9, 10, 11, 12, 13

Char. 2: landmark(s) 0, 1, 2, 3, 4, 5, 6, 7, 8, 9, 10, 11

Char. 3: landmark(s) 1, 2, 3, 4, 5, 7, 8, 9, 10, 11

Microglanis eurystoma:

Char. 1: landmark(s) 1, 2, 3, 4, 5, 6, 7, 9, 10, 11, 12, 13

Char. 2: landmark(s) 1, 2, 3, 4, 5, 6, 7, 8, 9, 10, 11

Char. 3: landmark(s) 1, 2, 3, 4, 5, 6, 7, 8, 9, 10, 11

Microglanis garavelloi:

Char. 1: landmark(s) 0, 1, 2, 4, 5, 6, 7, 8, 9

Char. 2: landmark(s) 0, 1, 3, 4, 5, 6, 7, 8, 9, 10, 11

Char. 3: landmark(s) 0, 1, 2, 3, 4, 5, 7, 8, 10

Microglanis iheringi:

Char. 1: landmark(s) 0, 1, 2, 3, 4, 5, 6, 7, 8, 9, 10, 11, 13

Char. 2: landmark(s) 2, 3, 4, 6, 7, 9, 10, 11

Char. 3: landmark(s) 0, 2, 5, 6, 7, 8

Microglanis leniceae:

Char. 1: landmark(s) 0, 1, 2, 3, 4, 7, 8, 9, 10, 11, 12

Char. 2: landmark(s) 1, 3, 7, 10

Char. 3: landmark(s) 0, 2, 3, 4, 5, 7, 8, 9, 11

Microglanis leptostriatus:

Char. 1: landmark(s) 3, 4, 10, 11, 13

Char. 2: landmark(s) 0, 1, 2, 3, 4, 6, 8, 10, 11

Char. 3: landmark(s) 0, 1, 2, 5, 6, 7, 10, 11

Microglanis lundbergi:

Char. 1: landmark(s) 0, 1, 2, 3, 5, 6, 7, 8, 9, 10, 11, 12

Char. 2: landmark(s) 0, 1, 2, 3, 4, 5, 6, 7, 8, 9

Char. 3: landmark(s) 0, 1, 2, 3, 4, 5, 6, 7, 9, 11

Microglanis maculatus:

Char. 1: landmark(s) 0, 1, 2, 3, 4, 5, 7, 8, 9, 10, 11, 12

Char. 2: landmark(s) 1, 2, 3, 5, 6, 7, 8, 9, 10

Char. 3: landmark(s) 0, 1, 2, 3, 4, 5, 6, 8, 10, 11

Microglanis malabarbai:

Char. 1: landmark(s) 0, 1, 2, 4, 6, 7, 8, 9, 13

Char. 2: landmark(s) 0, 5, 6, 7, 8, 9, 11

Char. 3: landmark(s) 1, 2, 6, 7, 8, 9, 10

Microglanis nigripinnis:

Char. 1: landmark(s) 4, 5, 6, 7, 8, 9, 10, 11, 13

Char. 2: landmark(s) 0, 2, 3, 5, 7, 8, 9, 10, 11

Char. 3: landmark(s) 1, 2, 3, 4, 6, 8, 9, 10, 11

Microglanis nigrolineatus:

Char. 1: landmark(s) 0, 1, 2, 3, 5, 6, 7, 8, 9, 10, 11, 12, 13

Char. 2: landmark(s) 0, 1, 2, 3, 6, 8, 9, 10, 11

Char. 3: landmark(s) 0, 1, 2, 3, 4, 5, 6, 7, 8, 10, 11

Microglanis oliveirai:

Char. 1: landmark(s) 0, 1, 2, 4, 5, 6, 7, 9, 10, 11, 12, 13

Char. 2: landmark(s) 0, 1, 3, 4, 5, 6, 7, 8, 9, 11

Char. 3: landmark(s) 0, 1, 2, 3, 4, 6, 7, 8, 9, 11

Microglanis parahybae:

Char. 1: landmark(s) 0, 2, 3, 5, 6, 7, 8, 9, 10, 11, 12, 13

Char. 2: landmark(s) 2, 3, 4, 5, 6, 7, 8, 9, 10

Char. 3: landmark(s) 0, 1, 2, 3, 5, 6, 7, 8, 9, 10, 11

Microglanis pataxo:

Char. 1: landmark(s) 0, 1, 2, 4, 5, 6, 7, 8, 11, 12, 13

Char. 2: landmark(s) 0, 1, 3, 4, 5, 6, 7, 8, 10

Char. 3: landmark(s) 0, 1, 2, 3, 4, 6, 7, 8, 9, 10, 11

Microglanis poecilus:

Char. 1: landmark(s) 1, 2, 3, 4, 5, 6, 7, 8, 9, 10, 11, 12, 13

Char. 2: landmark(s) 0, 1, 4, 7, 8, 9, 10, 11

Char. 3: landmark(s) 1, 2, 4, 7, 8, 9, 10

Microglanis robustus:

Char. 1: landmark(s) 0, 1, 3, 5, 6, 7, 8, 9, 10, 12

Char. 2: landmark(s) 0, 1, 2, 4, 5, 7, 9, 10

Char. 3: landmark(s) 0, 1, 2, 3, 4, 5, 6, 7, 8, 10, 11

Microglanis secundus:

Char. 1: landmark(s) 0, 1, 2, 3, 5, 6, 7, 8, 10, 11, 12, 13

Char. 2: landmark(s) 0, 1, 2, 3, 4, 6, 7, 8, 9, 10, 11

Char. 3: landmark(s) 0, 1, 2, 4, 5, 6, 7, 8, 9

Microglanis variegatus:

Char. 1: landmark(s) 0, 3, 5, 8, 11, 12

Char. 2: landmark(s) 0, 4, 5, 6, 8

Char. 3: landmark(s) 1, 2, 3, 4, 5, 6, 7, 9, 10, 11

Microglanis xylographicus:

Char. 1: landmark(s) 0, 2, 4, 5, 6, 7, 8, 10, 11

Char. 2: landmark(s) 2, 5, 6, 7, 8, 9, 11

Char. 3: landmark(s) 1, 3, 4, 6, 7, 8, 10, 11

Microglanis pellopterygius:

Char. 1: landmark(s) 1, 2, 3, 4, 5, 7, 8, 9, 10

Char. 2: landmark(s) 0, 1, 3, 6, 7, 8, 9, 10

Char. 3: landmark(s) 0, 1, 2, 3, 4, 5, 6, 8, 9, 10, 11

Pseudopimelodus bufonius:

Char. 1: landmark(s) 1, 2, 3, 4, 5, 6, 7, 8, 9, 10, 11, 12, 13

Char. 2: landmark(s) 0, 2, 4, 5, 6, 7, 8, 9, 11

Char. 3: landmark(s) 2, 3, 4, 5, 6, 7, 8, 9, 10

Pseudopimelodus charus:

Char. 1: landmark(s) 0, 2, 3, 4

Char. 2: landmark(s) 4, 5, 6, 7, 8, 9, 10, 11

Char. 3: landmark(s) 0, 3, 4, 8, 11

Pseudopimelodus mangurus:

Char. 1: landmark(s) 1, 3, 4, 6, 8, 9, 10, 11, 12, 13

Char. 2: landmark(s) 0, 1, 2, 3, 4, 5, 7, 8

Char. 3: landmark(s) 0, 1, 2, 3, 5, 6, 7, 8, 9, 10, 11

Pseudopimelodus schultzi:

Char. 1: landmark(s) 0, 2, 3, 4, 6, 7, 9, 10, 11, 12, 13

Char. 2: landmark(s) 0, 1, 2, 3, 6, 8, 10, 11

Char. 3: landmark(s) 0, 1, 2, 3, 4, 5, 6, 7, 8, 9, 11

Rhyacoglanis paranae:

Char. 1: landmark(s) 0, 3, 4, 5, 6, 7, 8, 9, 10, 11

Char. 2: landmark(s) 0, 1, 3, 4, 6, 7, 9, 10, 11

Char. 3: landmark(s) 0, 1, 2, 3, 5, 6, 7, 10

Rhyacoglanis epiblepsis:

Char. 1: landmark(s) 0, 1, 2, 3, 4, 5, 6, 7, 8, 11, 12, 13

Char. 2: landmark(s) 0, 1, 2, 4, 5, 7, 8, 9, 10, 11

Char. 3: landmark(s) 1, 2, 3, 4, 5, 6, 7, 8, 9, 10, 11

Char. 17: 0 > 1

Rhyacoglanis seminiger:

Char. 1: landmark(s) 0, 4, 9, 10, 11, 12, 13

Char. 2: landmark(s) 1, 2, 3, 5, 6, 8, 9, 10, 11

Char. 3: landmark(s) 0, 1, 2, 3, 4, 5, 6, 11

Char. 4: 0 > 1

Steindachneridion melanodermatum:

Char. 1: landmark(s) 0, 1, 2, 3, 4, 5, 9, 10

Char. 2: landmark(s) 0, 2, 3, 4, 5, 11

Char. 3: landmark(s) 1, 2, 3, 7, 8, 9, 10

Steindachneridion parahybae:

Char. 1: landmark(s) 1, 4, 5, 6, 7, 8, 11, 13

Char. 2: landmark(s) 0, 3, 6, 7, 8, 10, 11

Char. 3: landmark(s) 3, 6, 8, 9, 10, 11

Steindachneridion scripta:

Char. 1: landmark(s) 0, 1, 2, 3, 4, 5, 6, 7, 8, 9, 10, 11, 12, 13

Char. 2: landmark(s) 0, 1, 2, 3, 4, 5, 6, 7, 8, 9, 10, 11

Char. 3: landmark(s) 0, 1, 3, 4, 5, 6, 7, 8, 9, 10, 11

Synapomorphies

Node 1:

No autapomorphies

Node 2:

Char. 1: landmark(s) 0, 3, 10, 11, 12

Char. 2: landmark(s) 0, 1, 2, 3, 5, 6, 7, 9, 10

Char. 3: landmark(s) 1, 2, 4, 5, 6, 9, 10

Node 3:

Char. 1: landmark(s) 3, 4, 12, 13

Char. 2: landmark(s) 1, 3, 5, 7, 8, 9, 10, 11

Char. 3: landmark(s) 4, 5, 10, 11

Node 4:

Char. 1: landmark(s) 1, 2, 5, 6, 9, 10, 11, 12

Char. 2: landmark(s) 2, 3, 7, 8, 9

Char. 5: 0 > 1

Char. 15: 0 > 1

Node 5:

Char. 1: landmark(s) 0, 1, 2, 3, 4, 5, 6, 7, 8, 9, 10, 11, 12

Char. 2: landmark(s) 1, 2, 4, 7, 8, 11

Char. 3: landmark(s) 4, 7, 8, 9, 10

Char. 7: 0 > 1

Node 6:

Char. 1: landmark(s) 1, 2, 3, 4, 11, 12, 13

Char. 2: landmark(s) 0, 4, 5, 6, 8, 9, 10

Char. 3: landmark(s) 1, 7, 8, 9, 10, 11

Node 7:

Char. 1: landmark(s) 1, 2, 4, 7, 8, 10

Char. 2: landmark(s) 0, 2, 3, 4, 7, 9, 11

Char. 3: landmark(s) 0, 2, 3, 5, 6, 11

Char. 8: 0 > 1

Char. 13: 2 > 1

Node 8:

Char. 1: landmark(s) 0, 1, 2, 5, 6, 7, 8, 11, 12, 13

Char. 2: landmark(s) 1, 2, 6, 11

Char. 3: landmark(s) 0, 1, 2, 3, 5, 6, 7, 8, 10

Char. 13: 0 > 1

Node 9:

Char. 1: landmark(s) 0, 1, 2, 3, 4, 5, 6, 7, 8, 10, 12, 13

Char. 2: landmark(s) 7, 8, 9, 10

Char. 3: landmark(s) 8, 10, 11

Node 10:

Char. 1: landmark(s) 0, 2, 4, 5, 6, 10, 11, 12

Char. 2: landmark(s) 0, 1, 2, 3, 4, 9, 10

Char. 3: landmark(s) 1, 2, 5, 8, 11

Node 11:

Char. 1: landmark(s) 3, 4, 5, 6, 7, 8, 9, 10

Char. 2: landmark(s) 1, 4, 7, 11

Char. 3: landmark(s) 0, 1, 2, 3, 4, 6, 7, 8, 9, 10

Char. 14: 0 > 2

Node 12:

Char. 1: landmark(s) 0, 1, 2, 5, 6, 9, 13

Char. 2: landmark(s) 1, 2, 3, 4, 5, 6, 9, 10

Char. 3: landmark(s) 5, 6, 7, 9, 10

Char. 4: 0 > 1

Char. 13: 0 > 1

Node 13:

Char. 1: landmark(s) 0, 1, 2, 5, 6, 12

Char. 2: landmark(s) 2, 3, 5, 7, 8, 9

Char. 3: landmark(s) 0, 1, 2, 4, 5, 7, 9, 11

Node 14:

Char. 1: landmark(s) 4, 6, 7, 8, 11

Char. 2: landmark(s) 0, 2, 3, 4, 5, 6, 7, 8

Char. 3: landmark(s) 0, 3, 6, 9, 11

Node 15:

Char. 1: landmark(s) 5, 6, 7, 8

Char. 2: landmark(s) 0, 4, 5, 8, 9, 11

Char. 3: landmark(s) 1, 2, 6, 7, 8, 9, 10, 11

Node 16:

Char. 1: landmark(s) 0, 1, 2, 3, 4, 5, 6, 7, 8, 13

Char. 2: landmark(s) 1, 5, 6, 9, 10

Char. 3: landmark(s) 1, 2, 3, 4, 6, 9

Char. 12: 0> 1

Node 17:

Char. 1: landmark(s) 4, 5, 6

Char. 3: landmark(s) 2, 3, 4, 7, 8

Char. 6: 0 > 1

Char. 8: 0 > 1

Char. 9: 0 > 2

Char. 17: 0 > 1

Node 18:

Char. 1: landmark(s) 0, 1, 2, 3, 10

Char. 2: landmark(s) 0, 1, 2, 3, 4, 9, 10, 11

Char. 3: landmark(s) 6, 9, 11

Node 19:

Char. 1: landmark(s) 1, 2, 4, 5, 7, 8, 9, 10, 11, 12, 13

Char. 2: landmark(s) 4, 7, 8

Char. 3: landmark(s) 3, 4, 8, 10

Node 20:

Char. 1: landmark(s) 3, 4, 6

Char. 2: landmark(s) 4, 7, 10

Char. 3: landmark(s) 0, 2, 4, 5, 7, 8, 9, 10, 11

Node 21:

Char. 1: landmark(s) 6, 8, 11, 12

Char. 2: landmark(s) 2, 3, 6, 7, 8

Char. 3: landmark(s) 3, 5, 7, 8, 11

Node 22:

Char. 1: landmark(s) 1, 2, 3, 4, 5, 6, 7, 8, 11, 13

Char. 2: landmark(s) 1, 2, 3, 5, 9, 11

Char. 3: landmark(s) 2, 4

Char. 11: 1 > 0

Char. 14: 2 > 3

Char. 16: 0 > 2

Char. 17: 1 > 2

Node 23:

Char. 1: landmark(s) 0, 2, 3, 4, 6, 11, 13

Char. 2: landmark(s) 0, 1, 2, 3, 4, 6, 7, 9, 11

Char. 3: landmark(s) 6, 11

Node 24:

Char. 1: landmark(s) 0, 1, 3, 4, 7, 8, 13

Char. 2: landmark(s) 1, 2, 3, 4, 7, 8, 9, 10

Char. 3: landmark(s) 1, 2, 3, 4, 5, 6, 8

Node 25:

Char. 1: landmark(s) 0, 11, 12

Char. 2: landmark(s) 0, 4

Char. 3: landmark(s) 0, 1, 2, 3, 4, 5, 7, 8, 10, 11

Node 26:

Char. 1: landmark(s) 1, 2, 4, 5, 10, 11, 12

Char. 2: landmark(s) 1, 7, 8

Char. 3: landmark(s) 4, 9, 10

Node 27:

Char. 1: landmark(s) 0, 1, 2, 3, 4, 5, 7, 8, 12, 13

Char. 2: landmark(s) 1, 2, 3, 9, 10

Char. 3: landmark(s) 0, 1, 3, 8, 9, 10

Node 28:

Char. 1: landmark(s) 0, 1, 2, 7, 8, 9, 10, 11, 12

Char. 2: landmark(s) 0, 1, 2, 3, 5, 6, 8, 10, 11

Char. 3: landmark(s) 0, 4, 6

Node 29:

Char. 1: landmark(s) 0, 1, 2, 3, 4, 6, 7, 8, 9, 10, 13

Char. 2: landmark(s) 0, 3, 6, 7, 8, 9, 10

Char. 3: landmark(s) 1, 2, 3, 4, 5, 6, 7

Node 30:

Char. 1: landmark(s) 0, 2, 4, 6, 8, 9, 10, 11, 12

Char. 2: landmark(s) 0, 1, 2, 4, 5, 6, 7, 8, 9, 10

Char. 3: landmark(s) 0, 1, 2, 6

Node 31:

Char. 1: landmark(s) 0, 1, 2, 5, 6, 10, 13

Char. 2: landmark(s) 3, 4, 8, 9, 11

Char. 3: landmark(s) 0, 5, 6, 7, 11

Node 32:

Char. 1: landmark(s) 1, 5, 8, 10, 12

Char. 2: landmark(s) 0, 3, 6, 7, 8

Char. 3: landmark(s) 0, 2, 5, 7, 9, 10, 11

Node 33:

Char. 1: landmark(s) 0, 1, 10, 13

Char. 2: landmark(s) 0, 2, 3, 5, 6, 9

Char. 3: landmark(s) 1, 5

Node 34:

Char. 1: landmark(s) 3, 4, 10

Char. 2: landmark(s) 0, 1, 4, 5, 6, 7, 8, 9, 10, 11

Char. 3: landmark(s) 1, 3, 5, 7, 8

Node 35:

Char. 1: landmark(s) 3, 4, 9, 10

Char. 2: landmark(s) 0, 1, 2, 6, 8, 9, 10, 11

Char. 3: landmark(s) 0, 2, 5, 6, 10

Node 36:

Char. 1: landmark(s) 3, 4, 6, 7, 8, 9

Char. 2: landmark(s) 2, 3, 4, 7, 8, 9

Char. 3: landmark(s) 1, 2, 3, 4, 7, 9, 10

Node 37:

Char. 1: landmark(s) 0, 4, 9, 10, 13

Char. 2: landmark(s) 4, 5, 11

Char. 3: landmark(s) 1, 4, 7, 8, 9, 10

Node 38:

Char. 1: landmark(s) 8, 9, 10, 13

Char. 2: landmark(s) 2, 3, 6, 9

Char. 3: landmark(s) 0, 1, 3, 4, 5, 6, 9, 10

Node 39:

Char. 1: landmark(s) 3, 9, 13

Char. 2: landmark(s) 0, 2, 3, 6, 8, 10

Char. 3: landmark(s) 1, 2, 3, 4, 6, 10, 11

Node 40:

Char. 1: landmark(s) 1, 4, 5, 6, 9, 11, 12

Char. 2: landmark(s) 0, 2, 3, 5, 8, 10, 11

Char. 3: landmark(s) 0, 3, 8, 11

Node 41:

Char. 1: landmark(s) 0, 2, 3, 4, 5, 6, 8, 11

Char. 2: landmark(s) 1, 2, 4, 6, 7, 8, 10, 11

Char. 3: landmark(s) 8, 9, 11

Node 42:

Char. 1: landmark(s) 3, 4, 12, 13

Char. 2: landmark(s) 1, 3, 5, 7, 8, 9, 10, 11

Char. 3: landmark(s) 4, 5, 10, 11

Appendix 2. Character mapping. The ancestral configurations are in gray dotted lines. Red line represents reconstructed shapes. Blue line indicates the change in position of each landmark from the ancestor to the corresponding node a) character 1; b) character 2; c) character 3.

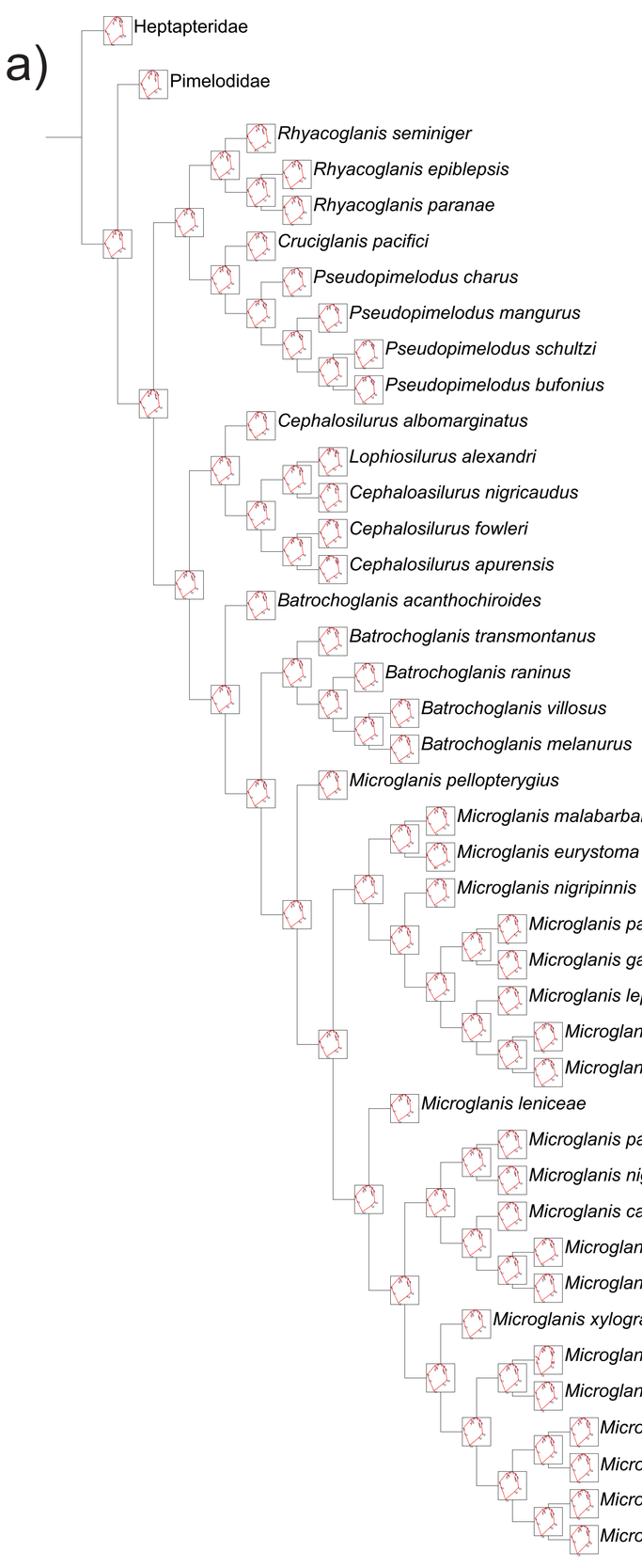

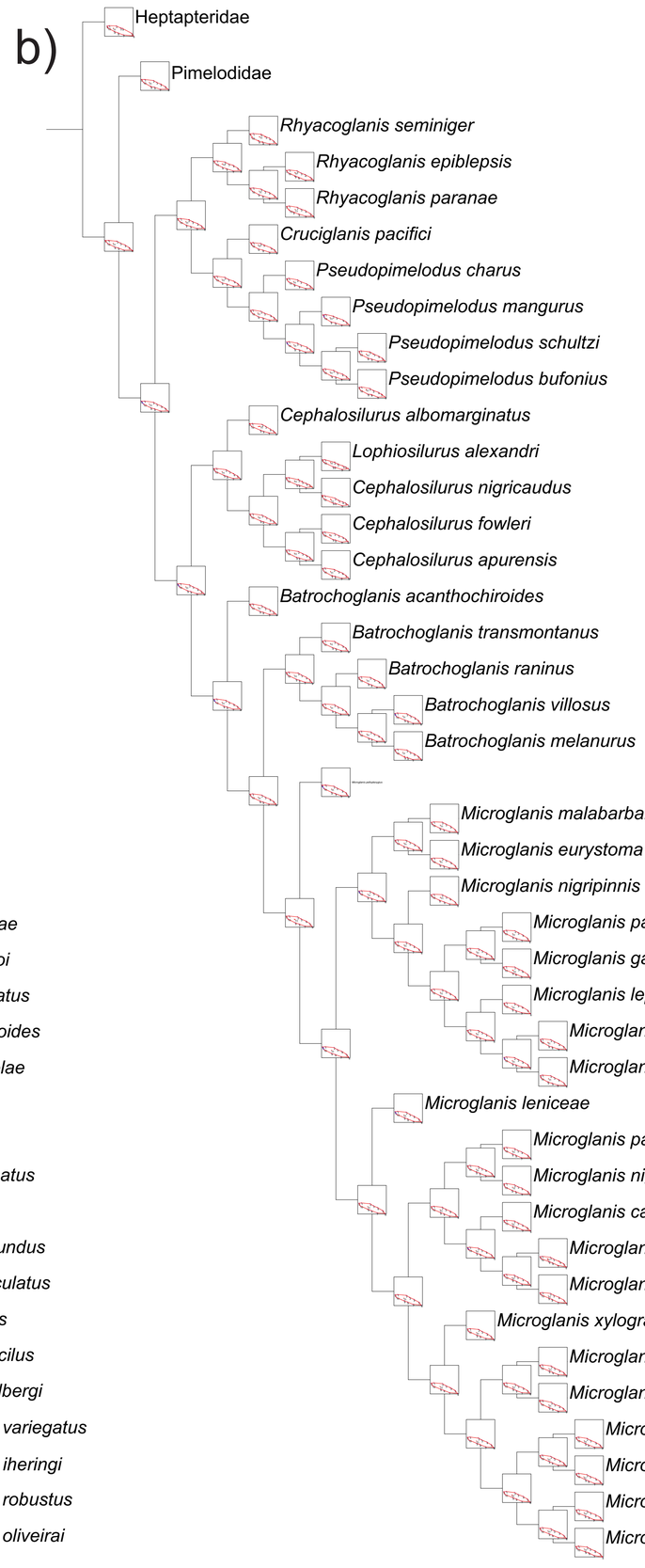

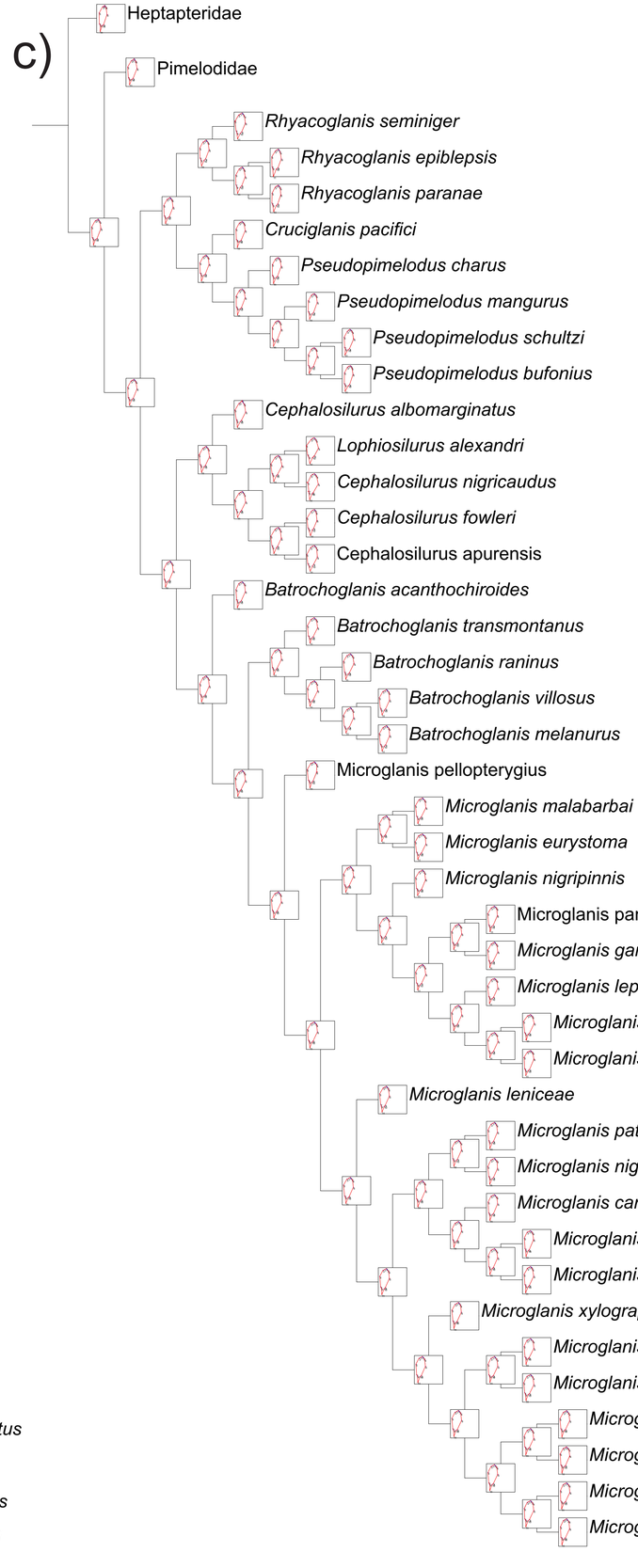

Appendix 3. Dataset in TNT format with combined matrix, user defined wireframe and best tree obtained considering the three configurations with dynamic alignment and discrete characters. Missing data or character inapplicable to particular taxa are indicated by "?".

nstates 16 ;

'Bloque 1 = Dorsal

Bloque 2 = Lateral

Bloque 3 = Ventral

'Data saved from TNT'

xread

17 44

&[landmark 2D]

Rhamdia quelen +0.07077,+0.19034 +0.01689,+0.19380 +0.12066,+0.16494 -0.03759,+0.16032 +0.15599,+0.10950 +0.00397,+0.13159 +0.10408,+0.10444 -0.05690,+0.04303 +0.11844,-0.00229 -0.24069,-0.13218 +0.19146,-0.24161 -0.18850,-0.19897 +0.11185,-0.26372 -0.09561,-0.45400

Batrochoglanis acanthochiroides +0.07346,+0.18955 -0.01561,+0.19640 +0.14368,+0.15540 -0.07503,+0.15513 +0.17500,+0.08225 -0.02502,+0.11154 +0.11091,+0.07564 -0.07111,+0.06694 +0.13148,+0.01528 -0.25478,-0.07310 +0.20743,-0.20573 -0.18602,-0.21710 +0.08869,-0.29299 -0.08776,-0.42784

Batrochoglanis melanurus +0.06911,+0.18580 -0.01971,+0.19078 +0.14210,+0.14457 -0.07112,+0.14746 +0.16733,+0.07663 -0.02235,+0.11605 +0.11308,+0.08066 -0.07762,+0.06887 +0.13914,+0.00918 -0.26594,-0.08609 +0.21298,-0.21408 -0.19824,-0.20580 +0.11970,-0.29529 -0.07314,-0.41761

Batrochoglanis raninus +0.06725,+0.19235 -0.02166,+0.19065 +0.14366,+0.14501 -0.08267,+0.14541 +0.17459,+0.08178 -0.01960,+0.11782 +0.11869,+0.07759 -0.07834,+0.06947 +0.14524,+0.00949 -0.25770,-0.08070 +0.21350,-0.21660 -0.20682,-0.20982 +0.12736,-0.29678 -0.06836,-0.40272

Batrochoglanis transmontanus +0.06919,+0.18494 -0.01934,+0.19057 +0.15010,+0.14775 -0.07666,+0.14563 +0.17482,+0.09054 -0.02457,+0.11606 +0.11573,+0.07955 -0.06903,+0.06788 +0.13683,+0.01311 -0.25563,-0.08389 +0.20800,-0.21088 -0.19388,-0.20867 +0.10284,-0.28216 -0.09252,-0.42889

Batrochoglanis villosus +0.06594,+0.18426 -0.02004,+0.18417 +0.14867,+0.14104 -0.07233,+0.14885 +0.17134,+0.08301 -0.02683,+0.12025 +0.12144,+0.08421 -0.08005,+0.06435 +0.13678,+0.00437 -0.25382,-0.07733 +0.21415,-0.21381 -0.19573,-0.20590 +0.10844,-0.28935 -0.08572,-0.42726

Cephalocilurus albomarginatus +0.07111,+0.18551 -0.02330,+0.19486 +0.14963,+0.14558 -0.07134,+0.15650 +0.17196,+0.08809 -0.02118,+0.12004 +0.11629,+0.08226 -0.07483,+0.07049 +0.13736,+0.01170 -0.24876,-0.09523 +0.18673,-0.20182 -0.21361,-0.22187 +0.11377,-0.30061 -0.07902,-0.41187

Cephalocilurus apurensis +0.06379,+0.17623 -0.03993,+0.18834 +0.15595,+0.13719 -0.08966,+0.15264 +0.18189,+0.07844 -0.04288,+0.12859 +0.13550,+0.08148 -0.08772,+0.09652 +0.15812,+0.02904 -0.25767,-0.08559 +0.21003,-0.20710 -0.18731,-0.21413 +0.09890,-0.29695 -0.07567,-0.40022

Cephalocilurus fowleri +0.07017,+0.18231 -0.01785,+0.19022 +0.15170,+0.14732 -0.06915,+0.15149 +0.17274,+0.09075 -0.03270,+0.12517 +0.12416,+0.08611 -0.08009,+0.07925 +0.13841,+0.02592 -0.23660,-0.10108 +0.20113,-0.20177 -0.17945,-0.22893 +0.08346,-0.28860 -0.09852,-0.43144

Cephalocilurus nigricaudus +0.07701,+0.19619 -0.02800,+0.19493 +0.15610,+0.15408 -0.07671,+0.15396 +0.17923,+0.09538 -0.02389,+0.12482 +0.12384,+0.08714 -0.06846,+0.05387 +0.12076,+0.00597 -0.23911,-0.09571 +0.20605,-0.20681 -0.17874,-0.22019 +0.08615,-0.29032 -0.08808,-0.42473

Cruciglanis pacifici +0.07173,+0.19110 -0.00545,+0.16931 +0.12566,+0.13256 -0.08091,+0.15558 +0.17974,+0.09156 -0.01295,+0.11027 +0.10659,+0.07877 -0.06132,+0.07462 +0.13251,+0.02115 -0.24843,-0.08118 +0.20839,-0.19425 -0.19660,-0.21329 +0.10917,-0.29737 -0.09262,-0.44589

Lophiosilurus alexandri +0.06474,+0.16626 -0.02226,+0.16982 +0.13825,+0.12229 -0.07546,+0.16666 +0.17956,+0.09617 -0.02107,+0.14229 +0.12619,+0.09770 -0.04661,+0.06985 +0.11172,+0.02546 -0.27089,-0.07987 +0.22505,-0.21260 -0.16488,-0.23527 +0.07065,-0.30043 -0.08880,-0.42825

Microglanis carlae +0.07304,+0.18850 -0.00111,+0.19279 +0.13259,+0.15702 -0.07000,+0.16585 +0.17972,+0.08699 -0.03429,+0.10680 +0.12452,+0.05952 -0.08155,+0.06244 +0.13980,-0.00133 -0.26312,-0.05917 +0.21860,-0.19666 -0.21040,-0.18731 +0.12567,-0.27361 -0.08584,-0.42608

Microglanis cibelae +0.06661,+0.17766 -0.00432,+0.18181 +0.12974,+0.14613 -0.07244,+0.15464 +0.17556,+0.08368 -0.03203,+0.11217 +0.12779,+0.06431 -0.08075,+0.07186 +0.14843,+0.00429 -0.25871,-0.03152 +0.23140,-0.18128 -0.22227,-0.18522 +0.13507,-0.28213 -0.09360,-0.43399

Microglanis cottoides +0.06505,+0.17003 +0.00065,+0.17442 +0.12495,+0.13640 -0.05496,+0.15870 +0.16759,+0.08713 -0.02954,+0.10806 +0.12013,+0.06413 -0.08141,+0.07242 +0.14713,+0.00535 -0.25335,-0.02709 +0.22127,-0.17867 -0.20861,-0.17257 +0.13207,-0.27910 -0.09277,-0.47892

Microglanis eurystoma +0.07296,+0.18968 -0.00702,+0.19474 +0.13932,+0.15430 -0.09006,+0.16568 +0.19054,+0.07960 -0.02348,+0.11425 +0.11204,+0.07565 -0.09110,+0.06270 +0.14493,-0.00446 -0.27421,-0.06797 +0.22697,-0.21930 -0.21361,-0.19974 +0.10733,-0.29440 -0.07667,-0.37601

Microglanis garavelloi +0.07348,+0.19384 +0.00130,+0.19630 +0.13701,+0.15601 -0.06630,+0.15671 +0.16884,+0.08901 -0.03131,+0.10238 +0.12316,+0.05667 -0.06393,+0.06010 +0.13193,-0.00226 -0.26275,-0.05901 +0.21151,-0.18838 -0.21828,-0.18455 +0.12310,-0.27149 -0.09151,-0.44267

Microglanis iheringi +0.07118,+0.19009 +0.00195,+0.18545 +0.13049,+0.14204 -0.06880,+0.15969 +0.17500,+0.08649 -0.03196,+0.11619 +0.12125,+0.07405 -0.07988,+0.06430 +0.14161,+0.00451 -0.24742,-0.06513 +0.20800,-0.18164 -0.20225,-0.17455 +0.12032,-0.27547 -0.10050,-0.46089

Microglanis leniceae +0.06814,+0.20213 -0.00244,+0.18702 +0.13140,+0.15278 -0.06472,+0.17277 +0.18047,+0.08766 -0.03243,+0.10848 +0.12134,+0.06259 -0.07595,+0.06253 +0.13459,-0.00122 -0.25526,-0.04477 +0.20356,-0.19547 -0.20661,-0.18211 +0.12505,-0.28560 -0.09105,-0.43452

Microglanis leptostriatus +0.07093,+0.18442 -0.00232,+0.18959 +0.13394,+0.14809 -0.07811,+0.15772 +0.18305,+0.08056 -0.03138,+0.11106 +0.12265,+0.06750 -0.07877,+0.06569 +0.14023,+0.00311 -0.26383,-0.04115 +0.22653,-0.18339 -0.22868,-0.18860 +0.13202,-0.27954 -0.08231,-0.42228

Microglanis lundbergi +0.07348,+0.19304 +0.00232,+0.19465 +0.13465,+0.15607 -0.07410,+0.14873 +0.17887,+0.08201 -0.03549,+0.10252 +0.12097,+0.05854 -0.07860,+0.06187 +0.13506,+0.00435 -0.24642,-0.04283 +0.22121,-0.16680 -0.20530,-0.18376 +0.11590,-0.26489 -0.10274,-0.46691

Microglanis maculatus +0.07666,+0.19615 -0.00203,+0.19562 +0.14032,+0.15867 -0.06384,+0.15907 +0.17253,+0.09496 -0.03573,+0.10545 +0.11746,+0.06321 -0.07648,+0.06427 +0.12830,+0.00852 -0.25048,-0.08762 +0.20284,-0.21032 -0.20382,-0.18833 +0.11793,-0.27855 -0.09234,-0.43203

Microglanis malabarbai +0.06809,+0.18127 -0.01135,+0.19231 +0.13946,+0.14195 -0.08166,+0.16041 +0.18265,+0.07556 -0.02573,+0.11470 +0.12725,+0.06682 -0.08390,+0.06881 +0.15072,-0.00275 -0.26440,-0.04424 +0.20715,-0.20493 -0.21639,-0.18593 +0.12422,-0.28364 -0.07180,-0.42418

Microglanis nigripinnis +0.07330,+0.19115 -0.00411,+0.19287 +0.13851,+0.15189 -0.07690,+0.15777 +0.17791,+0.07755 -0.01782,+0.11881 +0.11943,+0.07898 -0.06748,+0.05706 +0.12992,-0.00032 -0.26429,-0.05895 +0.20257,-0.20988 -0.21560,-0.17998 +0.12465,-0.28354 -0.08270,-0.42694

Microglanis nigrolineatus +0.07505,+0.19134 +0.00176,+0.19718 +0.13457,+0.15603 -0.07964,+0.14745 +0.18167,+0.07916 -0.03087,+0.10025 +0.11577,+0.06059 -0.07260,+0.05929 +0.12724,+0.00441 -0.25974,-0.04033 +0.23601,-0.18008 -0.20736,-0.20388 +0.11138,-0.29100 -0.09223,-0.42756

Microglanis oliveirai +0.07209,+0.19687 -0.00571,+0.19499 +0.13862,+0.14814 -0.07475,+0.15537 +0.16979,+0.08207 -0.03193,+0.11432 +0.12253,+0.06544 -0.07739,+0.07271 +0.13844,+0.00486 -0.24732,-0.05310 +0.18111,-0.19380 -0.19005,-0.17048 +0.11321,-0.26503 -0.10258,-0.47732

Microglanis parahybae +0.07505,+0.19244 +0.00088,+0.19640 +0.12974,+0.15538 -0.05866,+0.15418 +0.17091,+0.08622 -0.03689,+0.10906 +0.12400,+0.06845 -0.08173,+0.05756 +0.13229,-0.00256 -0.24768,-0.04488 +0.20383,-0.18363 -0.20317,-0.18698 +0.11461,-0.26401 -0.08929,-0.47012

Microglanis pataxo +0.07278,+0.18701 -0.00715,+0.19172 +0.13680,+0.15445 -0.07989,+0.14917 +0.18800,+0.07597 -0.03602,+0.10896 +0.13173,+0.06723 -0.08232,+0.06298 +0.14148,+0.00481 -0.26148,-0.05516 +0.22250,-0.19182 -0.20774,-0.17120 +0.12301,-0.26783 -0.09408,-0.43839

Microglanis poecilus +0.07313,+0.19326 -0.01678,+0.19315 +0.14650,+0.15541 -0.08177,+0.15291 +0.18554,+0.07907 -0.03948,+0.11689 +0.12971,+0.06757 -0.08448,+0.07148 +0.14590,+0.00675 -0.17808,-0.09038 +0.13888,-0.18708 -0.22069,-0.18998 +0.12914,-0.28462 -0.10830,-0.48072

Microglanis robustus +0.07475,+0.19025 -0.00062,+0.18652 +0.13581,+0.15467 -0.08479,+0.14200 +0.17531,+0.08022 -0.03521,+0.10800 +0.12167,+0.06994 -0.07688,+0.05817 +0.13873,+0.00899 -0.24687,-0.04478 +0.22104,-0.17531 -0.20224,-0.17525 +0.12036,-0.25380 -0.10308,-0.47685

Microglanis secundus +0.07273,+0.18627 -0.00297,+0.18926 +0.13559,+0.14894 -0.07030,+0.15487 +0.17782,+0.08629 -0.02955,+0.10936 +0.11139,+0.07199 -0.07835,+0.06941 +0.13566,+0.01582 -0.25539,-0.06597 +0.23418,-0.18337 -0.22375,-0.18988 +0.13232,-0.28078 -0.10201,-0.42101

Microglanis variegatus +0.07096,+0.19445 -0.00116,+0.18728 +0.13207,+0.14338 -0.07175,+0.16084 +0.17845,+0.08369 -0.03014,+0.11133 +0.12114,+0.06958 -0.07796,+0.06412 +0.13952,+0.00168 -0.24749,-0.05113 +0.20772,-0.18083 -0.19975,-0.17406 +0.11720,-0.27343 -0.10132,-0.46448

Microglanis xylographicus +0.07304,+0.19432 -0.00159,+0.19207 +0.13005,+0.15773 -0.07467,+0.15628 +0.17935,+0.08170 -0.03169,+0.09763 +0.11498,+0.05611 -0.07187,+0.06540 +0.13253,+0.00488 -0.24955,-0.04857 +0.22029,-0.18405 -0.21058,-0.18749 +0.12204,-0.27761 -0.09553,-0.44798

Microglanis pellopterygius +0.07180,+0.18994 +0.00026,+0.19252 +0.13837,+0.15437 -0.05549,+0.16408 +0.17671,+0.08835 -0.02757,+0.10954 +0.12090,+0.06623 -0.08104,+0.06598 +0.13972,+0.00373 -0.25563,-0.09696 +0.18350,-0.22033 -0.20312,-0.19350 +0.10558,-0.28802 -0.08700,-0.42853

Pseudopimelodus bufonius +0.07346,+0.18989 -0.02059,+0.16648 +0.13248,+0.12199 -0.08791,+0.16050 +0.17922,+0.08639 -0.02666,+0.11730 +0.11767,+0.07680 -0.07641,+0.09262 +0.14897,+0.02726 -0.25982,-0.08055 +0.19357,-0.23016 -0.19348,-0.19946 +0.11754,-0.29175 -0.06826,-0.42913

Pseudopimelodus charus +0.07615,+0.19668 -0.00701,+0.16697 +0.12477,+0.13092 -0.07105,+0.15541 +0.17117,+0.09724 -0.01446,+0.11064 +0.10962,+0.07793 -0.06914,+0.07901 +0.13474,+0.02189 -0.25579,-0.08338 +0.20824,-0.20393 -0.19530,-0.21235 +0.10539,-0.29195 -0.08783,-0.44200

Pseudopimelodus mangurus +0.07378,+0.19059 -0.01713,+0.16239 +0.13081,+0.12312 -0.08293,+0.15023 +0.17972,+0.09055 -0.02051,+0.11623 +0.11723,+0.08340 -0.07950,+0.08448 +0.15314,+0.02724 -0.26576,-0.08113 +0.21317,-0.21960 -0.19511,-0.21273 +0.10413,-0.29000 -0.07713,-0.42135

Pseudopimelodus schultzi +0.07378,+0.18444 -0.01365,+0.16695 +0.13696,+0.13028 -0.07168,+0.14477 +0.17337,+0.08773 -0.02398,+0.11787 +0.12325,+0.08447 -0.08008,+0.08379 +0.14852,+0.02652 -0.24215,-0.09636 +0.20578,-0.20677 -0.19906,-0.20001 +0.11279,-0.27846 -0.08428,-0.45323

Rhyacoglanis paranae +0.07142,+0.20126 +0.00735,+0.17697 +0.11467,+0.15049 -0.05010,+0.16651 +0.15872,+0.11366 -0.00821,+0.09315 +0.09323,+0.06632 -0.05912,+0.04874 +0.11520,+0.00201 -0.24687,-0.03603 +0.22833,-0.16882 -0.20783,-0.21809 +0.11906,-0.30360 -0.09308,-0.45678

Rhyacoglanis epiblepsis +0.07009,+0.19295 +0.01272,+0.17474 +0.11294,+0.15115 -0.05290,+0.15342 +0.15753,+0.09315 +0.00264,+0.11519 +0.09098,+0.08814 -0.04531,+0.06230 +0.10760,+0.01732 -0.25913,-0.07920 +0.21189,-0.20471 -0.20751,-0.19090 +0.13692,-0.28459 -0.09482,-0.46236

Rhyacoglanis seminiger +0.06989,+0.20222 +0.00323,+0.17884 +0.12055,+0.14549 -0.06524,+0.16337 +0.16795,+0.10542 -0.00550,+0.10152 +0.09449,+0.07500 -0.05416,+0.05483 +0.11306,+0.00557 -0.27839,-0.06087 +0.23244,-0.21501 -0.20494,-0.22240 +0.11027,-0.31398 -0.07264,-0.40264

Steindachneridion melanodermatum +0.07397,+0.19124 -0.00146,+0.19191 +0.13742,+0.15256 -0.05888,+0.17046 +0.16592,+0.11240 +0.00195,+0.13184 +0.10452,+0.10472 -0.05048,+0.02251 +0.10082,-0.02098 -0.23348,-0.12077 +0.17477,-0.23465 -0.17943,-0.23074 +0.08841,-0.29877 -0.08816,-0.44234

Steindachneridion parahybae +0.07078,+0.19040 -0.00415,+0.18849 +0.13615,+0.15044 -0.06121,+0.15965 +0.17406,+0.09873 +0.00306,+0.13803 +0.11131,+0.10888 -0.05966,+0.02201 +0.11149,-0.02871 -0.24838,-0.10898 +0.19003,-0.23647 -0.17845,-0.21104 +0.09570,-0.28695 -0.08732,-0.44109

Steindachneridion scripta +0.07152,+0.19968 -0.00105,+0.18706 +0.13268,+0.14976 -0.05287,+0.17232 +0.16022,+0.10878 +0.00430,+0.13273 +0.10404,+0.10650 -0.05231,+0.00744 +0.09868,-0.03431 -0.22368,-0.10682 +0.18141,-0.20750 -0.14780,-0.23642 +0.06761,-0.29880 -0.09898,-0.48236

&[landmark 2D]

Rhamdia quelen -0.32834,+0.05483 -0.26873,+0.06872 -0.06126,+0.05767 +0.05836,+0.00368 +0.11672,-0.01186 +0.37762,-0.14752 +0.42497,-0.22105 +0.13804,-0.19697 -0.01369,-0.13651 -0.11990,-0.09550 -0.29727,+0.00369 -0.14819,-0.00707

Batrochoglanis acanthochiroides -0.37328,+0.09197 -0.29202,+0.09553 -0.03908,+0.04452 +0.05741,-0.00981 +0.18719,-0.06652 +0.29142,-0.12044 +0.37658,-0.19399 +0.17309,-0.19822 -0.00225,-0.13882 -0.09308,-0.11360 -0.32380,-0.00204 -0.13785,-0.00601

Batrochoglanis melanurus -0.37225,+0.07335 -0.29633,+0.09062 -0.02449,+0.05826 +0.06380,+0.00226 +0.17564,-0.04841 +0.29719,-0.11389 +0.38210,-0.19650 +0.14117,-0.20924 -0.00917,-0.16075 -0.08546,-0.14960 -0.32099,-0.01159 -0.14155,-0.00136

Batrochoglanis raninus -0.36902,+0.06514 -0.29748,+0.08435 -0.03835,+0.06862 +0.07222,+0.00914 +0.20622,-0.05065 +0.29752,-0.12348 +0.36211,-0.21436 +0.14083,-0.20203 -0.01048,-0.14392 -0.09719,-0.10857 -0.32791,-0.00024 -0.13952,-0.00747

Batrochoglanis transmontanus -0.37194,+0.06881 -0.29786,+0.08562 -0.02439,+0.06021 +0.06415,+0.00242 +0.20413,-0.06470 +0.29751,-0.12348 +0.36073,-0.20862 +0.15324,-0.19888 +0.00592,-0.14433 -0.08878,-0.11468 -0.32783,-0.00114 -0.14468,+0.00287

Batrochoglanis villosus -0.37070,+0.07114 -0.29954,+0.08475 -0.02805,+0.06368 +0.07125,+0.00587 +0.19422,-0.04886 +0.29750,-0.12400 +0.36665,-0.21012 +0.13932,-0.20253 -0.00482,-0.14420 -0.09226,-0.11313 -0.33101,-0.01279 -0.14106,-0.00293

Cephalocilurus albomarginatus -0.39345,+0.07086 -0.30777,+0.07448 -0.02618,+0.05337 +0.07392,-0.00152 +0.20164,-0.07504 +0.29612,-0.13318 +0.36656,-0.19321 +0.16438,-0.18779 +0.00142,-0.13591 -0.07761,-0.11076 -0.33160,-0.00098 -0.07476,-0.00236

Cephalocilurus apurensis -0.36039,+0.08060 -0.29739,+0.08816 -0.03761,+0.05058 +0.08762,-0.00676 +0.19909,-0.05238 +0.29474,-0.11792 +0.36874,-0.19150 +0.16586,-0.20388 -0.01403,-0.15238 -0.10370,-0.13407 -0.32864,-0.00499 -0.13412,-0.02162

Cephalocilurus fowleri -0.36973,+0.08034 -0.30916,+0.08353 -0.01952,+0.03858 +0.08735,-0.01638 +0.20955,-0.06178 +0.28964,-0.11366 +0.34675,-0.18362 +0.17942,-0.20207 -0.00530,-0.14314 -0.07511,-0.12999 -0.33633,+0.00675 -0.17001,+0.00218

Cephalocilurus nigricaudus -0.38595,+0.09638 -0.30218,+0.08586 -0.01167,+0.01824 +0.09866,-0.05251 +0.20396,-0.09129 +0.29275,-0.12186 +0.36574,-0.17888 +0.18682,-0.19940 -0.00635,-0.13013 -0.06488,-0.12983 -0.33417,-0.00160 -0.11774,-0.04158

Cruciglanis pacifici -0.34630,+0.05805 -0.27752,+0.06920 -0.06794,+0.05194 +0.01729,+0.01070 +0.23068,-0.07371 +0.32209,-0.12893 +0.38094,-0.20395 +0.17197,-0.19615 -0.00599,-0.14024 -0.13766,-0.10365 -0.30824,-0.00463 -0.13459,+0.00850

Lophiosilurus alexandri -0.37665,+0.07967 -0.29647,+0.07707 -0.03170,+0.00276 +0.06315,-0.04315 +0.22937,-0.10618 +0.29190,-0.13095 +0.38061,-0.17775 +0.18102,-0.19733 -0.01885,-0.12722 -0.07488,-0.11709 -0.32149,+0.01011 -0.13846,+0.00752

Microglanis carlae -0.36213,+0.06976 -0.29057,+0.08052 -0.05894,+0.05466 +0.04029,+0.00243 +0.16755,-0.05501 +0.30478,-0.13859 +0.39813,-0.22101 +0.16818,-0.19997 -0.00007,-0.12084 -0.10829,-0.09158 -0.31504,+0.00786 -0.12051,-0.02051

Microglanis cibelae -0.35155,+0.06809 -0.28551,+0.08312 -0.05221,+0.06507 +0.04476,+0.01648 +0.17036,-0.04181 +0.31825,-0.13195 +0.39099,-0.21834 +0.14169,-0.20161 -0.00738,-0.15452 -0.13276,-0.11466 -0.32105,+0.00030 -0.10369,-0.01457

Microglanis cottoides -0.34701,+0.06831 -0.28798,+0.08396 -0.04328,+0.06105 +0.03577,+0.01060 +0.18188,-0.05696 +0.30957,-0.12884 +0.39264,-0.21189 +0.16132,-0.20538 -0.01511,-0.14512 -0.11157,-0.11344 -0.31725,+0.01031 -0.13233,-0.01612

Microglanis eurystoma -0.36597,+0.06712 -0.28091,+0.07891 -0.04940,+0.07194 +0.04860,+0.02245 +0.18953,-0.03754 +0.31640,-0.13267 +0.37809,-0.22267 +0.13768,-0.19959 -0.01185,-0.14793 -0.12135,-0.11438 -0.31618,-0.01304 -0.11426,-0.00253

Microglanis garavelloi -0.37452,+0.06982 -0.29334,+0.08462 -0.04520,+0.06843 +0.05588,+0.01294 +0.16820,-0.03496 +0.31655,-0.13398 +0.38604,-0.22407 +0.13745,-0.19997 -0.01913,-0.12881 -0.10723,-0.09374 -0.32602,-0.00622 -0.07813,-0.03862

Microglanis iheringi -0.36011,+0.07498 -0.29298,+0.08642 -0.05139,+0.04558 +0.03532,-0.00327 +0.19593,-0.06286 +0.31568,-0.13265 +0.38087,-0.20395 +0.15780,-0.20115 -0.00938,-0.12853 -0.09783,-0.08953 -0.31745,+0.01171 -0.13950,-0.01578

Microglanis leniceae -0.36703,+0.07277 -0.29570,+0.08272 -0.04427,+0.06025 +0.05180,+0.00163 +0.17396,-0.05386 +0.31298,-0.13370 +0.38256,-0.21705 +0.15543,-0.19827 -0.00509,-0.13184 -0.10291,-0.09398 -0.32062,+0.00428 -0.11130,-0.02127

Microglanis leptostriatus -0.35433,+0.07083 -0.28198,+0.08203 -0.05181,+0.06338 +0.04494,+0.01208 +0.16423,-0.03171 +0.31647,-0.13057 +0.40170,-0.23060 +0.14232,-0.19768 -0.01402,-0.14186 -0.11451,-0.10358 -0.31583,-0.00510 -0.12251,-0.02309

Microglanis lundbergi -0.36509,+0.10531 -0.28348,+0.10459 -0.03258,+0.04488 +0.05552,-0.00869 +0.18926,-0.05812 +0.30121,-0.11986 +0.38628,-0.20086 +0.14908,-0.20472 -0.00779,-0.14035 -0.09760,-0.11222 -0.32582,+0.00179 -0.10832,-0.02767

Microglanis maculatus -0.36213,+0.06976 -0.28494,+0.08104 -0.06580,+0.05392 +0.02738,+0.00967 +0.17684,-0.05548 +0.32099,-0.13506 +0.40083,-0.22184 +0.14719,-0.19436 -0.01906,-0.11504 -0.11209,-0.07832 -0.31250,+0.00641 -0.12018,-0.02056

Microglanis malabarbai -0.36295,+0.06635 -0.28826,+0.07983 -0.05115,+0.06951 +0.05025,+0.01981 +0.18832,-0.04518 +0.31122,-0.13584 +0.38602,-0.22019 +0.14205,-0.19527 -0.01293,-0.13953 -0.12120,-0.10262 -0.32056,-0.00224 -0.09873,-0.02090

Microglanis nigripinnis -0.36884,+0.06408 -0.28863,+0.08045 -0.05631,+0.07156 +0.05626,+0.01080 +0.17087,-0.04239 +0.31357,-0.13714 +0.38354,-0.21996 +0.14743,-0.19548 +0.00245,-0.13701 -0.12794,-0.09007 -0.32282,+0.00236 -0.09148,-0.00980

Microglanis nigrolineatus -0.36168,+0.07911 -0.28334,+0.09142 -0.05020,+0.05286 +0.04497,-0.00284 +0.15205,-0.04134 +0.32501,-0.13311 +0.39188,-0.20762 +0.14704,-0.20358 -0.01954,-0.14074 -0.12427,-0.10550 -0.32667,-0.00567 -0.09974,-0.01623

Microglanis oliveirai -0.36305,+0.05230 -0.29139,+0.06966 -0.04590,+0.04948 +0.03628,+0.00113 +0.17377,-0.06396 +0.32441,-0.14970 +0.39310,-0.23974 +0.14671,-0.18837 +0.00650,-0.11518 -0.09655,-0.08238 -0.32122,-0.00386 -0.12421,-0.00378

Microglanis parahybae -0.36858,+0.06448 -0.29187,+0.08481 -0.03850,+0.07157 +0.05083,+0.01873 +0.17880,-0.04591 +0.30699,-0.13520 +0.37469,-0.21856 +0.14672,-0.19540 -0.00813,-0.14651 -0.10839,-0.10703 -0.33063,+0.00420 -0.10654,-0.01777

Microglanis pataxo -0.35859,+0.07730 -0.28247,+0.09023 -0.05377,+0.05546 +0.03457,+0.00246 +0.14767,-0.04126 +0.32543,-0.13316 +0.40484,-0.21466 +0.14153,-0.20729 -0.01792,-0.13159 -0.11583,-0.09821 -0.31825,-0.00334 -0.11021,-0.02005

Microglanis poecilus -0.36918,+0.07252 -0.29516,+0.08130 -0.04226,+0.05011 +0.05057,-0.00733 +0.18928,-0.06985 +0.31239,-0.13367 +0.38838,-0.20714 +0.14672,-0.19249 +0.00059,-0.13022 -0.10161,-0.09094 -0.32732,+0.00612 -0.09603,-0.02391

Microglanis robustus -0.35853,+0.07787 -0.28275,+0.08470 -0.04769,+0.04537 +0.04219,-0.00087 +0.19264,-0.05984 +0.32215,-0.13061 +0.38769,-0.21175 +0.14154,-0.20235 -0.00918,-0.12756 -0.10508,-0.09268 -0.32078,-0.00576 -0.12993,-0.00844

Microglanis secundus -0.35440,+0.06853 -0.29285,+0.07676 -0.05909,+0.05018 +0.02796,+0.00333 +0.21255,-0.07507 +0.31839,-0.13496 +0.38154,-0.22364 +0.15412,-0.17638 -0.00142,-0.10695 -0.09946,-0.06840 -0.32000,+0.00799 -0.14770,+0.01444

Microglanis variegatus -0.36091,+0.07618 -0.29298,+0.08642 -0.04715,+0.04866 +0.04381,-0.00078 +0.19657,-0.06139 +0.31745,-0.13064 +0.37893,-0.20495 +0.15463,-0.20058 -0.01735,-0.12778 -0.10069,-0.09266 -0.31946,+0.00213 -0.13093,-0.01855

Microglanis xylographicus -0.36653,+0.07275 -0.29069,+0.08540 -0.04458,+0.06174 +0.04753,+0.00328 +0.19045,-0.06019 +0.30679,-0.13363 +0.38533,-0.21991 +0.14961,-0.19552 -0.00528,-0.12729 -0.10348,-0.09913 -0.32290,-0.00078 -0.10811,-0.02789

Microglanis pellopterygius -0.38733,+0.09292 -0.27731,+0.09841 -0.04317,+0.06014 +0.03923,+0.01251 +0.19285,-0.05736 +0.30096,-0.12251 +0.36069,-0.20868 +0.15636,-0.20796 +0.00120,-0.15135 -0.11384,-0.11029 -0.32094,-0.01031 -0.10968,-0.01838

Pseudopimelodus bufonius -0.36277,+0.07786 -0.29662,+0.08658 -0.05343,+0.04388 +0.04265,-0.00859 +0.19356,-0.06500 +0.27715,-0.11279 +0.38976,-0.19888 +0.17245,-0.20049 -0.00601,-0.12619 -0.10484,-0.11596 -0.32538,-0.00242 -0.15475,+0.02161

Pseudopimelodus charus -0.35998,+0.07897 -0.29323,+0.08651 -0.05415,+0.04409 +0.03956,-0.00824 +0.20635,-0.06979 +0.30307,-0.12332 +0.39295,-0.19513 +0.17272,-0.19826 -0.00524,-0.13712 -0.14554,-0.08781 -0.28430,-0.02200 -0.16365,-0.00143

Pseudopimelodus mangurus -0.33567,+0.08078 -0.27798,+0.09075 -0.06830,+0.04127 +0.02442,+0.00381 +0.21581,-0.06220 +0.30698,-0.11702 +0.38975,-0.19888 +0.16721,-0.20402 -0.00458,-0.14754 -0.12995,-0.11778 -0.31516,+0.00032 -0.15292,-0.00280

Pseudopimelodus schultzi -0.36035,+0.07999 -0.29853,+0.08570 -0.05012,+0.05811 +0.06888,-0.00590 +0.19478,-0.06384 +0.30433,-0.12307 +0.36205,-0.18313 +0.16814,-0.20386 -0.00086,-0.14916 -0.11179,-0.11843 -0.33040,-0.00193 -0.13918,-0.02077

Rhyacoglanis paranae -0.36645,+0.07599 -0.28615,+0.09043 -0.05844,+0.05257 +0.05067,-0.00231 +0.17378,-0.04328 +0.31181,-0.12764 +0.41148,-0.20959 +0.17344,-0.19985 -0.01586,-0.14237 -0.16619,-0.08722 -0.27246,-0.04199 -0.10867,-0.01851

Rhyacoglanis epiblepsis -0.36596,+0.06355 -0.27602,+0.07666 -0.05906,+0.05293 +0.05130,-0.00485 +0.16846,-0.05450 +0.33033,-0.13466 +0.39658,-0.19763 +0.16877,-0.20590 -0.02200,-0.12310 -0.11410,-0.08666 -0.30782,-0.00344 -0.12031,+0.01172

Rhyacoglanis seminiger -0.37419,+0.07882 -0.27783,+0.08967 -0.05251,+0.06902 +0.07832,-0.00036 +0.18260,-0.04351 +0.29593,-0.11851 +0.38096,-0.19893 +0.17038,-0.20258 -0.00696,-0.16469 -0.12184,-0.13194 -0.32200,-0.03193 -0.08594,-0.00609

Steindachneridion melanodermatum -0.39632,+0.07266 -0.27792,+0.07741 -0.03379,+0.05155 +0.06503,-0.00023 +0.16391,-0.03340 +0.30164,-0.12033 +0.38842,-0.20069 +0.15144,-0.19863 -0.00078,-0.14274 -0.09899,-0.13006 -0.31146,-0.00280 -0.13791,+0.00126

Steindachneridion parahybae -0.36630,+0.04071 -0.26873,+0.06872 -0.04473,+0.05823 +0.05672,+0.00730 +0.18919,-0.05545 +0.31923,-0.14387 +0.40979,-0.23221 +0.13218,-0.18333 +0.01066,-0.12940 -0.11018,-0.10364 -0.30091,-0.02207 -0.15953,+0.00554

Steindachneridion scripta -0.36844,+0.09804 -0.27763,+0.08568 -0.03418,+0.01714 +0.04892,-0.02512 +0.16926,-0.05643 +0.31314,-0.12218 +0.39774,-0.18654 +0.15485,-0.19036 +0.01617,-0.15328 -0.10012,-0.13631 -0.31886,+0.00153 -0.15734,-0.00636

&[landmark 2D]

Rhamdia quelen +0.10107,+0.47667 +0.05278,+0.41994 +0.12615,+0.40709 +0.00941,+0.41237 +0.16428,+0.38732 -0.15395,+0.12625 +0.20849,+0.06255 -0.14636,-0.36967 +0.05242,-0.40333 -0.09962,-0.42921 -0.00773,-0.44502 -0.10844,-0.72432

Batrochoglanis acanthochiroides +0.09429,+0.47141 +0.01591,+0.44351 +0.17654,+0.41327 -0.05058,+0.38844 +0.20952,+0.35469 -0.18385,+0.11038 +0.24561,+0.02115 -0.14461,-0.34161 +0.05752,-0.39852 -0.12333,-0.42221 +0.00116,-0.44342 -0.12301,-0.71183

Batrochoglanis melanurus +0.10851,+0.49275 +0.01909,+0.44108 +0.17844,+0.40904 -0.05298,+0.39804 +0.22685,+0.33915 -0.21978,+0.12413 +0.25647,+0.04089 -0.17027,-0.35317 +0.07129,-0.39084 -0.12576,-0.42666 +0.00269,-0.44852 -0.09098,-0.66842

Batrochoglanis raninus +0.09996,+0.48184 +0.02446,+0.43543 +0.16215,+0.41071 -0.05515,+0.39282 +0.22064,+0.34803 -0.21263,+0.12581 +0.27909,+0.03468 -0.15826,-0.34621 +0.05905,-0.38790 -0.12415,-0.42404 +0.00000,-0.44686 -0.10328,-0.68735

Batrochoglanis transmontanus +0.10060,+0.48411 +0.02953,+0.44345 +0.15803,+0.41879 -0.04625,+0.39987 +0.20728,+0.34994 -0.20885,+0.11518 +0.25623,+0.01983 -0.16268,-0.35517 +0.05602,-0.38725 -0.12315,-0.43175 -0.00500,-0.44558 -0.09156,-0.68081

Batrochoglanis villosus +0.10980,+0.49477 +0.02195,+0.43952 +0.17872,+0.40941 -0.06316,+0.40103 +0.22579,+0.34166 -0.22043,+0.11587 +0.24478,+0.00023 -0.17149,-0.35188 +0.06954,-0.39710 -0.13300,-0.42555 +0.00985,-0.45300 -0.08735,-0.66575

Cephalocilurus albomarginatus +0.10310,+0.52294 +0.00781,+0.42019 +0.16465,+0.39026 -0.04146,+0.39066 +0.20099,+0.34926 -0.22479,+0.08249 +0.26514,-0.00260 -0.16781,-0.34551 +0.06883,-0.39034 -0.13714,-0.40971 +0.01672,-0.43803 -0.12301,-0.70237

Cephalocilurus apurensis +0.10216,+0.48154 +0.01815,+0.45894 +0.17558,+0.42169 -0.05869,+0.39486 +0.21778,+0.32793 -0.23923,+0.07239 +0.24637,-0.04470 -0.19386,-0.33723 +0.07664,-0.37036 -0.14562,-0.42875 +0.02108,-0.44847 -0.08465,-0.68914

Cephalocilurus fowleri +0.10179,+0.47824 +0.03251,+0.45323 +0.15929,+0.42749 -0.03819,+0.39033 +0.18730,+0.33604 -0.23638,+0.09324 +0.22649,-0.01441 -0.19081,-0.35131 +0.07288,-0.37760 -0.14711,-0.42058 +0.01885,-0.44388 -0.06209,-0.70650

Cephalocilurus nigricaudus +0.10200,+0.47421 +0.01698,+0.44238 +0.15763,+0.42457 -0.04635,+0.38001 +0.21878,+0.34895 -0.19102,+0.05224 +0.28248,+0.00316 -0.14524,-0.32499 +0.04716,-0.40643 -0.14281,-0.40336 -0.00232,-0.44712 -0.10309,-0.72216

Cruciglanis pacifici +0.09752,+0.47341 +0.02878,+0.43867 +0.15511,+0.41851 -0.03303,+0.39055 +0.19432,+0.35208 -0.17924,+0.11272 +0.23823,+0.05111 -0.15673,-0.35823 +0.05337,-0.39899 -0.11167,-0.40897 -0.00667,-0.42882 -0.12159,-0.72982

Lophiosilurus alexandri +0.09634,+0.46611 +0.02249,+0.44191 +0.15353,+0.41570 -0.03948,+0.38976 +0.19425,+0.33892 -0.26690,+0.10609 +0.29896,-0.00635 -0.20379,-0.31677 +0.10940,-0.36399 -0.14973,-0.41016 +0.02757,-0.43471 -0.10088,-0.71554

Microglanis carlae +0.09429,+0.46714 +0.02470,+0.43692 +0.15603,+0.40990 -0.04904,+0.39890 +0.21036,+0.34780 -0.18966,+0.13076 +0.25093,+0.05010 -0.16436,-0.35798 +0.06148,-0.40118 -0.11962,-0.41098 -0.00474,-0.43594 -0.10759,-0.71349

Microglanis cibelae +0.09881,+0.46726 +0.02863,+0.43125 +0.15322,+0.41295 -0.04134,+0.39468 +0.20592,+0.36092 -0.18514,+0.15655 +0.25670,+0.08337 -0.16403,-0.35916 +0.06076,-0.40194 -0.12473,-0.43378 -0.00536,-0.45260 -0.11419,-0.67861

Microglanis cottoides +0.09853,+0.46711 +0.02864,+0.43125 +0.15563,+0.40363 -0.02847,+0.40622 +0.19403,+0.35602 -0.22144,+0.14724 +0.26710,+0.06349 -0.16453,-0.36110 +0.05584,-0.39152 -0.11995,-0.41776 -0.00495,-0.43046 -0.08544,-0.70649

Microglanis eurystoma +0.10017,+0.48222 +0.00965,+0.43973 +0.18997,+0.40407 -0.07491,+0.39969 +0.24019,+0.33615 -0.22508,+0.11891 +0.26216,+0.02222 -0.16623,-0.34886 +0.07146,-0.38624 -0.12857,-0.42400 +0.00295,-0.44506 -0.10159,-0.67904

Microglanis garavelloi +0.10073,+0.49065 +0.02807,+0.43573 +0.15520,+0.41334 -0.04484,+0.39949 +0.20745,+0.35583 -0.20165,+0.10384 +0.25418,+0.03052 -0.16005,-0.35579 +0.04471,-0.39026 -0.12100,-0.42946 -0.01687,-0.44556 -0.11248,-0.68400

Microglanis iheringi +0.09233,+0.45849 +0.02332,+0.43567 +0.15612,+0.41237 -0.04904,+0.39558 +0.21160,+0.34939 -0.18950,+0.15673 +0.24702,+0.06732 -0.15650,-0.35477 +0.05151,-0.38127 -0.11620,-0.41202 -0.00695,-0.43213 -0.11182,-0.73241

Microglanis leniceae +0.09583,+0.47966 +0.02466,+0.43675 +0.16573,+0.40317 -0.03845,+0.40598 +0.20501,+0.34400 -0.20573,+0.13414 +0.24387,+0.03395 -0.15873,-0.34932 +0.05641,-0.38508 -0.12493,-0.42472 -0.00102,-0.44642 -0.09301,-0.70641

Microglanis leptostriatus +0.09717,+0.46474 +0.02904,+0.44159 +0.15739,+0.42060 -0.04572,+0.39565 +0.20701,+0.35713 -0.20759,+0.12401 +0.25949,+0.02998 -0.15849,-0.34701 +0.05752,-0.39311 -0.12117,-0.42915 -0.00875,-0.45412 -0.12719,-0.68299

Microglanis lundbergi +0.09955,+0.47847 +0.01352,+0.44058 +0.16423,+0.41394 -0.06439,+0.39650 +0.22167,+0.34143 -0.21398,+0.10645 +0.25835,+0.01264 -0.16610,-0.34891 +0.05283,-0.38743 -0.12797,-0.41182 -0.00695,-0.43196 -0.10642,-0.70827

Microglanis maculatus +0.10363,+0.48375 +0.02823,+0.44038 +0.15230,+0.41838 -0.04122,+0.38713 +0.19715,+0.34340 -0.19231,+0.11582 +0.24813,+0.03719 -0.14847,-0.34804 +0.05411,-0.37855 -0.12072,-0.41863 +0.00352,-0.43549 -0.12732,-0.72518

Microglanis malabarbai +0.10017,+0.48222 +0.01909,+0.43015 +0.17259,+0.39893 -0.05479,+0.39803 +0.22661,+0.34523 -0.21951,+0.12614 +0.26586,+0.03358 -0.15877,-0.35103 +0.05453,-0.38474 -0.11680,-0.42583 -0.00420,-0.44597 -0.10371,-0.69486

Microglanis nigripinnis +0.10016,+0.48222 +0.03112,+0.44021 +0.15523,+0.41955 -0.04387,+0.38917 +0.20266,+0.34328 -0.20704,+0.12733 +0.24634,+0.04789 -0.16340,-0.35851 +0.06740,-0.40264 -0.12317,-0.42132 -0.00120,-0.44981 -0.12157,-0.68276

Microglanis nigrolineatus +0.09744,+0.48314 +0.00717,+0.43914 +0.16602,+0.40678 -0.05983,+0.39979 +0.22259,+0.35040 -0.20604,+0.09567 +0.24421,+0.01287 -0.16014,-0.34275 +0.06123,-0.38841 -0.12021,-0.41760 -0.00370,-0.44032 -0.11074,-0.70855

Microglanis oliveirai +0.09785,+0.48209 +0.02503,+0.43399 +0.15852,+0.40893 -0.04016,+0.39866 +0.21430,+0.35777 -0.18093,+0.11198 +0.24270,+0.03317 -0.14665,-0.36581 +0.04167,-0.39993 -0.11500,-0.41302 -0.00707,-0.43377 -0.11550,-0.71131

Microglanis parahybae +0.09405,+0.48460 +0.03273,+0.43806 +0.15521,+0.42105 -0.04132,+0.39380 +0.20748,+0.35584 -0.20313,+0.13581 +0.23582,+0.04658 -0.16321,-0.36778 +0.04150,-0.40044 -0.12436,-0.43833 -0.02030,-0.45415 -0.08631,-0.66654

Microglanis pataxo +0.10026,+0.47846 +0.02280,+0.43990 +0.15787,+0.41580 -0.05594,+0.39274 +0.20658,+0.34363 -0.19235,+0.12616 +0.23958,+0.03940 -0.16233,-0.34239 +0.06038,-0.38425 -0.12918,-0.41909 +0.00136,-0.43960 -0.10658,-0.71853

Microglanis poecilus +0.09905,+0.47852 +0.00783,+0.43165 +0.17679,+0.40549 -0.05757,+0.40032 +0.22440,+0.35274 -0.19816,+0.12137 +0.25525,+0.02708 -0.14582,-0.36120 +0.03844,-0.39292 -0.11334,-0.41433 -0.00740,-0.43156 -0.10717,-0.70924

Microglanis robustus +0.09816,+0.47756 +0.02126,+0.43742 +0.16014,+0.41696 -0.05818,+0.38837 +0.21799,+0.35758 -0.17795,+0.11166 +0.25815,+0.03815 -0.16438,-0.34332 +0.05643,-0.37965 -0.11582,-0.41384 -0.00683,-0.43507 -0.12938,-0.71906

Microglanis secundus +0.09823,+0.47016 +0.02845,+0.43715 +0.15350,+0.41908 -0.04947,+0.39668 +0.20320,+0.35548 -0.18348,+0.13871 +0.24107,+0.06800 -0.14325,-0.35259 +0.04699,-0.39678 -0.12110,-0.41902 +0.00047,-0.43691 -0.10759,-0.71349

Microglanis variegatus +0.09836,+0.47783 +0.02060,+0.43610 +0.16153,+0.40824 -0.04078,+0.39930 +0.21018,+0.34916 -0.20660,+0.11342 +0.24879,+0.02488 -0.15550,-0.34147 +0.05166,-0.38300 -0.11751,-0.40835 -0.00593,-0.42766 -0.11102,-0.73347

Microglanis xylographicus +0.09959,+0.47931 +0.02459,+0.43538 +0.15883,+0.41081 -0.04590,+0.40029 +0.20613,+0.35275 -0.19334,+0.12954 +0.23407,+0.03863 -0.15404,-0.35280 +0.03729,-0.39292 -0.11658,-0.41631 -0.01688,-0.43185 -0.10577,-0.71912

Microglanis pellopterygius +0.11174,+0.48070 +0.01726,+0.43992 +0.19045,+0.39599 -0.05401,+0.41350 +0.22257,+0.32730 -0.22768,+0.11764 +0.20515,+0.00420 -0.16192,-0.35184 +0.05497,-0.38525 -0.12083,-0.41839 +0.00023,-0.44264 -0.09226,-0.71500

Pseudopimelodus bufonius +0.09777,+0.46842 +0.02884,+0.44591 +0.14627,+0.42849 -0.02645,+0.38810 +0.18196,+0.35603 -0.16190,+0.13333 +0.22512,+0.07562 -0.16921,-0.34953 +0.07687,-0.39881 -0.12629,-0.42420 +0.01429,-0.44314 -0.13507,-0.70920

Pseudopimelodus charus +0.09837,+0.46760 +0.03054,+0.44272 +0.15051,+0.41803 -0.02745,+0.38531 +0.18894,+0.34813 -0.16791,+0.14388 +0.23902,+0.06811 -0.16864,-0.34871 +0.06994,-0.38955 -0.12149,-0.42398 -0.00119,-0.44678 -0.11018,-0.72174

Pseudopimelodus mangurus +0.09759,+0.46833 +0.03590,+0.43722 +0.14869,+0.41508 -0.02715,+0.39053 +0.19384,+0.35080 -0.16742,+0.14677 +0.23862,+0.07317 -0.17309,-0.34930 +0.07227,-0.38926 -0.12621,-0.43373 -0.00012,-0.45541 -0.10254,-0.70846

Pseudopimelodus schultzi +0.09152,+0.48535 +0.02342,+0.44664 +0.15206,+0.42151 -0.03480,+0.38623 +0.19621,+0.35141 -0.17952,+0.10958 +0.26150,+0.04109 -0.14779,-0.34048 +0.06786,-0.39471 -0.11900,-0.42142 +0.00076,-0.45422 -0.14604,-0.69509

Rhyacoglanis paranae +0.10035,+0.48138 +0.03254,+0.43963 +0.15476,+0.41171 -0.03484,+0.39300 +0.19414,+0.34588 -0.17023,+0.11400 +0.21711,+0.03818 -0.18602,-0.33636 +0.08380,-0.37707 -0.14375,-0.42163 +0.01540,-0.44686 -0.10523,-0.73088

Rhyacoglanis epiblepsis +0.10024,+0.48223 +0.02603,+0.42540 +0.15607,+0.39916 -0.03682,+0.37416 +0.19222,+0.33037 -0.19775,+0.12719 +0.25027,+0.03958 -0.18411,-0.31231 +0.09029,-0.37438 -0.14539,-0.39211 +0.01611,-0.42462 -0.12093,-0.78565

Rhyacoglanis seminiger +0.10131,+0.48890 +0.02453,+0.44234 +0.16009,+0.40958 -0.05927,+0.39171 +0.20889,+0.33138 -0.23235,+0.10823 +0.25268,+0.01372 -0.17359,-0.33397 +0.08074,-0.37858 -0.13269,-0.42809 +0.00906,-0.44774 -0.10570,-0.69908

Steindachneridion melanodermatum +0.10495,+0.49380 +0.04012,+0.42323 +0.14295,+0.40546 -0.01443,+0.39991 +0.18521,+0.36295 -0.18550,+0.11384 +0.23803,+0.04414 -0.16189,-0.36655 +0.06644,-0.40835 -0.11406,-0.42796 -0.00248,-0.44367 -0.10132,-0.69722

Steindachneridion parahybae +0.10166,+0.48508 +0.04633,+0.42564 +0.13741,+0.40921 -0.02225,+0.40325 +0.18517,+0.37075 -0.17242,+0.11832 +0.23015,+0.06439 -0.16115,-0.36872 +0.06359,-0.41939 -0.10972,-0.44238 -0.00785,-0.46303 -0.11375,-0.67028

Steindachneridion scripta +0.10574,+0.49555 +0.04226,+0.43103 +0.14525,+0.40642 -0.01501,+0.41334 +0.18314,+0.36452 -0.18441,+0.10249 +0.19030,+0.02684 -0.14865,-0.39733 +0.04935,-0.41128 -0.09933,-0.44376 -0.00373,-0.44894 -0.10088,-0.67914

&[num]

Rhamdia quelen ?00?0001000010

Batrochoglanis acanthochiroides 00101211102001

Batrochoglanis melanurus 00101211102001
Batrochoglanis raninus 00101211102001
Batrochoglanis transmontanus 00101211102001
Batrochoglanis villosus 00101211102001
Cephalocilurus albomarginatus 10000001112000
Cephalocilurus apurensis 10000001112000
Cephalocilurus fowleri 10000001112000
Cephalocilurus nigricaudus 10000001112000
Cruciglanis pacifici 01001111001111
Lophiosilurus alexandri 10000001111000
Microglanis carlae 00101210103022
Microglanis cibelae 00101210103022
Microglanis cottoides 00101210103022
Microglanis eurystoma 00101210103022
Microglanis garavelloi 00101210103022
Microglanis iheringi 00101210103022
Microglanis leniceae 00101210103022
Microglanis leptostriatus 00101210103022
Microglanis lundbergi 00101210103022
Microglanis maculatus 00101210103022
Microglanis malabarbai 00101210103022
Microglanis nigripinnis 00101210103022
Microglanis nigrolineatus 00101210103022
Microglanis oliveirai 00101210103022
Microglanis parahybae 00101210103022
Microglanis pataxo 00101210103022
Microglanis poecilus 00101210103022
Microglanis robustus 00101210103022
Microglanis secundus 00101210103022
Microglanis variegatus 00101210103022
Microglanis xylographicus 00101210103022
Microglanis pellopterygius 00101210103022

Pseudopimelodus bufonius 01001011011100

Pseudopimelodus charus 01001011011100

Pseudopimelodus mangurus 01001011011100

Pseudopimelodus schultzi 01001011011100

Rhyacoglanis paranae 01010011002110

Rhyacoglanis epiblepsis 01010011002111

Rhyacoglanis seminiger 11010011002110

Steindachneridion melanodermatum ?00?0001000000

Steindachneridion parahybae ?00?0001000000

Steindachneridion scriptwa ?00?0001000000

;

lmark connect 0 0-1 1-3 9-11 11-13 13-12 12-10 8-6 4-2 2-0 0-1 9-3 4-10 5-7 5-1 2-6/1 0-1 1-2 2-3 3-4 4-5 5-6 6-7 7-8 8-9 9-10 10-0/2 0-1 1-3 3-5 5-7 7-9 9-11 11-10 10-8 8-6 6-4 4-2 2-0

;

tread

(0 (42 ((((1 ((4 (3 (2 5)))(33 ((18 (((12 (21 30))(24 27))(32 (((17 31)(25 29))(20 28)))))((23 ((19 (13 14))(16 26)))(15 22))))))(6 ((7 8)(9 11))))((10 (35 (36 (34 37))))(40 (38 39))))(41 43))))

;

proc/;

Appendix 4. *Microglanis nigrolineatus*, a new species from northwestern Argentina (Ostariophysi: Pseudopimelodidae).

Os resultados apresentados a seguir referem-se ao artigo publicado na revista Ichthyological Exploration of Freshwaters, Volume 27, Número 3 de novembro de 2016, no qual é descrita uma espécie nova de *Microglanis* da bacia do rio Bermejo, Argentina.

Verlag Dr. Friedrich Pfeil
ISSN 0936-9902

Excerpt from

Ichthyological Exploration of Freshwaters

An international journal for field-orientated ichthyology

Volume 27
Number 3

Ichthyological Exploration of Freshwaters

An international journal for field-orientated ichthyology

Volume 27 · Number 3 · November 2016
pages 193–288, 57 figs., 18 tabs.

Ichthyological Exploration of Freshwaters is published quarterly

Subscriptions should be addressed to the Publisher:

Verlag Dr. Friedrich Pfeil, Wolfratshauser Str. 27, 81379 München, Germany
PERSONAL SUBSCRIPTION : EURO 100 per Year/volume - 4 issues (includes surface mail shipping)
INSTITUTIONAL SUBSCRIPTION : EURO 180 per Year/volume - 4 issues (includes surface mail shipping)

Manuscripts should be addressed to the Managing Editor:
Maurice Kottelat, Rue des Rauraques 6, CH–2800 Delémont, Switzerland

CIP-Titelaufnahme der Deutschen Bibliothek

Ichthyological exploration of freshwaters : an international journal for field-orientated ichthyology. – München : Pfeil.
Erscheint jährl. viermal. – Aufnahme nach Vol. 1, No. 1 (1990)
ISSN 0936-9902

Vol. 1, No. 1 (1990) –

Printed by PBtisk a.s., Příbram I – Balonka

ISSN 0936–9902
Printed in the European Union

Verlag Dr. Friedrich Pfeil, Wolfratshauser Str. 27, 81379 München, Germany
Phone +49 89 742827–0 · Fax +49 89 7242772 · E-mail: info@pfeil-verlag.de · www.pfeil-verlag.de

Ichthyol. Explor. Freshwaters, Vol. 27, No. 3, pp. 193–202, 6 figs., 2 tabs., November 2016

Microglanis nigrolineatus, a new species from northwestern Argentina (Ostariophysi: Pseudopimelodidae)

Guillermo E. Terán*, Lucas R. Jarduli,***, Felipe Alonso****, J. Marcos Mirande* and Oscar A. Shibatta****

Microglanis nigrolineatus, new species, is described from streams of Bermejo River basin, northwestern Argentina. It is distinguished from all congeners by a combination of characters including a unique coloration pattern: a thin dark line that runs along middle body from vertical line through dorsal-fin origin to end of adipose fin, delimiting two dark-brown areas ending in a dark blotch crossing entire body depth just anterior to caudal-fin origin and dorsal region of head uniformly dark, lacking a paler area on nuchal region. Also, thorn serrae on anterior margin of pectoral-fin spine are short.

Microglanis nigrolineatus, nueva especie, se describe de arroyos de la cuenca del Río Bermejo, Noroeste de Argentina. Esta nueva especie se distingue de los congéneres por una combinación de caracteres que incluyen un patrón de coloración único: una delgada línea oscura que atraviesa longitudinalmente la parte media del cuerpo, que va desde la aleta dorsal hasta el final de la adiposa delimitando dos áreas pardo oscuras que terminan en una mancha negra que atraviesa toda la altura del cuerpo justo anterior a la aleta caudal, y la región dorsal de la cabeza uniformemente oscura, sin un área más clara en la región nucal. Además, los ganchos en el margen anterior de la espina pectoral son cortos.

Introduction

Microglanis was proposed by Eigenmann (1912) and is the most diverse genus of Pseudopimelodidae, with 24 known species (Shibatta, 2014). Many of those species have been described in the latest years (Ruiz & Shibatta, 2011; Jarduli & Shibatta, 2013; Mattos et al., 2013; Shibatta, 2014) and more are waiting discovery.

Shibatta (1998) included the presumably monophyletic genus *Microglanis* in the Pseudopimelodidae, differing from other members of

* Fundación Miguel Lillo, UEL-CONICET, Miguel Lillo 251, 4000. San Miguel de Tucumán, Argentina. E-mail: guilloteran@gmail.com, mcmirande@gmail.com

** Departamento de Biologia Animal e Vegetal, Universidade Estadual de Londrina, Caixa Postal 10.011, 8657-090, Londrina, PR, Brazil. E-mail: oscar.shibatta@gmail.com

*** Faculdades Integradas de Ourinhos, BR 153, Km 338, Água do Cateto, 19909-100, Ourinhos, SP, Brazil. E-mail: lucasjarduli@gmail.com (corresponding author)

**** División de Ictiología, Museo Argentino de Ciencias Naturales, CONICET, Av. Ángel Gallardo 470, 1405 Buenos Aires, Argentina. E-mail: felipealonso@gmail.com

Fig. 1. *Microglanis nigrolineatus*, CI-FML 6596, holotype, 32.5 mm SL; Argentina: Salta province: Quebrada Colorada stream, Bermejo River basin.

the family by a smaller body size, rarely reaching 80 mm of standard length, an incomplete lateral line, and a premaxillary tooth patch with rounded margin, without posterior projection (Schultz, 1944; Gomes, 1946; Mees, 1974, 1978).

Microglanis has the widest distribution within the Pseudopimelodidae (Shibatta, 2003a). This genus occurs in the cis-andean rivers between Venezuela and Uruguay, and in the trans-andean coastal rivers of Ecuador (Shibatta, 2003b; Bertaco & Cardoso, 2005).

Two species are reported from Argentina: *M. cottoides* Boulenger, 1891 (Mirande & Koerber, 2015) and *M. carlae* Vera Alcaraz, da Graça & Shibatta, 2008 (Almirón et al., 2015). A recent collecting expedition to northwestern Argentina allowed us to discover an additional species from the upper Bermejo River basin. The aim of this work is to describe this new species of *Microglanis*.

Material and methods

Counts and morphometric variables of ten specimens were taken according to Shibatta (2014), with addition of measurements of the dorsal-fin to adipose-fin distance, totaling 23 morphometric variables. Standard length (SL) is expressed in mm and all measurements are presented as percents of standard length (SL). Subunits of the head are also presented as percents of head length (HL). Roman numerals indicate unbranched rays and Arabic numerals represent branched rays. Numbers in parentheses indicate the number of specimens with a given count; counts of the holotype are marked by asterisks. Weberian-apparatus vertebrae are counted as five elements and included in the vertebral counts, and the compound caudal centrum (i. e., preural 1 fused to ural 1) of the caudal region was counted as a single element. The holotype (CI-FML 6596) and paratype (CI-FML 6595) were x-rayed to count ribs, vertebrae, and branchiostegal rays. Specimens of the new species were collected with hand nets, euthanized by overdose in benzocaine solution, fixed in 4 % formalin solution for 7 days and preserved in 70 % ethanol. Species with similar color pattern and those present in the basins of southern Brazil and Argentina were used for a Principal Components Analysis, with PAST (Hammer et al., 2001).

Institutional abbreviations are: ANSP, Academy of Natural Sciences of Drexel University, Philadelphia; CAS, California Academy of Sciences, San Francisco; CI-FML, Colección ictiológica, Fundación Miguel Lillo, San Miguel de Tucumán; INPA, Instituto Nacional de Pesquisas da Amazônia, Manaus; LBP, Laboratório de Biologia e Genética de Peixes, Botucatu; MCP, Museu de Ciências e Tecnologia, Pontifícia Universidade Católica do Rio Grande do Sul, Porto Alegre; MEPN, Museo de la Escuela Politécnica Nacional, Quito; MHNG, Muséum d'Histoire Naturelle, Geneva; MNHNP, Museu Nacional de Historia Natural del Paraguay, San Lorenzo; MNRJ, Museu Nacional, Rio de Janeiro; MZUEL, Museu de Zoologia da Universidade Estadual de Londrina, Londrina; MZUSP, Museu de Zoologia da Universidade de São Paulo, São Paulo; ROM, Royal Ontario Museum, Toronto; USNM, National Museum of Natural History, Smithsonian Institution,Washington.

Fig. 2. *Microglanis nigrolineatus*, CI- FML6595, paratype, 43.6 mm SL; live specimen, before fixation; Argentina: Salta province: Quebrada Colorada stream, Bermejo River basin.

Microglanis nigrolineatus, new species
(Figs. 1–3)

Holotype. CI-FML 6596, 32.6 mm SL; Argentina: Salta Province: San Ramón de la Nueva Orán, Bermejo River basin: Quebrada Colorada stream at RN50; 22°48'12"S 64°21'10"W; G. E. Terán, F. Alonso & J. M. Mirande, 19 May 2015.

Paratypes. All from Argentina. CI-FML 6595, 4, 27.6–43.6 mm SL; MZUEL 14122, 2, 17.5–30.1 mm SL; collected with holotype. – CI-FML 6260, 1, 21.8 mm SL; Salta Province: San Ramón de la Nueva Orán, Bermejo River basin: unnamed stream between Blanco and Pescado River at RN50; 23°00'46"S 64°21'54"W; G. E. Terán et al., 19 May 2015. – CI-FML 6261, 1, 34.2 mm SL; Salta Province: San Ramón de la Nueva Orán, Bermejo River basin: Pescado River at RN50; J. M. Mirande & G. Aguilera 01 Aug 2003. – CI-FML 4841, 1, 40.1 mm SL; Salta Province: San Martín, Bermejo River basin: Grande de Tarija River; 22°35'28"S 64°14'24"W; F. Cancino, 25 Sep 2005.

Diagnosis. *Microglanis nigrolineatus* differs from all its congeners by having a longitudinal stripe along middle of trunk, by the absence of a crossbar or light spot on nuchal region, and by having short serrae on anterior margin of pectoral-fin spine. *Microglanis nigrolineatus* is further distinguished from *M. carlae* by a longer head (28–33 % SL vs. 25–26), wider mouth (27–54 % HL vs. 21–24), 13–14 principal caudal-fin rays (vs. 11–12), caudal-fin emarginate (vs. caudal fin weakly forked), and ventral region slightly pigmented (vs. pigmented ventral region). It further differs from *M. cibelae* by a longer head (28–33 % SL vs.

23–26), longer maxillary barbels (29–37 % SL vs. 19–25), longer pelvic fin (17–20 % SL vs. 13–14), smaller distance from dorsal to adipose fins (5–15 % SL vs. 15–21), 8 branchiostegal rays (vs. 9), 28 free vertebral centra (vs. 29) and caudal fin with a dark bracket shaped stripe (vs. black distal band); from *M. cottoides* by the longer head (28–33 % SL vs. 26–27), smaller dorsal-fin spine length (8–13 % SL vs. 14–19), smaller pectoral-fin spine length (9–18 % SL vs. 18–23), smaller posterior cleithral process length (11–14 % SL vs. 15–19), smaller distance from dorsal to adipose fins (5–15 % SL vs. 18–21), longer adipose-fin base (24–29 % SL vs. 15–20) and 28 free vertebral centra (vs. 29); from *M. eurystoma* by a smaller distance from dorsal to adipose fins (5–15 % SL vs. 17–21), longer adipose-fin base (24–29 % SL vs. 15–21), smaller mouth width (27–54 % HL vs. 55–63), smaller interorbital width (36–43 % HL vs. 44–47), and 8 branchiostegal rays (vs. 9); from *M. garavelloi* by a longer head (28–33 % SL vs. 25–28), smaller snout length (33–40 % HL vs. 41–45) and anal fin hyaline (vs. anal fin mottled dark brown); from *M. maculatus* by a deeper head (14–17 % SL vs. 11–13), longer maxillary barbels (29–37 % SL vs. 20–25), smaller distance from dorsal to adipose fins (5–15 % SL vs. 15–18), absence of rounded spots in the flank (vs. presence), and caudal-fin with upper lobe hardly longer than lower lobe (vs. upper lobe slightly, but noticeably, longer than the lower).

Microglanis nigrolineatus differs from *M. malabarbai* by a smaller dorsal-fin spine (8–13 % SL vs. 14–17), deeper caudal peduncle (11–12 % SL vs. 9–10), longer adipose-fin base (24–29 % SL vs. 17–21), smaller distance from dorsal to adipose fins (5–15 % SL vs. 16–22), higher number of lateral-line pores 7–18 (vs. 6–7), and caudal-fin

Table 1. Morphometric data for *Microglanis nigrolineatus* (n = 10). SD, standard deviation. Range, mean and SD include holotype.

	holotype	range	mean	SD
Standard length (mm)	32.5	17.5–43.6	32.1	8.5
Percents of standard length				
Head length	28	28–33	30.7	1.7
Head depth	14	14–17	15.3	1.1
Interorbital width	12	11–14	12.3	1.0
Orbital diameter	2	2–4	3.1	0.6
Snout length	11	11–14	11.6	1.2
Mouth width	14	8–16	14.0	2.6
Maxillary barbel length	33	29–37	31.0	2.6
Pelvic fin length	18	17–20	18.0	1.0
Dorsal-fin spine length	9	8–13	11.1	1.6
Pectoral-fin spine length	18	9–18	15.5	2.5
Posterior cleithral process length	14	11–14	12.4	0.9
Predorsal length	36	35–40	37.1	1.2
Prepelvic length	52	47–58	52.6	3.3
Preanal length	69	68–76	71.0	3.3
Caudal peduncle depth	12	11–12	11.6	0.6
Caudal peduncle length	18	14–19	16.9	1.7
Body width	27	26–31	28.4	1.6
Body depth at dorsal fin	21	16–25	20.7	2.7
Dorsal-fin base length	15	13–16	14.2	0.9
Adipose-fin base length	28	24–29	27.0	2.0
Anal-fin base length	16	12–16	13.7	1.0
Distance dorsal-fin to adipose-fin	11	5–15	10.8	2.5
Percents of head length				
Interorbital width	42	36–43	40.0	2.4
Orbital diameter	8	8–11	9.5	0.9
Snout length	39	33–40	37.1	1.9
Mouth width	50	27–54	45.6	7.8
Maxillary barbel length	118	42–118	90.8	25.7
Head depth	51	45–53	50.0	2.3

with dark stripe (vs. caudal fin almost completely black); and differs from *M. xylographicus* by the longer adipose-fin base (24–29 % SL vs. 18–21), smaller interorbital width (36–43 % HL vs. 47–49), smaller orbital diameter 8–11 % HL (vs. 12–14), smaller snout length (33–40 % HL vs. 41–44), 7 ribs (vs. 5), and absence of melanophores surrounding neuromasts (vs. presence).

Description. Morphometric data in Table 1. Head and anterior portion of body (from mouth to dorsal-fin origin) depressed, becoming laterally compressed posteriorly; body depth highest at dorsal-fin origin; body width largest at pectoral-fin base (Fig. 1). Lateral profile of head from snout tip to opercular margin slightly convex; becoming straight until dorsal-fin origin. Lateral line incomplete, reaching vertical through the end of dorsal-fin base, surpassing it in some specimens (Figs. 1–2); 7–18 pores. Ventral profile of head and abdomen almost straight. Ventral profile of body gently curved posterior to anal fin (Fig. 1).

Head as wide as long, strongly depressed, anteriorly rounded in dorsal view. Mouth terminal, slightly prognathous. Eyes small, situated dorsolaterally, covered by skin and positioned at midlength of HL. Snout short. Anterior nostril tubular, close to upper lip; posterior nostril larger, rounded, close to eye. Maxillary barbel reaching dorsal-fin spine. Mental barbels arranged in arch along ventral surface of jaw; outer pair surpassing base of pectoral-fin spine; inner pair, slightly shorter than one-half length of outer mental barbel. Gill rakers filiform; total gill rakers on first arch 5*(8) or 6 (2). Branchiostegal membranes free from isthmus; 8*(10) branchiostegal rays.

Dorsal-fin posterior margin rounded, entire base anterior to middle of standard length; one spinelet, I,6*(10) rays. Dorsal spine (lepidotrichium) short, not extended as much as longest dorsal-fin rays; posterior margin distal portion serrated. Adipose fin elongated, with free posterior margin; base longer than length of anal-fin base, almost reaching posteriorly to vertical of caudal-fin base. Pectoral fin completely covered by thin skin; not reaching pelvic-fin origin when adpressed; I,5*(10). Pectoral-fin spine slightly flattened dorsoventrally, strong, with developed serrations on both margins; serrae on anterior margin retrorse on proximal third, antrorse and apical serrae distally, very short; serrae on posterior margin retrorses, greater than those from anterior margin, increasing in size from proximal to distal portion (Fig. 3). Pelvic fin rounded, origin at vertical through last dorsal-fin ray insertion, not reaching anal-fin origin when adpressed; i,5*(4). Anal fin short and rounded in distal profile, its base shorter than adipose fin base and not confluent posteriorly with caudal fin; iii,7 (7), iii,8*(3). Caudal fin emarginated, with distal profile of lobes rounded, upper lobe hardly longer than lower lobe; principal caudal-fin rays i,13,i (2); i,14,i*(8). Seven ribs; free vertebral centra 28 (total 34 vertebrae) in holotype and paratype (CI-FML 6595).

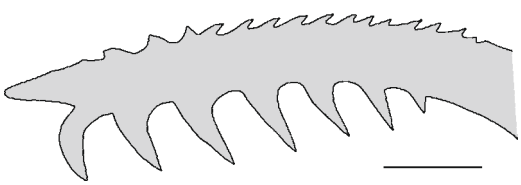

Fig. 3. *Microglanis nigrolineatus*, CI- FML 6596, holotype, 32.5 mm SL; dorsal view of left pectoral-fin spine. Scale bar 1 mm.

Color in alcohol. Head in dorsal view dark brown from tip of snout to nuchal region, in dorsal view, with small light blotches on posterior nares and small light blotch on posterior cheek extending posteroventrally below eye. Barbels light with dark brown spots. Head ventral region light yellow. Trunk between occipital region and posterior base of dorsal fin with dark brown blotch extending to ventral region near pelvic-fin base. Dorsal region between dorsal and adipose fins with a dark longitudinal stripe. Dark stripe running longitudinally along midline body from a vertical through dorsal fin to adipose fin end, sometimes confluent with triangular dark brown blotch of caudal peduncle. Body ventral surfaces light yellow with dark spots. First pectoral-fin ray dark brown; branched rays of pectoral fin with dark brown spots from proximal to distal regions. Dorsal fin hyaline with dark brown base and broad dark brown band crossing middle portions of fin spine, rays and membranes. Adipose fin with dark blotch in its middle region and light brown margin. Pelvic fin hyaline. Anal fin hyaline, with two dark spots on base. Caudal fin with a dark bracket shaped stripe, broad, not reaching caudal-fin dorsal and ventral margins.

Color in life. Similar coloration as in preserved specimens, some specimens darker (Fig. 2).

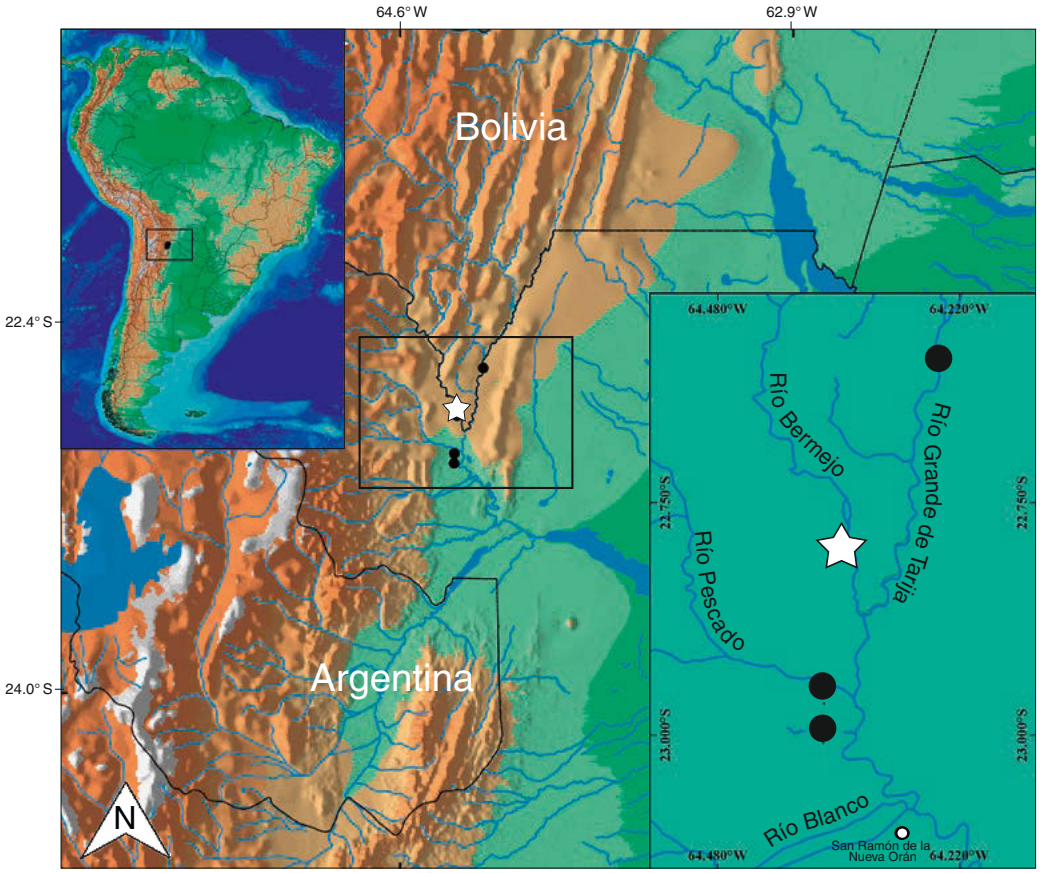

Fig. 4. Northwestern Argentina, showing the distribution of *Microglanis nigrolineatus*. ☆, type locality at Quebrada Colorada stream, Bermejo River basin. ●, paratype localities.

Distribution. All known specimens of *M. nigrolineatus* were collected in the upper Bermejo River basin, in the province of Salta, Argentina. The upper Bermejo River basin extends to the province of Jujuy, in Argentina, and southern Bolivia (Fig. 4). Considering the relatively wide known distribution of this species in the upper Bermejo River basin in Argentina, close to the limit with Bolivia, *M. nigrolineatus* is most probably present also in that country.

Etymology. The specific name *nigrolineatus* is formed by two Latin adjectives *niger*: black and *lineatus*: with lines; in allusion to the dark stripes running along trunk of the new species. An adjective.

Habitat notes. (CI-FML 6596*, CI-FML 6595, MZUEL 14122). Habitats where specimens of *M. nigrolineatus* were collected are between 345–390 m asl. in the piedmont of Yungas. Although many samplings were done above that altitude, no specimen of *Microglanis* was collected there, suggesting a preference for plain habitats (Fig. 5). While mountain environments present high flow velocity and gravel substrate, the habitats of *M. nigrolineatus* have slow water flow and sandy or muddy substrate. The region has marked seasonality, with precipitations in the area concentrated in summer (80 % from November to March), and a dry winter (June to October). Average temperatures range from 14 °C in July to 26 °C in December and January (Servicio Meteorológico Nacional, 2015). In May, when most of the specimens were collected, the streams had clean waters, with slow flow velocity, water slightly alkaline (pH 7.4) and relatively high conductivity (770 $\mu S \cdot cm^{-1}$). Maximum depth

was approximately 40 cm at the type locality. The river shores had abundant marginal macrophytes as *Ludwigia* sp., *Equisetum* sp. and watercress (Brassicaceae). Individuals of *M. nigrolineatus* were associated with driftwood and leaves and never in open water. Other fish species collected syntopically at the type locality include: *Aphyocharax anisitsi*, *Astyanax chico*, *A. lacustris*, *A. lineatus*, *Bryconamericus exodon*, *Characidium* cf. *zebra*, *Cichlasoma dimerus*, *Loricariichthys* sp., *Loricaria holmbergi*, *Moenkhausia* cf. *intermedia*, *Otocinclus vittatus*, *Rhamdia quelen*, *Serrapinnus microdon*, and *Synbranchus* cf. *marmoratus*.

Fig. 5. Type locality: Quebrada Colorada stream, Bermejo River basin, Salta, Argentina. May 2015.

Discussion

Coloration pattern in *Microglanis* is quite variable and complex, resulting in a large number of configurations among the species of the genus (Shibatta, 2014). *Microglanis nigrolineatus* is distinguished from all its congeners by a unique coloration pattern besides a combination of morphological characters. The coloration pattern is very important in the systematic of this genus since it has been used for the diagnosis of many species (e. g., Mees, 1978; Shibatta & Benine, 2005; Bertaco & Cardoso, 2005; Mori & Shibatta, 2006; Vera Alcaraz et al, 2008; Ottoni et al, 2010; Ruiz & Shibatta, 2011; Mattos et al, 2013; Jarduli & Shibatta, 2013; Shibatta, 2014). Two longitudinal black stripes along body, similar to the color pattern of *M. nigrolineatus*, are observed in *M. maculatus* Shibatta, 2014 and *M. xylographicus* Ruiz & Shibatta, 2011. However, *M. maculatus* has light spots in the nuchal region, an U-shaped dark-brown blotch on the trunk between nape and end of dorsal fin, and rounded dark blotches (Shibatta, 2014), and *M. xylographicus* has a light spot on the occipital region, and dark streaks on the trunk (Ruiz & Shibatta, 2011). Although these species share similar color patterns, a phylogenetic analysis is needed to assess if that coloration is more parsimoniously attributed to common ancestry or parallelisms.

Morphometric differences are observed through principal components analysis (PCA) between *M. nigrolineatus* and species with similar color pattern or geographically close. Results reveal a separation between *M. nigrolineatus* and other species along the second and third principal component (Fig. 6; Table 2). The PC2 retains 3.44 % and PC3 retainis 1.38 % of the total variance and corresponds primarily to differences in shape (vs. size). *Microglanis nigrolineatus* differs from *M. eurystoma*, *M. maculatus* and *M. xylographicus* by higher values of orbital diameter, mouth width, adipose-fin base length and body depth at dorsal fin (positive highest values) and differs from *M. carlae*, *M. cibelae*, *M. cottoides*, *M. garavelloi*, and *M. malabarbai* by smaller values of dorsal-fin to adipose-fin distance, dorsal-fin spine length, mouth width and pectoral-fin spine length (negative highest values; Table 2).

Other important diagnostic character of *M. nigrolineatus* is the serrae on the anterior margin of the pectoral-fin spine shorter than in other species of the genus (Fig. 3). However, according to Shibatta (2014), this character should be used with caution due to ontogenetic variation on the serrae morphology observed in *Microglanis*.

Microglanis nigrolineatus is the first species described from Argentina. *Microglanis cottoides* and *M. parahybae* Steindachner, 1880 have been reported in Argentina (Gonzo, 2003) but, according to Liotta (2005) and Mirande & Koerber (2015), only *M. cottoides* occurs in this country. *Microglanis parahybae* was considered a senior synonym of *M. cottoides* by Mees (1974), which may have caused some confusion regarding the identification of the species in Argentina. Malabarba & Mahler (1998) recognized the validity of both species, but they have cited only *M. cottoides* in the Uruguay River basin, a drainage shared with Brazil and Argentina. The know distribution of *M. parahybae* is restricted to coastal rivers of Rio de Janeiro, Brazil. Other species reported in several streams of Parque Nacional Pre Delta (lower Paraná basin), Argentina, is *M. carlae* (Almirón et al., 2015). Several endemic species

had been described for the upper portion of Bermejo River basin, in the last decade: e. g. *Astyanax latens* Mirande, Aguilera & Azpelicueta, 2004; *A. chico* Casciotta & Almirón, 2004; *A. tumbayaensis* Miquelarena & Menni, 2005; *A. endy* Mirande, Aguilera & Azpelicueta, 2006; *Bryconamericus indefessus* (Mirande, Aguilera & Azpelicueta, 2006); *Loricaria holmbergi* Rodríguez & Miquelarena, 2005; *Oligosarcus itau* Mirande, Aguilera & Azpelicueta, 2011. According to Hales & Petry (2015), the study site (upper Bermejo basin) and lower Bermejo basin belong to Chaco Ecoregion. This ecoregion includes the drainages of the western Paraguay basin across Bolivia, Paraguay, and Argentina. There are presently more than 150 fish species recorded in this ecoregion, of which 16 are endemic.

Material examined. All from Brazil, except where noted. *Microglanis carlae*: MHNHP 3667, holotype, 34.1 mm SL; MZUSP 98255, 5 paratypes, 23.4–29.1 mm SL; Paraguay: Salado River, Paraguay River basin.

M. cibelae: MCP 19822, 3 paratypes, 34.9–48.7 mm SL; arroio do Ouro, Maquiné River basin. – MCP 21190, 9, 24.6–42.4 mm SL; Osório, Tramandaí River basin.

M. cottoides: LBP 17014, 15, 39.3–51.3 mm SL; Cabeça stream, Lagoa dos Patos basin. – MCP 10826, 5, 38.2–49.5 mm SL; Sanga das Águas Frias River. – MCP 17706, 4, 45.3–25.1 mm SL; Quarizinho stream, tributary of Buricá River, Uruguai River basin.

M. eurystoma: MCP 13405, holotype, 77.6 mm SL; MCP 12698, 10 paratypes, 26.3–41.1 mm SL; do Passo Alto stream, Uruguai River basin.

M. garavelloi: MZUSP 88006, holotype, 31.7 mm SL; MZUSP 1732, 2 paratypes, 23.7–30.8 mm SL; MCP 1678, 4 paratypes, 24.6–27.9 mm SL; Taquari stream, Paraná River basin.

M. iheringi: USNM 121985, paratype, 31.3 mm SL; Venezuela**:** Turmero River basin. – CAS 64403, 3, 27.4–41.0 mm SL; Venezuela: Orinoco River basin.

M. leptostriatus: MZUSP 47456, 2 paratypes, 28.4–28.7 mm SL; Verde River. – MZUEL 3733, 6 paratypes, 19.3–27.4 mm SL; Cruz River, São Francisco River basin.

M. lundbergi: INPA 28577, holotype, 27.7 mm SL; INPA 18774, 3 paratypes, 22.3–24.7 mm SL; Solimões River basin. – MZUSP 112217, paratype, 23.3 mm SL; MZUSP 112218, paratype, 23.1 mm SL; MZUSP 112219, 2 paratypes, 21.2–25.7 mm SL; MZUSP 112220, paratype,

Table 2. Morphometric data loadings, eigenvalues and percentages relating to the first (PC1), second (PC2) and third (sheared PC3) eigenvectors of Principal Components obtained from the analysis of combined samples of *Microglanis nigrolineatus* (n = 10), *M. carlae* (n = 5), *M. cibelae* (n = 6), *M. cottoides* (n = 5), *M. eurystoma* (n = 8), *M. garavelloi* (n = 10), *M. maculatus* (n = 4), *M. malabarbai* (n = 4) and *M. xylographicus* (n = 6).

	PC1	PC2	PC3
Standard length	0.194	−0.042890	0.033410
Head length	0.2016	0.090820	−0.020160
Head depth	0.1911	0.038250	0.150100
Interorbital width	0.2106	0.059740	−0.194600
Orbital diameter	0.1481	0.277000	0.065820
Snout length	0.2067	0.031670	−0.148700
Mouth width	0.3023	0.591900	−0.439800
Maxillary barbel length	0.1707	0.060510	0.124600
Pelvic fin length	0.1639	−0.048280	0.043340
Dorsal-fin spine length	0.2107	−0.369000	0.015000
Pectoral-fin spine length	0.2246	−0.296800	0.064110
Posterior cleithral process length	0.2353	−0.136400	0.119700
Predorsal length	0.1964	−0.020890	−0.029800
Prepelvic length	0.2067	−0.009036	0.012310
Preanal length	0.2017	0.010810	−0.016840
Caudal peduncle depth	0.1755	0.154100	−0.069190
Caudal peduncle length	0.1903	0.077250	−0.046640
Body width	0.2117	−0.054120	−0.013780
Body depth at dorsal fin	0.2649	−0.137600	0.282100
Dorsal-fin base length	0.2015	−0.047870	0.101800
Adipose-fin base length	0.1875	0.262700	0.588700
Anal-fin base length	0.1937	−0.030420	0.151500
Distance dorsal-fin to adipose-fin	0.2476	−0.428300	−0.462900
Eigenvalue	0.876594	0.033075	0.013310
Percents of total variance	91.08%	3.44%	1.38%

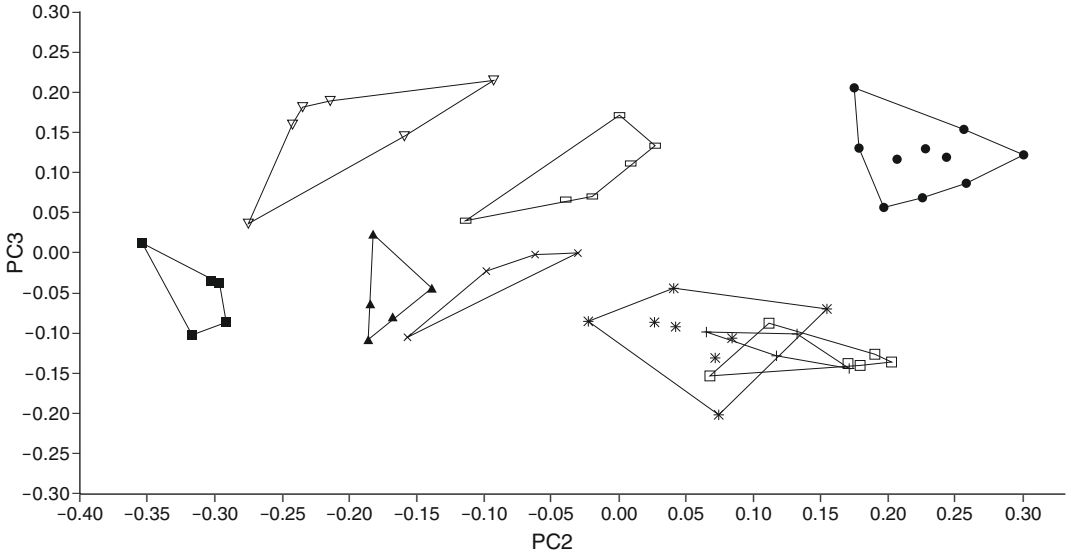

Fig. 6. Principal component analysis (PC2 vs. PC3) of combined samples of *Microglanis nigrolineatus* (●; n = 10) *M. carlae* (■; n = 5), *M. cibelae* (▭; n = 6), *M. cottoides* (▲; n = 5), *M. eurystoma* (✳; n = 8), *M. garavelloi* (▽; n = 10), *M. maculatus* (+; n = 4), *M. malabarbai* (×; n = 4) and *M. xylographicus* (□; n = 6).

24.5 mm SL; MZUSP 112221, paratype, 20.8 mm SL; Amazonas River basin.

M. maculatus: INPA 41133, holotype, 36.5 mm SL; Pouso Alegre stream. – INPA 24044, 2 paratypes, 21.4–25.8 mm SL; igarapé Veredas; dos Patos River, Tocantins basin.

M. malabarbai: MCP 37252, 1, 47.7 mm SL; Alexandrino stream. – MCP 37187, 1, 50.1 mm SL, das Pedras stream, Ijuí River basin.

M. nigripinnis: MZUSP 80223, 1, 47.2 mm SL; MZUSP 80229, 2, 38.3–43.5 mm SL; tributary of São João River, Eastern basin.

M. oliveirai: INPA 35623, holotype, 26.3 mm SL; Corrente River. – MZUEL 5175, 11 paratypes, 19.6–25.4 mm SL; Corrente River, Araguaia River basin.

M. parahybae: MNRJ 15989, 5, 30.3–34.2 mm SL; Dois Rios River. – MNRJ 16047, 5, 28.6–38.9 mm SL; Muriaé River, Paraíba do Sul River basin.

M. pataxo: MZUSP 54516, 10, 24.9–31.4 mm SL; Mucuri River, East coast basin.

M. pellopterygius: ANSP 130437, holotype, 68.1 mm SL; MEPN 88.4–12, 2, 22.4–23.1 mm SL; Ecuador: tributary of Aguarico River.

M. poecilus: ROM 60738, 1, 22.5 mm SL; unknown stream from Essequibo River. – ROM 62390, 1, 17,1 mm SL; Shimiri River. – ROM 62391, 1, 17.1 mm SL; Guiana: Essequibo River basin. – INPA 28575, 3, 18.6–20.6 mm SL; Aripuanã River, Madeira River basin. – INPA 28576, 3, 19.8–20.4 mm SL; igarapé Ano Bom. – INPA 8052, 3, 24.8–26.2 mm SL; igarapé Maracá, Branco River basin. – INPA 6828, 3, 19.2–25.8 mm SL; Jamanxin River, Tapajós River basin.

M. robustus: INPA 8053, holotype, 20.3 mm SL; INPA 32885, 11 paratypes, 18.4–23.3 mm SL; INPA 7943, paratypes, 2, 20.0–22.2 mm SL; INPA 7957, 3 paratypes, 19.2–21.7 mm SL; lower Tocantins River, Tocantins-Araguaia River basin.

M. secundus: INPA 5730, 7, 18.5–31.1 mm SL; INPA 7950, 3, 24.4–28.1 mm SL; Trombetas River, Amazonas River basin. – MHNG 2621.038, 6, 18.9–27.1 mm SL; Suriname: Mindrineti River.

M. variegatus: USNM 083653, 1 paratype, 29.1 mm SL; pools in forests near Vinces. – MHNG 298.033, 2, 25.2–27.7 mm SL; MHNG 1232.11, 2, 23.6–26.2 mm SL; Ecuador**:** Palengue River basin.

M. xylographicus: INPA 35624, holotype, 27.8 mm SL; MZUEL 5174, 2 paratypes, 23.1–26.2 mm SL; Jaraguá stream. – MZUEL 5173, 4 paratypes, 18.2–22.3 mm SL; Corrente River, Araguaia River basin.

Acknowledgments

We thank P. J. dos Reis (Department of Physics, UEL) for the radiograph of the holotype and paratype. J. L. O. Birindelli, F. Jerep (UEL), G. Aguilera, F. Cancino, C. Butí (FML), M. Azpelicueta (CONICET), L. Lobo; G. Scrocchi and P. Goloboff (UEL-CONICET) for their valuable suggestions on the manuscript. We are also thankful to the Universidade Estadual de Londrina, CNPq for financial support and Fundación Miguel Lillo, CONICET (PIP-11420110100301 to J. M. Mirande) and FONCyT (PICT-2011-0992 to J. M. Mirande).

Literature cited

Almirón, A., J. Casciotta, L. Ciotek & P. Giorgis. 2015. Guía de los peces del Parque Nacional Pre-Delta. Administración de Parques Nacionales Ciudad Autónoma de Buenos Aires, 300 pp.

Alcaraz, H. S. V., W. J. Graça & O. A. Shibatta. 2008. *Microglanis carlae*, a new species of bumblebee catfish (Siluriformes: Pseudopimelodidae) from the río Paraguay basin in Paraguay. Neotropical Ichthyology, 6: 425–432.

Bertaco, V. A. & A. R. Cardoso. 2005. A new species of *Microglanis* (Siluriformes: Pseudopimelodidae) from the rio Uruguay drainage, Brazil. Neotropical Ichthyology, 1: 61–67.

Eigenmann, C. H. 1912. The freshwater fishes of British Guiana, including a study of the ecological grouping of species, and the relation of the fauna of the plateau to that of the lowlands. Memoirs of the Carnegie Museum, 5: 1–578.

Gomes, A. L. 1946. A review of *Microglanis*, a genus of South American catfishes, with notes of related genera. Occasional Papers of the Museum of Zoology, 494: 1–19.

Gonzo, G. M. 2003. Peces de los Ríos Bermejo, Juramento y Cuencas Endorreicas de la Provincia de Salta. Museo Ciencias Naturales y Consejo de Investigación, Universidad Nacional de Salta, Salta, 243 pp.

Hales, J. & P. Petry, 2015. Chaco in Freshwater Ecoregions of the World. http://www.feow.org/ecoregions/details/342. Electronic version accessed 30/10/2015.

Hammer, Ø., D. A. T. Harper & P. D. Ryan. 2001. PAST: Paleontological Statistics Software Package for Education and Data Analysis. Palaeontologia Electronica 4: 1–9.

Jarduli, L. R. & O. A. Shibatta. 2013. Description of a new species of *Microglanis* (Siluriformes: Pseudopimelodidae) from the Amazon basin, Amazonas State, Brazil. Neotropical Ichthyology, 11: 507–512.

Liotta, J. 2005. Distribución geográfica de peces de aguas continentales de la República Argentina. ProBiota FCNyM, UNLP, La Plata, 653 pp.

Malabarba, L. R. & J. K. F. Mahler. 1998. Review of the genus *Microglanis* in the rio Uruguay and coastal drainages of southern Brazil (Ostariophysi: Pimelodidae). Ichthyological Exploration of Freshwaters, 9: 243–254.

Mattos, J. L. O., F. P. Ottoni & M. A. Barbosa. 2013. *Microglanis pleriqueater*, a new species of catfish from the rio São João basin, eastern Brazil (Teleostei: Pseudopimelodidae). Ichthyological Exploration of Freshwaters, 24: 147–154.

Mees, G. F. 1974. The Auchenipteridae and Pimelodidae of Suriname (Piscer, Nematognathi). Zoologische Verhandelingen, 132: 1–246.

— 1978. Two new species of Pimelodidae from Northwestern South America (Pisces, Nematognathi). Zoologische Mededelingen, 53: 253–261.

Mirande, J. M. & S. Koerber. 2015. Checklist of the freshwater fishes of Argentina (CLOFFAR). Ichthyological Contributions of Peces Criollos, 36: 1–68.

Mori, H. & O. A. Shibatta. 2008. A new species of Microglanis Eigenmann, 1912 (Siluriformes, Pseudopimelodidae) from rio São Francisco basin, Brazil. Zootaxa, 1302: 31–42.

Ottoni, F. P., J. L. O. Mattos & M. A. Barbosa. 2010. Description of a new species of *Microglanis* from the rio Barra Seca basin, southeastern Brazil (Telestei: Siluriformes: Pseudopimelodidae). Vertebrate Zoology, 60: 187–192.

Ruiz, W. B. G & O. A. Shibatta. 2010. A new species of *Microglanis* (Siluriformes: Pseudopimelodidae) from lower Rio Tocantins basin, Pará, Brazil, with a description of superficial neuromasts and pores of lateral line system. Zootaxa, 2632: 53–66.

Schultz, L. P. 1944. The catfishes of Venezuela, with descriptions of thirty-eight new forms. Proceedings of the United States National Museum, 94: 173–338.

Servicio Meteorológico Nacional. 2015. Secretaría de Ciencia, Tecnología y Producción. Ministerio de Defensa. Presidencia de La Nación. República Argentina. http://www.smn.gov.ar/ Accessed: 11/05/2015.

Shibatta, O. A. 1998. Sistemática e evolução da família Pseudopimelodidae (Ostariophysi, Siluriformes), com a revisão taxonômica do gênero *Pseudopimelodus*. Unpublished Ph.D. Dissertation, Universidade Federal de São Carlos, São Carlos, 357 pp.

— 2003a. Phylogeny and classification of 'Pimelodidae'. Pp. 385–400 in: G. Arratia, B. G. Kapoor, M. Chardon & R. Diogo (eds.), Catfishes. Vol. 1. Sciences Publishers, Enfield, 487 pp.

— 2003b. Family Pseudopimelodidae (Bumblebee catfishes, dwarf marbled catfishes). Pp. 401–405 in: R. E. Reis, S. O. Kullander & C. J. Ferraris (eds.), Check list of the freshwater fishes of South and central America. Editora Edipucrs, Porto Alegre.

— 2014. A new species of *Microglanis* (Siluriformes: Pseudopimelodidae) from the upper rio Tocantins basin, Goiás State, Central Brazil. Neotropical Ichthyology, 12: 81-87.

Shibatta, O. A. & R. C. Benine. 2005. A new species of *Microglanis* (Siluriformes: Pseudopimelodidae) from upper rio Paraná basin, Brazil. Neotropical Ichthyology, 3: 579–585.

Vera Alcaraz, H. S., W. J. da Graça & O. A. Shibatta. 2008. *Microglanis carlae*, a new species of bumblebee catfish (Siluriformes: Pseudopimelodidae) from the río Paraguay basin in Paraguay. Neotropical Ichthyology, 6: 425–432.

Received 23 November 2015
Revised 10 June 2016
Accepted 9 August 2016

Ichthyological Exploration of Freshwaters

An international journal for field-orientated ichthyology

INSTRUCTIONS TO CONTRIBUTORS

Warning
Prospective authors should read carefully the following instructions and follow them when submitting a manuscript. Doing so significantly hastens publication and saves money and efforts. Manuscripts which do not satisfy the instructions below may be rejected at the Editor's discretion and will not be returned.

Submission of manuscripts
The original manuscript should be sent to the Editor, Maurice Kottelat, by e-mail (mkottelat@dplanet.ch). Additional information is requested:
1) the name, postal and e-mail addresses, telephone and fax numbers of the corresponding author;
2) the names, postal and e-mail addresses of up to four persons outside the authors' institutions who are qualified to review the paper; and
3) a statement that the material has not been published and is not considered for publication elsewhere and that it will not be submitted elsewhere unless it is rejected or withdrawn. In submitting a manuscript, the author(s) accept(s) transfer of the copyright to the Publisher.

Co-authors, corresponding author
Authors are those who have played a significant role in designing and conducting the research and in writing the manuscript. Individuals who have only collected data, provided material or financial support, or reviewed the manuscript should be listed in acknowledgments. Honorary authorship is not accepted.

Co-authors should designate a single corresponding author to whom correspondence and proofs will be sent. All correspondence regarding the paper should go through the corresponding author. Correspondence will not be sent to other co-authors and correspondence from other co-authors regarding the manuscript will neither be answered nor taken into consideration.

Format
Files. The manuscript should be submitted in DOC or RTF format only. The text, captions, tables etc. must all be included in the same file. It the manuscript includes only a few illustrations, include them in low resolution in the word file. If the manuscript includes numerous illustrations they must be submitted in a separate PDF file; send all figures in low resolution and with caption in a single file. The files should be less than 8 MB.

Text. All manuscripts are subject to editorial revision before final acceptance for publication. Nothing in the manuscript should be underlined. Titles with numerical series designations are not permitted. Titles should be brief, fewer than 20 words and should indicate clearly the field of study and the group of fishes investigated. All abbreviations should be explained in the Method section (or figure caption when appropriate) or a reference to published explanations should be provided; exceptions are very common abbreviations, such as mm, km, kg, sec, min, yr, vs., SL. Footnotes are not permitted. All measurements must be in metric units. The first page should include: title of the paper, author(s), addresses and abstract, all left justified. The text should be followed by Material Examined (if appropriate), Acknowledgments (if any), Appendix (if any) and Literature Cited, in that order. Keys are desirable in taxonomic papers. They should be dichotomous and not serially indented.

Nomenclature. Names of living organisms should follow the appropriate and current International Codes of Nomenclature. Only formal names of genera and species should be written in italics. Names of authors and publication dates of scientific names should be mentioned once, in introduction or discussion, depending where most convenient, exceptionally as a table; bibliographical references must be included in the Literature cited section. Very old and classical works can be omitted if not absolutely justified.

Language. Manuscripts should be written in English. All papers must have a concise but informative abstract in English. In taxonomic papers, the abstract must include at least clear diagnosis of the new taxa. This maybe omitted for papers including the descriptions of many new taxa; consult the editor first. A second abstract, provided by the author(s), in the language of the country or area concerned by the text is acceptable. A maximum of two abstracts is permitted.

Acknowledgments. Identify individuals by first name(s) and surname. Do not list titles, position or institution. Acknowledge individuals, not positions. Idiosyncrasy and private jokes are not permitted.

Literature cited. Format for Literature Cited is that of the most recent issue. Do not abbreviate the names of journals. For books, give full name of publishing company or institution, and city. Manuscripts in preparation, abstracts, in-house reports and other literature not obtainable through normal library channels cannot be cited. In-press manuscripts can be cited only if they have been formally accepted.

Tables. Tables should be included in the text file, at the end. Use Word format and do not anchor them. Tables must be numbered sequentially with Arabic numerals; they should have concise but self-explanatory headings. Do not insert frames, vertical rules, dotted lines or footnotes. The location of first citation of each table should be clearly indicated in the text.

Figures. Detailed instructions for the preparation of digital images are here: http://pfeil-verlag.de/div/eimag.php

For the submission of new manuscript only low resolution copies are needed. Do not send large files at this stage. Case by case, if needed, we may ask you to send the original files at the time of submission.

All maps, graphs, charts, drawings and photographs are regarded as figures and are to be numbered consecutively and in the sequence of their first citation in the text. When several charts or photographs are grouped as one figure, they must be trimmed and spaced as intended for final reproduction. Each part of such a group figure should be lettered with a lower case block letter in the lower left corner. Where needed, scale should be indicated on the figure by a scale bar.

All illustrations should be designed to fit a width of 68 or 140 mm and a depth no greater than 200 mm. Lettering should be large enough to be easily seen when reduced onto a journal column (68 mm).

If a vector-graphics program is used, the original files saved by this program and all linked files must be submitted. Do not export or save the figure in a different format (for more details see the informations on http://pfeil-verlag.de/div/eimag.php
If line drawings are scanned, the resolution must be 1200 dpi or more and the format must be bitmap (1 pixel = 1 bit).
If halftones are scanned, the resolution should never be lower than 400 dpi, applied to a width of 14 cm, even for photographs designed for column width.

Photographic prints and slides and original drawings must be scanned for submission. We will ask to send the original after acceptance of the manuscript.

Colour illustrations should preferably be submitted as slides (photographic slides, not slides prepared by a printer). Digital images should be only unmodified (raw) data files as originally saved by the camera or the scanner. If the data files are modified, a copy of the original, unmodified file should be submitted too.

The decision to print in colour or in black and white any figure originally submitted in colour remains with the editor and publisher. This decision will be based on scientific justification, quality of the original, layout and other editorial, financial and production constraints. By submitting colour originals, the authors know and accept that they may be published in black and white.

Review
Each manuscript will be sent to two reviewers for confidential evaluation. When justified, the reviewer's comments will be forwarded to the corresponding author. When submitting a revised manuscript, authors should briefly indicate the reasons for disregarding any suggestion they consider unacceptable. Remember that if a reviewer had questions or did not understand you, other readers may make the same experience and the answers should be in the manuscript and not in a letter to the editor. Changes in style, format and layout requested by the Editor are non-negotiable and non-observance will result in rejection of the manuscript.

Revised manuscripts received more than 6 months after the reviewers' comments had been sent will not be considered or will be treated as new submissions.

Proofs, Reprints and Page Charges
A PDF proof file will be sent to the corresponding author; it should be checked and returned to the Editor within one week. If corrections are not received within this delay, they may be done by the Editor, at the author's risks. Authors may be charged for any changes other than printer's error. Reprint orders must be forwarded with the corrections. The corresponding author is responsible for contacting the co-authors and forwarding their reprint orders.

The authors will receive a PDF file for personal use free of charge; high-resolution PDF files for unlimited use may be ordered. There will be no page charges and no charges for justified colour illustrations.

Ichthyological Exploration of Freshwaters

An international journal for field-orientated ichthyology

Volume 27 · Number 3 · November 2016

CONTENTS

Cover photograph
Liniparhomaloptera macrostoma (Photograph by Jiahu Lan)
Tiejun Wu, Lihui Xiu and Jian Yang
(this volume pp. 275–282)

Articles appearing in this journal are indexed in:

AQUATIC SCIENCES and FISHERIES ABSTRACTS
BIOLIS – BIOLOGISCHE LITERATUR INFORMATION SENCKENBERG
CAMBRIDGE SCIENTIFIC ABSTRACTS
CURRENT CONTENTS/AGRICULTURE, BIOLOGY & ENVIRONMENTAL SCIENCES and SCIE
FISHLIT
ZOOLOGICAL RECORD